OAK RIDGE NATIONAL LABORATORY LIBRARY
3 4456 0021622 8

NUREG/CR-3303
(ORNL/TM-8774)

ornl

OAK RIDGE NATIONAL LABORATORY

UNION CARBIDE

Use of Neutron Noise for Diagnosis Of In-Vessel Anomalies in Light-Water Reactors

D. N. Fry
J. March-Leuba
F. J. Sweeney

Prepared for the
Instrumentation and Control Branch
Division of Facility Operations
Office of Nuclear Regulatory Research
U.S. Nuclear Regulatory Commission
Under Interagency Agreement 40-551-75

OAK RIDGE NATIONAL LABORATORY
CENTRAL RESEARCH LIBRARY
CIRCULATION SECTION
4500N ROOM 175
LIBRARY LOAN COPY
DO NOT TRANSFER TO ANOTHER PERSON
If you wish someone else to see this report, send in name with report and the library will arrange a loan.

OPERATED BY
UNION CARBIDE CORPORATION
FOR THE UNITED STATES
DEPARTMENT OF ENERGY

NUREG/CR-3303
ORNL/TM-8774
NRC Dist. Category R1

Instrumentation and Controls Division

USE OF NEUTRON NOISE FOR DIAGNOSIS OF IN-VESSEL ANOMALIES IN LIGHT-WATER REACTORS

D. N. Fry
J. March-Leuba*
F. J. Sweeney

Manuscript Completed - June 1983

Date of Issue - January 1984

*The University of Tennessee, Knoxville, Tennessee 37816

Prepared for the
Instrumentation and Control Branch
Division of Facility Operations
Office of Nuclear Regulatory Research
U.S. Nuclear Regulatory Commission
Under Interagency Agreement 40-551-75

NRC Fin No. B0191

Prepared by the
Oak Ridge National Laboratory
Oak Ridge, Tennessee 37831
operated by
UNION CARBIDE CORPORATION
for the
U.S. DEPARTMENT OF ENERGY
under Contract No. W-7405-eng-26

OAK RIDGE NATIONAL LABORATORY LIBRARY
3 4456 0021622 8

TABLE OF CONTENTS

	Page
LIST OF FIGURES	v
LIST OF ACRONYMS	ix
ACKNOWLEDGEMENTS	x
ABSTRACT	xi
1. INTRODUCTION	1
2. THEORETICAL BASIS OF NEUTRON NOISE	2
3. COMPARISON OF BWR AND PWR NEUTRON NOISE	5
4. ACQUISITION OF NEUTRON NOISE DATA	8
5. ORNL NEUTRON NOISE LIBRARY	13
6. DATA REDUCTION AND ERROR ESTIMATION	16
6.1 Reduction of Noise Recordings	16
6.2 Uncertainties In Coherence Estimates	16
6.3 Normalization of Power Spectra	17
7. PWR EX-CORE NEUTRON NOISE	18
7.1 Overview	18
7.2 Sources of PWR Ex-Core Neutron Noise	18
7.2.1 Low-Frequency Region	18
7.2.2 Mid-Frequency Region	19
7.2.3 High-Frequency Region	19
7.3 Variation of PWR Ex-Core Neutron Noise Over a Fuel Cycle at Sequoyah 1	45
7.4 Application of Neutron Noise in PWRs	50
7.4.1 Measurement of Core Barrel Motion	50
7.4.2 Measurement of In-Core Coolant Velocity	55
7.4.3 Measurement of Fuel Motion	57
8. BWR NEUTRON NOISE	59
8.1 Sources of BWR Neutron Noise	61
8.2 Application of Neutron Noise in BWRs	61
8.2.1 Vibration Monitoring	62
8.2.2 Bypass Boiling Detection	65
8.2.3 Two-Phase Flow Measurement	71
8.2.4 Stability Monitoring	73
9. SUMMARY AND CONCLUSIONS	78
10. RECOMMENDATIONS	79
REFERENCES	81

LIST OF FIGURES

Figure		Page
1	Normalized power spectral density (NPSD) of ex-core neutron noise from a PWR at 75 and 96% of full power . . .	3
2	Comparison of BWR and PWR neutron noise signals when normalized to the dc signal level (signals bandpassed 0.01-40 Hz and sampled at 100 samples per s)	6
3	Comparison of BWR and PWR neutron noise amplitude probability densities (APDs) when normalized to the dc signal level and the total number of samples (signals bandpassed 0.01-40 Hz and sampled at 100 samples per s for 2048 s)	7
4	Comparison of BWR and PWR neutron noise spectra when normalized to the square of the dc signal level	7
5	Method of acquisition of neutron noise	8
6	Typical locations of ex-core power range neutron detectors in a PWR	9
7	Typical locations of local power range neutron detectors in a BWR	10
8	Signal amplifier for a BWR neutron detector	11
9	Sequoyah 1 ex-core neutron noise spectrum on August 8, 1982	18
10	Coherence between ex-core neutron noise and core exit temperature noise at Sequoyah 1	20
11	Typical ex-core neutron noise signatures from six PWRs . .	21
12	Calvert Cliffs 1 ex-core neutron detector locations and their noise signatures on January 30, 1979	22
13	Calvert Cliffs 2 ex-core neutron detector locations and their noise signatures on January 30, 1979	23
14	Sequoyah 1 ex-core neutron detector locations and their noise signatures on April 7, 1981	24
15	Trojan ex-core neutron detector locations and their noise signatures on October 21, 1980	25

LIST OF FIGURES (Continued)

Figure		Page
16	H. B. Robinson 2 ex-core neutron detector locations and their noise signatures on December 5, 1979	26
17	ANO 1 ex-core neutron detector locations and their noise signatures on March 27, 1980	27
18	Shell and beam mode vibration of a PWR core barrel	29
19	Calvert Cliffs 1 coherence and phase between ex-core neutron detectors, January 30, 1979	30
20	Calvert Cliffs 2 coherence and phase between ex-core neutron detectors, January 30, 1979	31
21	Sequoyah 1 coherence and phase between ex-core neutron detectors, April 7, 1981	32
22	Trojan coherence and phase between ex-core neutron detectors, October 21, 1980	33
23	H. B. Robinson 2 coherence and phase between lower ex-core neutron detectors, December 5, 1979	34
24	H. B. Robinson 2 coherence and phase between upper ex-core neutron detectors, December 5, 1979	35
25	ANO 1 coherence and phase between ex-core neutron detectors, March 27, 1980	36
26	Calvert Cliffs 1 phased coherence between ex-core neutron detectors, January 30, 1979	37
27	Calvert Cliffs 2 phased coherence between ex-core neutron detectors, January 30, 1979	38
28	Sequoyah 1 phased coherence between lower ex-core neutron detectors, April 7, 1981	39
29	Trojan phased coherence between ex-core neutron detectors, October 21, 1980	40
30	H. B. Robinson 2 phased coherence between lower ex-core neutron detectors, December 5, 1979	41
31	H. B. Robinson 2 phased coherence between upper ex-core neutron detectors, December 5, 1979	42

LIST OF FIGURES (Continued)

Figure		Page
32	ANO 1 phased coherence between ex-core neutron detectors, March 27, 1980	43
33	Sequoyah 1 ex-core neutron noise spectrum at the start of the first and second fuel cycles and at the end of the first cycle	47
34	Long-term variation in the amplitude of resonances in the Sequoyah 1 ex-core neutron noise spectrum	49
35	Palisades ex-core neutron detector signal when the core barrel was loose. Most of the steady-state signal is biased out to illustrate the noise detail	51
36	Cause of abnormal core barrel motion in Palisades	52
37	Comparison of ex-core and in-core power spectra obtained at Palisades when the core barrel was loose	53
38	Phase shift between a Sequoyah 1 ex-core neutron signal and a core-exit thermocouple before and after correction for thermocouple response time	56
39	NPSDs for the APRM and the four detectors in LPRM string 08-33 (Browns Ferry 3 on January 17, 1977)	59
40	NPSDs for the APRM and the B-level detectors in four LPRM strings (Browns Ferry 3 on January 17, 1977)	60
41	NPSD of a typical APRM signal in a BWR at full power (Browns Ferry 3 on January 18, 1977)	60
42	Bypass flow which caused in-core instrument tubes to vibrate in BWR-4s	63
43	Flow dependence of NCPSD between C and D detectors when instrument tubes were vibrating	64
44	NCPSD between C and D detectors before and after plugging	65
45	Coherence between C and D detectors before and after plugging	66
46	Comparison of a typical impact signature (C and D NCPSD) before plugging with signatures from 31 strings after bypass cooling holes were plugged	67

LIST OF FIGURES (Continued)

Figure		Page
47	NCPSD between C and D detectors for a BWR-4 following tie plate modifications	68
48	BWR in-core neutron noise as a function of bypass flow	69
49	Core elevation where bypass coolant bulk boiling is predicted to occur	70
50	Phase versus frequency for A-B, B-C, and C-D detector pairs in LPRM string 20-37 at Hatch 1 on January 14, 1976	71
51	Steam velocity and void fraction as a function of the channel height Z	74
52	Comparison of Browns Ferry 3 NPSDs obtained by using Fast Fourier Transform (FFT) and by using the optimal autoregressive (AR) model	76
53	Impulse response obtained from the optimal AR model fit to the Browns Ferry 3 APRM signal	76

LIST OF ACRONYMS

APD	Amplitude probability density
APRM	Average power-range monitor
AR	Autoregressive
ASME	American Society of Mechanical Engineers
BWR	Boiling-water reactor
CPSD	Cross power spectral density
CSB	Core support barrel
DOE	Department of Energy
FFT	Fast Fourier transform
FM	Frequency modulated
LOFT	Loss-of-Fluid Test
LPRM	Local power-range monitor
LWR	Light-water reactor
NCPSD	Normalized cross power spectral density
NPSD	Normalized power spectral density
ORNL	Oak Ridge National Laboratory
PWR	Pressurized-water reactor
PSD	Power spectral density
RMS	Root mean square
TIP	Traversing in-core probe
USNRC	U.S. Nuclear Regulatory Commission

ACKNOWLEDGMENTS

The authors wish to express their appreciation to the nuclear plant staff members who contributed to this work, including the following: Jim Steelman of Calvert Cliffs; Tom Cogburn of ANO 1 and 2; Royce Maner and his staff of the Tennessee Valley Authority (Sequoyah 1); and the staffs at the Peach Bottom, Browns Ferry, and Hatch nuclear plants.

We also wish to thank Ray Saxe of North Carolina State University, and George Kosály and Bob Albrecht of the University of Washington for the acquisition and interpretation of neutron noise from H. B. Robinson 2 and Trojan respectively. Charlie Mayo of Science Applications, Incorporated contributed the section on amplitude probability analysis.

Lao Holland, of the Institute for Energy and Nuclear Studies, Sao Paulo, Brazil, provided a valuable analysis and interpretation of the ANO 1 and 2 data.

ORNL staff members who contributed to this research are Bill Sides (aquisition of ANO data), Cy Smith (acquisition of Calvert Cliffs and Sequoyah data), and Willie King, who contributed the section on errors in coherence measurements. Jim Mullens (ORNL) and Eduardo Machado (Institute for Energy and Nuclear Studies, Sao Paulo, Brazil) provided valuable input to the computer programs used to process and display the noise signatures.

The authors are also indebted to Lew Lewis, Lambros Lois, and Bill Farmer of the USNRC for their guidance and helpful suggestions throughout this study.

ABSTRACT

The value of neutron noise analysis for diagnosis of in-vessel anomalies in light-water reactors (LWRs) was assessed by: (1) analyzing ex-core neutron noise from seven pressurized-water reactors (PWRs) to determine the degree of similarity in the noise signatures and the sources of ex-core neutron noise; (2) measuring changes in ex-core neutron noise over an entire fuel cycle at a commerical PWR; (3) applying PWR neutron noise analysis to diagnose a loose core barrel, to infer in-core coolant velocity, and to infer fuel assembly motion; and (4) applying BWR neutron noise analysis to diagnose in-core instrument tube vibrations and bypass coolant boiling, to infer in-core two-phase flow velocity and void fraction, and to infer stability associated with reactivity feedback.

This report summarizes these assessments and provides guidance for the acquisition and analysis of neutron noise in LWRs.

1. INTRODUCTION

This report presents our experiences with and assessments of neutron noise analysis in commercial light water reactors (LWRs) and is intended as a guide for the U.S. Nuclear Regulatory Commission (USNRC) and its consultants when using neutron noise analysis to detect and diagnose anomalous conditions within the reactor pressure vessel during power operation. The data used to prepare this report were obtained by the Oak Ridge National Laboratory (ORNL) and its consultants under the sponsorship of the USNRC Offices of Nuclear Regulatory Research and Nuclear Reactor Regulation.

Neutron noise is defined as the fluctuations in the neutron flux around the mean (dc) level. Neutron noise analysis is an accepted tool for diagnosing unusual conditions in a reactor core, where because of limited space, high temperature, and radiation, it is impossible or impractical to install diagnostic instrumentation such as vibration, flow, or temperature sensors. Neutron noise analysis is performed without disturbing normal operations by using existing plant instrumentation such as power range flux monitors. Since this report does not cover the state of the art or history of neutron noise analysis, we refer the reader to work by Uhrig,[1] Williams,[2] Thie,[3] and Kosály,[4] or the proceedings of the periodic international meetings of reactor noise analysis,[5-7] all of which contain excellent descriptions of the development and application of neutron noise analysis for reactor diagnosis.

The USNRC and ORNL were prompted to embark upon this project by the growing use of neutron noise analysis by reactor manufacturers and plant operators for diagnosing abnormal conditions in LWRs. Also, ORNL noise analysts have utilized neutron noise to aid the USNRC in the investigation of abnormal core conditions such as a loose core support barrel (CSB) in a pressurized-water reactor[8] (PWR) and the impacting of instrument tubes against fuel channel boxes in boiling-water reactors[9] (BWRs). These applications of neutron noise analysis would have been enhanced if the noise analysts had had baseline data before the anomalies occurred and had known the sources of neutron noise. The USNRC therefore requested that ORNL obtain a representative sample of PWR and BWR neutron noise under normal full-power operating conditions, interpret the sources of noise where possible, and provide guidance on the use of neutron noise for diagnosis and assessment of possible future core anomalies.

2. THEORETICAL BASIS OF NEUTRON NOISE

Previous theoretical studies[10,11] using point kinetics showed that the power spectral densities (PSDs) of the neutron flux noise induced by reactivity perturbations are proportional to the square of the reactor power, provided that the noise caused by the ionization chamber detection process or inherent statistical fluctuations in the fission process (zero-power noise) is small. In the present work, perturbations in the reactor system such as structural vibrations or coolant boiling are modeled as fluctuating neutron sources (Langevin sources). The Langevin sources are therefore the result of the static (steady state) flux distribution acting on changes in material properties (density or composition) of the reactor. The neutron detector response to these perturbations is then determined by a first-order perturbation approximation to the space-dependent reactor kinetics equations.

The following assumptions are made:

a. inherent statistical fluctuations in the multiplication process are negligible,
b. the noise due to the detection process is negligible,
c. the amount of vibration or boiling is small, and does not vary with power. Therefore, first-order perturbation theory is valid (i.e., the static flux distribution or detector spatial sensitivity are not changed as a result of the perturbation and the reactor system behaves in a linear manner), and
d. the critical, static flux distribution at all locations is proportional to the reactor power (fission rate).

The Langevin source δS is then expressed as:

$$\delta S(r,E,\omega) = \delta\Sigma(r,E,\omega)\ \bar{\phi}(r,E)\ , \tag{1}$$

where $\bar{\phi}$ is the static critical flux and $\delta\Sigma$ is the change in the macroscopic cross section resulting from a perturbation at location r, neutron energy E, and fluctuating at frequency ω.[12-14]

The detector response δR due to the perturbation is

$$\delta R\ (r_d,\omega) = \langle\phi^+(r,E,\omega)\ \delta S(r,E,\omega)\rangle_{v_p}\ , \tag{2}$$

and, substituting Eq. 1, becomes

$$\delta R(r_d,\omega) = \langle\phi^+(r,E,\omega)\ \delta\Sigma(r,E,\omega)\ \bar{\phi}(r,E)\rangle_{v_p}\ , \tag{3}$$

where ϕ^+ is the space-, energy-, and frequency-dependent detector sensitivity to neutron sources (i.e., the neutron source-to-detector transfer function), $\langle\ \rangle_{v_p}$ is an integration over neutron energy and spatial volume of the perturbation v_p, and r_d is the detector location. The power spectral density of Eq. 3 is

$$PSD(r_d,\omega) = \rho\{[\langle\phi^+(r,E,\omega)\ \delta\Sigma(r,E,\omega)\ \bar{\phi}(r,E)\rangle_{v_p}]^2\} \tag{4}$$

where $\rho\{\ \}$ is the expectation operator.[15]

It can be seen from Eq. 4 that the PSD of the neutron noise is proportional to the square of the static flux $\bar{\phi}$ and therefore to the reactor power, provided that ϕ^+ and $\delta\Sigma$ remain constant (i.e., the detector spatial sensitivity and amplitudes of noise sources do not change). Normalizaton of the neutron noise PSD by dividing by the square of the mean (dc) detector signal removes the power dependence as shown in the comparison of two normalized power spectral densities (NPSDs) at 75 and 96% power levels (Fig. 1). Equation 4 also implies that both in-core (reactivity) and ex-core (shielding) perturbations yield power spectral densities that are proportional to the square of the power level.

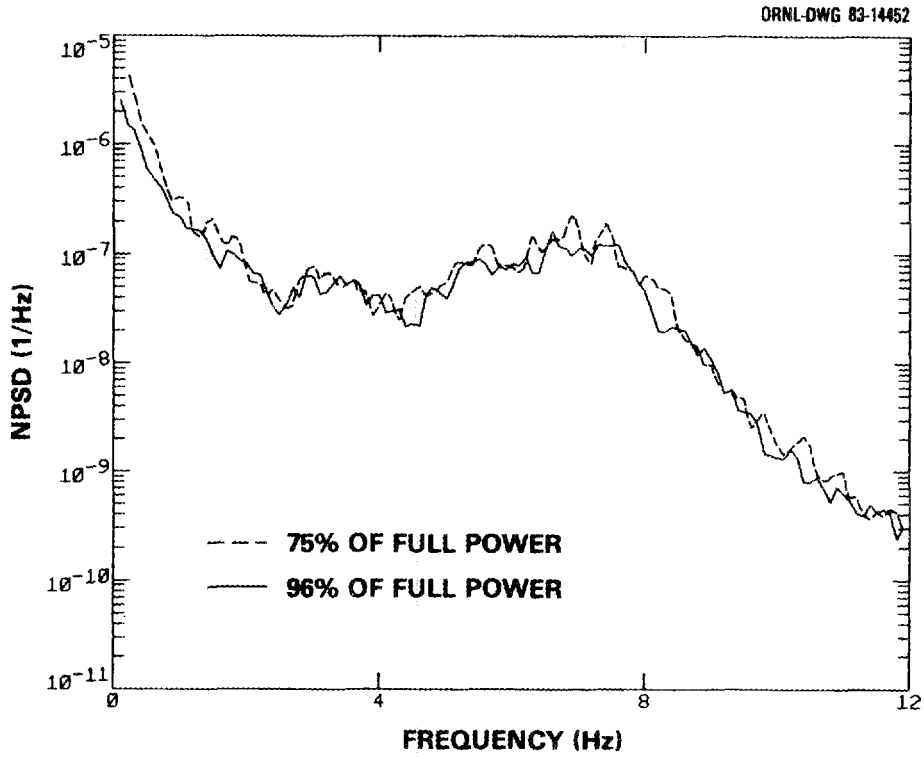

Fig. 1. Normalized power spectral density (NPSD) of ex-core neutron noise from a PWR at 75 and 96% of full power.

For multiple perturbations Eq. 4 becomes

$$\mathrm{PSD}\ (r_d,\omega) = \rho\{[\langle\phi^+(r,E,\omega_1)\ \delta\Sigma_1(r,E,\omega_1)\ \bar{\phi}(r,E)\rangle_{V_{p1}}]^2\}$$

$$+ \rho\{[\langle\phi^+(r,E,\omega_2)\ \delta\Sigma_2(r,E,\omega_2)\ \bar{\phi}(r,E)\rangle_{V_{p2}}]^2\} + \ldots \quad (5)$$

where $\delta\Sigma_i\ (r,E,\omega_i)$ $i = 1,2 \ldots N$ is a perturbation of type i occurring over the spatial volume V_{pi} with frequency ω_i. Equation 5 shows that multiple perturbations can be separated in the neutron noise, provided that the frequencies of the individual perturbations, ω_i, do not overlap and are statistically uncorrelated. Should the ω_i overlap it may be difficult to separate the effects of the individual perturbations in the neutron noise.

3. COMPARISON OF BWR AND PWR NEUTRON NOISE

Differences in the character of neutron noise in PWRs and BWRs can be traced to the basic design of the core internals and the principle of operation of the two systems, as well as the way in which neutron flux is measured in each type of plant. In PWRs the core is supported in a core barrel suspended from the vessel head in a cantilevered fashion, creating a vibratory system, whereas BWR cores are supported from the vessel bottom. PWR cores consist of open lattices of fuel rods, thus permitting the crossflow of coolant. Also, flow in a PWR is greater than in a BWR, thus providing stronger hydraulic forces to stimulate mechanical vibrations. In contrast, BWR fuel rods are contained in cans (called channel boxes) which confine the cooling flow within a given bundle of fuel rods. However, the major difference relative to neutron noise is that steam is produced in a BWR core, whereas PWRs have a negligible amount of boiling coolant in the core. Fluctuation and movement of steam voids are a major source of neutron flux perturbations and thus of neutron noise in BWRs. For this reason BWR neutron noise is generally of greater amplitude than PWR noise. Figure 2 illustrates this difference; note that the peak-to-peak noise (normalized to the dc level) is ~10% in a BWR in contrast to only 2% in a PWR. This difference is not due to the fact that BWR noise is measured with in-core detectors whereas PWR noise is generally measured with ex-core detectors (some PWRs don't have fixed in-core neutron detectors with a response time fast enough to measure neutron noise) but is in fact due to steam void formation, transport, and collapse in the BWR. Note that a noise signal can appear to have a completely different visual character, depending on the time over which it is viewed. Therefore, caution is advised when using strip chart recorders, oscilloscopes, or digital systems to view and analyze noise signals to draw conclusions regarding the amplitude or frequency content of the signals.

Another means of illustrating the differences in BWR and PWR neutron noise amplitude is the normalized amplitude probability densities (APDs) shown in Fig. 3. The APDs illustrate not only the difference in amplitude but also that the noise in both BWRs and PWRs is essentially Gaussian in nature, thus supporting the hypothesis that the amplitude of wideband (0-50 Hz) neutron noise is in general a random process (i.e., the amplitude of neutron noise cannot be predicted at any given time but must be analyzed by random signal analysis methods).

One such method (the one most commonly used) is power spectral density analysis as shown in Fig. 4.* The additional insight that this analysis provides is easily seen when compared to either the time traces of Fig. 2 or the APDs in Fig. 3. Here again the overall noise level is greater in BWRs, but spectral analysis shows that it does not have the resonant structure characteristic of PWR neutron noise.

---

*Note that the example of BWR in-core noise shown in Fig. 4 is from a detector near the top of the core. Section 8 will address in detail the spatial differences in in-core noise in BWRs.

ORNL–DWG 83-11482

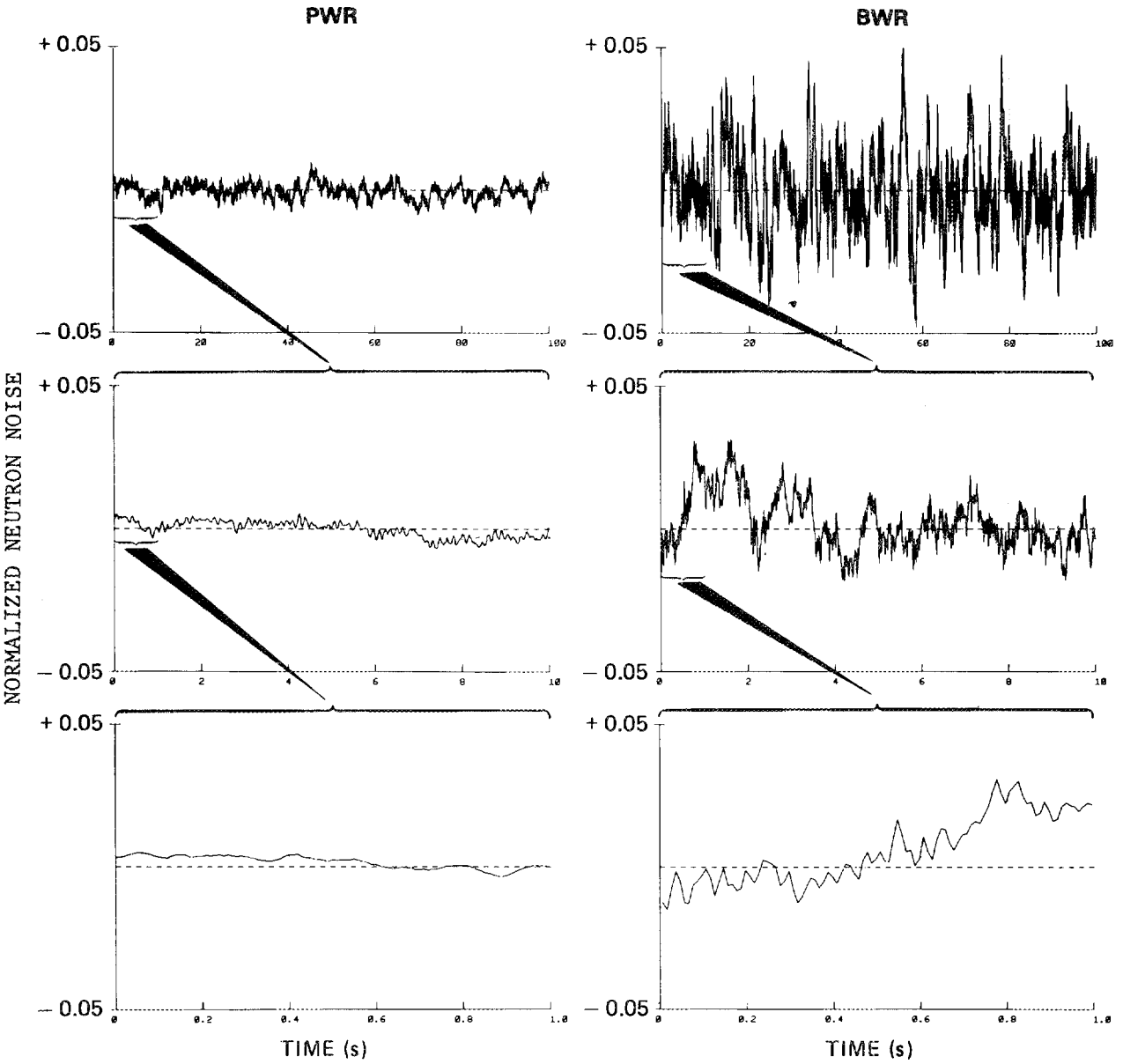

Fig. 2. Comparison of BWR and PWR neutron noise signals when normalized to the dc signal level (signals bandpassed 0.01–40 Hz and sampled at 100 samples per s).

In summary, the main points to keep in mind are that BWR neutron noise is generally of larger amplitude than PWR noise, and that PWR noise contains periodic components presumably related to internal vibration whereas BWR noise is caused mainly by core thermal-hydraulics and steam void fluctuations. More will be said about the causes of PWR and BWR neutron noise in Sect. 7 and 8.

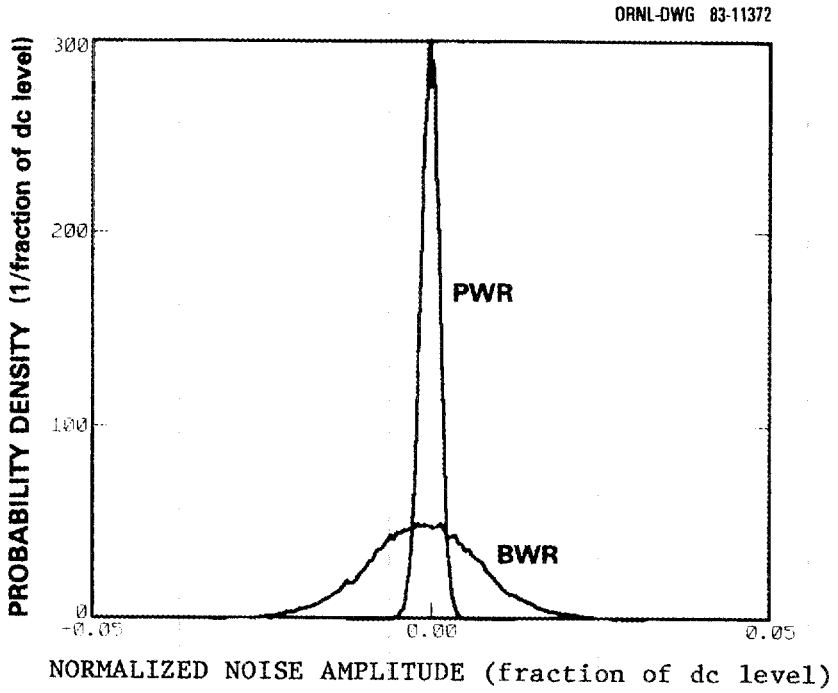

Fig. 3. Comparison of BWR and PWR neutron noise amplitude probability densities (APDs) when normalized to the dc signal level and the total number of samples (signals bandpassed 0.01-40 Hz and sampled at 100 samples per s for 2048 s).

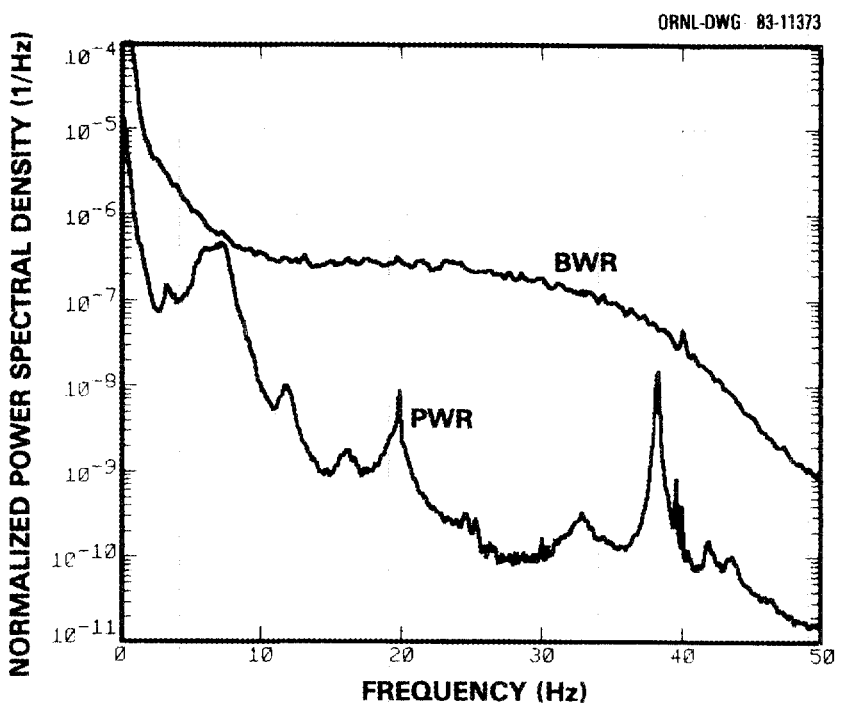

Fig. 4. Comparison of BWR and PWR neutron noise spectra when normalized to the square of the dc signal level.

4. ACQUISITION OF NEUTRON NOISE DATA

Neutron noise recordings in the ORNL library were obtained using the methodology shown in Fig. 5. Because the recordings were made over a period of ~8 years with a variety of equipment, no attempt will be made to describe each recording. However, some general comments can be made about the methods used to acquire the data.

Figure 6 shows the locations of the power-range neutron detectors used to monitor core power in a typical PWR. Power-range detectors used to obtain data for the ORNL noise library are located outside the core. The boron-coated ionization chambers extend approximately the full length of the core, with separate signals being available from the top and bottom halves of the detectors. Although most of the recordings in the ORNL library were obtained from the lower-half detectors, the upper-half signal and the total (sum of upper and lower) signal are also available and were recorded in some cases. Detectors are located at ~90° intervals around the core periphery. Some plants also have additional power-range detectors that are used as spares or for control of core power. These signals were also recorded in some cases.

Figure 7 shows the location of local power range monitor (LPRM) detectors in a typical BWR. Miniature fission detectors (1 in. long and 1/4 in. diam) are spaced 36 in. apart in in-core instrument tubes located in a bypass flow region at the junction of four fuel channel boxes. There are between 30 and 43 LPRM strings in a BWR, depending on core size. Individual LPRM signals from various radial and axial locations are summed to form the average power range monitor (APRM) signals used to monitor core power. The ORNL library contains recordings of both LPRM and APRM signals.

Personnel at the respective plants supplied ORNL representatives with flux signals which had been isolated from plant control and protection systems. In most cases ORNL did not obtain documentation or calibration data on plant equipment used to condition the signals. The absolute gain of the flux amplifiers and isolation circuits is not needed

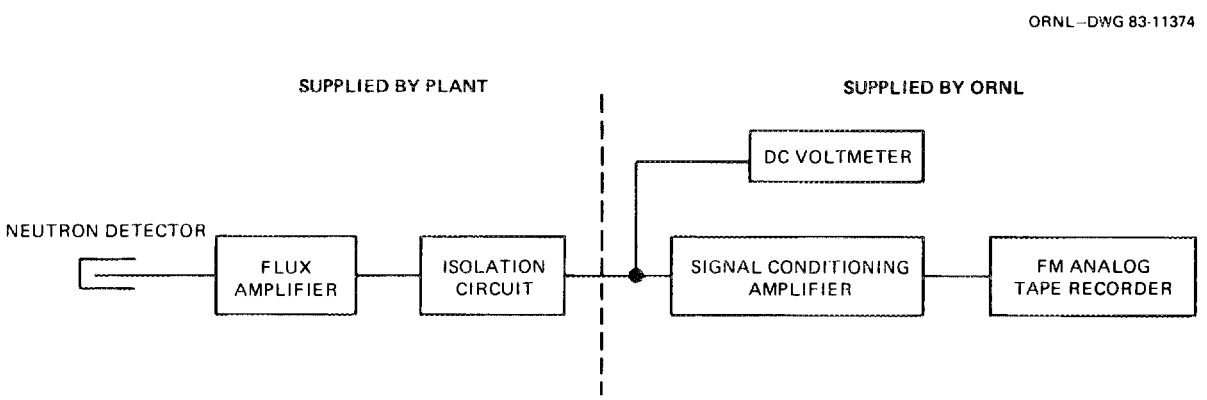

Fig. 5. Method of acquisition of neutron noise.

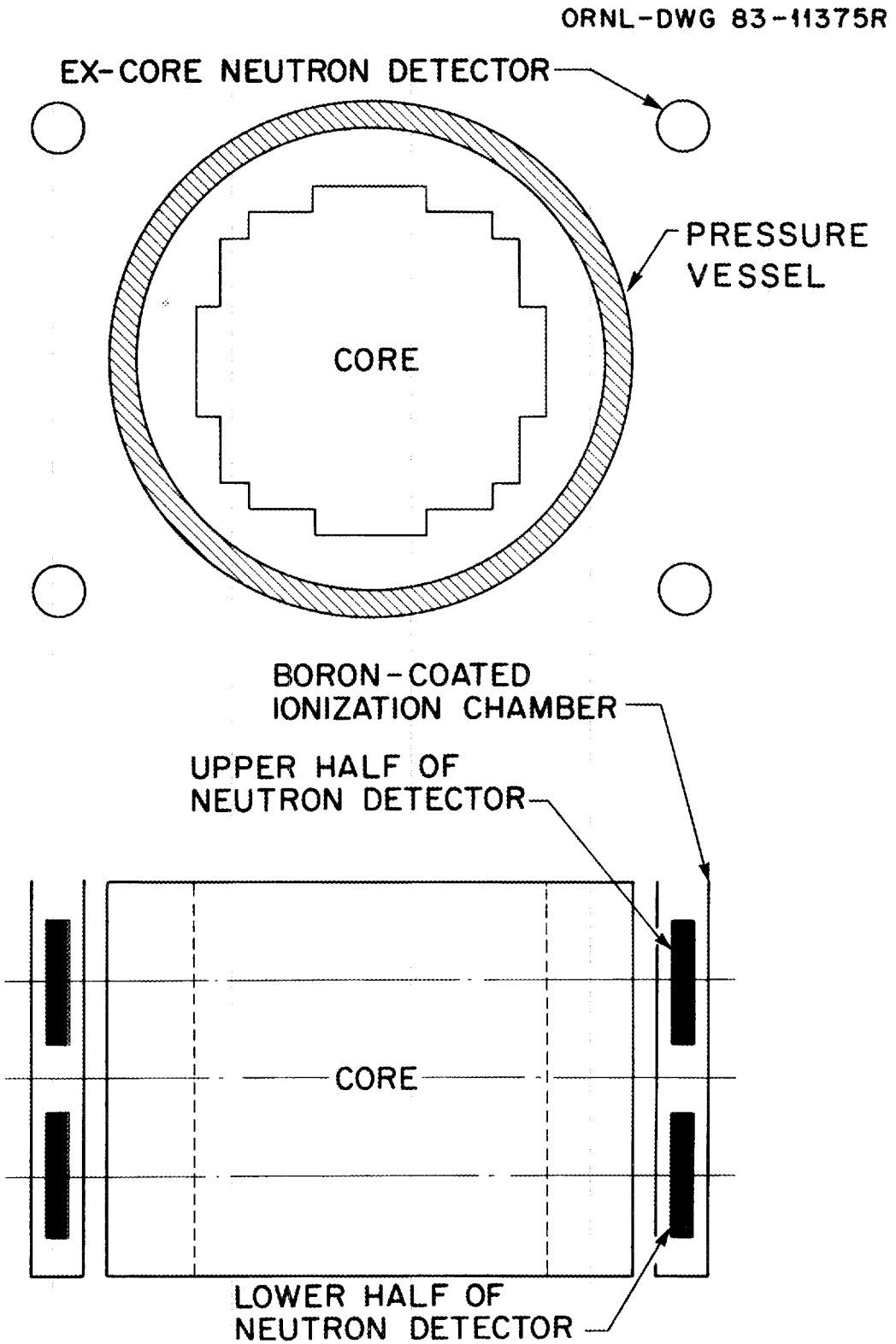

Fig. 6. Typical locations of ex-core power range neutron detectors in a PWR.

ORNL-DWG 83-11371

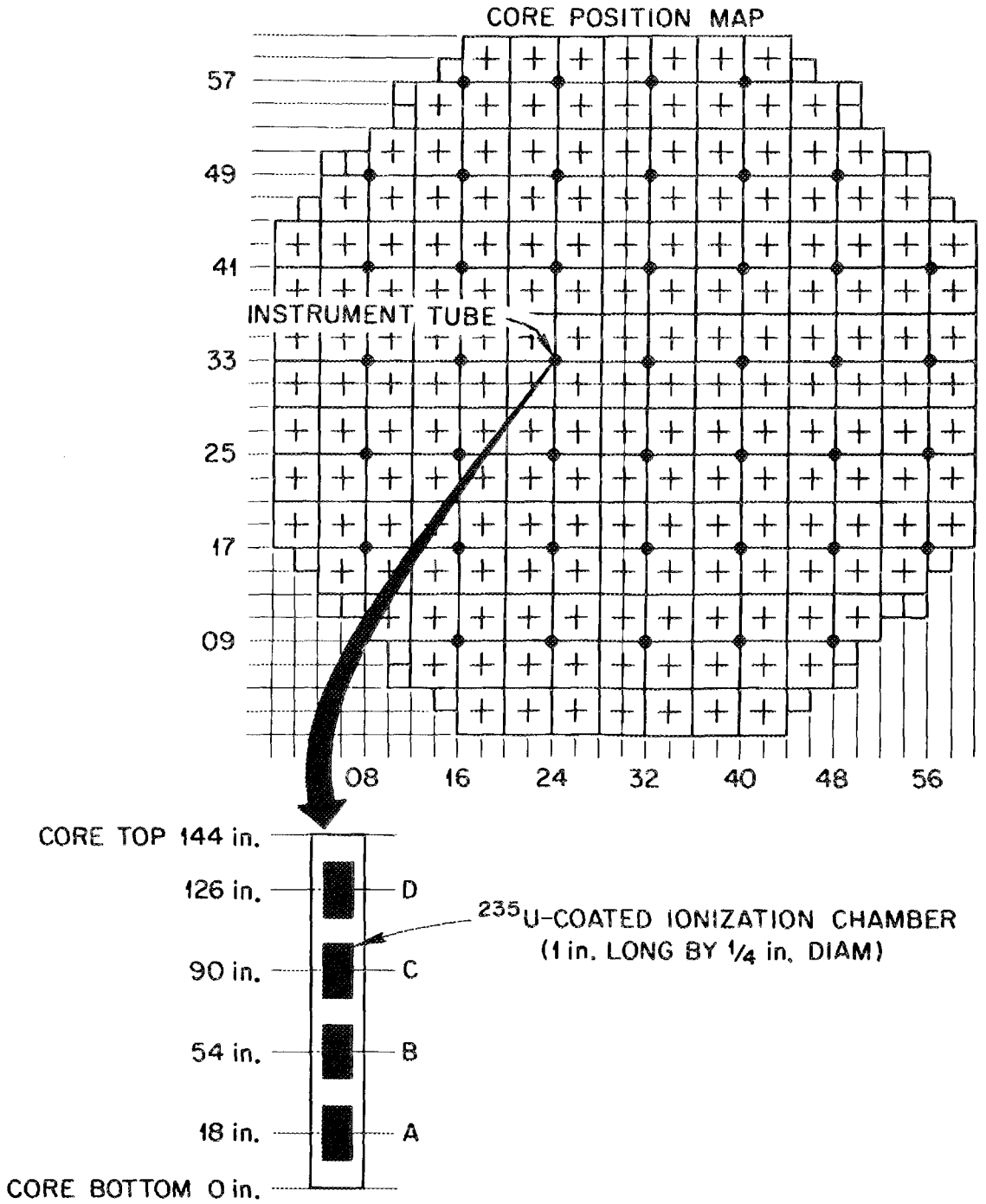

Fig. 7. Typical locations of local power range neutron detectors in a BWR.

because neutron noise is normalized to the dc level at the input to the signal conditioning amplifier before interpretation, which eliminates the effects of these gains (see Sect. 6.3).

However, some caution must be exercised in the interpretation of the flux signals because of a lack of knowledge about the frequency response of the plant-supplied instrumentation. For example, the flux amplifiers in BWRs have an adjustable gain to allow calibration and correction for burnup of the fissionable material in the detector. Figure 8 is the equivalent circuit for an LPRM amplifier, showing the selectable feedback resistance in parallel with a capacitor (C2). The amplifier frequency response (the frequency where the gain is -3dB compared to the dc gain) is given by:

$$f_B = \frac{1}{2\pi R_f C_2} \quad , \tag{6}$$

where R_f is the sum of the fixed resistor (R_1, R_2, or R_3) and the portion of variable resistance selected on R_4, R_5, or R_6, depending on the jumper position. The result is the higher the gain the lower the frequency bandwidth. (Table 1 lists the maximum and minimum frequency response on each gain range.) Theoretically, therefore, the bandpass of a BWR flux amplifier can vary from ~266 Hz for a new detector to ~3 Hz when the maximum gain setting is used as a result of burnup of the fissionable material in the detector. Although not specifically recorded for all

ORNL-DWG 83-12129

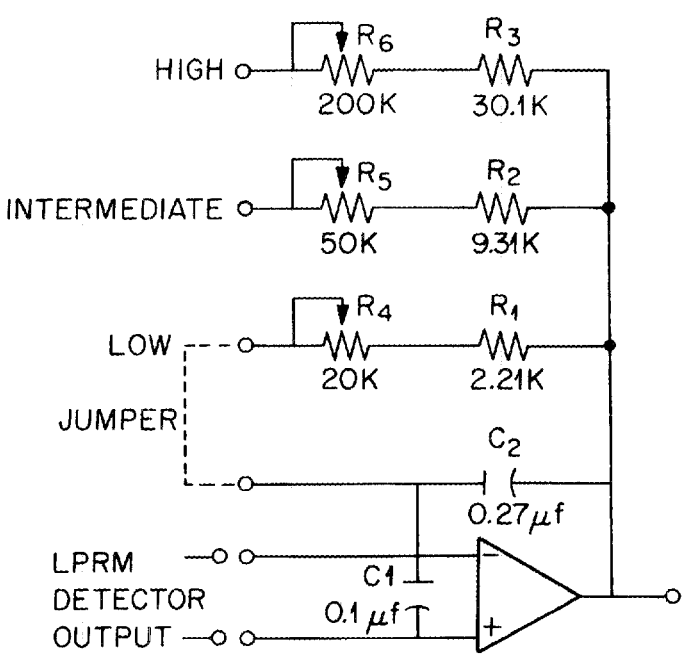

Fig. 8. Signal amplifier for a BWR neutron detector.

Table 1. Frequency response of LPRM amplifier

Gain range	f_B (Hz) Maximum	Minimum
Low	266	27
Intermediate	63	10
High	20	3

measurements, it is believed that most of the BWR data in the ORNL library were obtained with LPRM amplifiers set on the low gain range.

Because the amplitude dynamic range of analog tape recorders is limited, in order to obtain an optimum recording of the noise signal, the raw neutron signal was conditioned by eliminating the dc component with an ac-coupled amplifier, which also filtered the signal to the frequency range of interest (~100 Hz) and amplified the resulting signal to optimize the tape recording signal to noise. This was accomplished using Princeton Applied Research, Inc. Model 113 preamplifiers or comparable amplifiers with adjustable gain and bandwidth. The resulting signals recorded on tape have nominal levels of ±1.5 V and 0.01- to 100-Hz nominal bandwidth (actual bandwidths and amplifier gains vary between recordings but are recorded in the documentation of each measurement).

All tape-recorded signals in the ORNL neutron noise library were recorded on frequency-modulated (FM) magnetic tape. Because the data were recorded over a period of ~8 years, various recorders were used and the format included 1/4-, 1/2-, and 1-in.-wide tapes. All recordings are documented as to the recording speed (which determines the center frequency or frequency modulation) and tape format used in the measurement.

5. ORNL NEUTRON NOISE LIBRARY

Table 2 lists the 13 LWRs for which ORNL has obtained analog recordings of neutron noise. Note that in the case of PWRs we attempted to obtain data from a representative plant for each reactor supplier as well as from plants with different numbers of primary loops and pumps.

Most of the BWR data were obtained during ORNL's investigation of instrument tube vibrations in 1975 and 1976.[9] Therefore, much of the data were acquired under abnormal core conditions using existing plant instrumentation (more will be said about this later). However, data obtained under Department of Energy (DOE) funding during the startup of Browns Ferry 2 in 1974 and 1975 are included in the ORNL library but were not analyzed as part of this study.

Table 2. Plants included in ORNL neutron noise library*

Plant	Type	Reactor supplier	Number of primary pumps	Number of loops	Net MWe	Date of first commercial operation
Calvert Cliffs 1	PWR	C-E	4	2	850	5/75
Calvert Cliffs 2	PWR	C-E	4	2	850	4/77
ANO 1	PWR	B&W	4	2	836	12/74
ANO 2	PWR	C-E	2	2	858	3/80†
Trojan	PWR	W	4	4	1130	5/76
Sequoyah 1	PWR	W	4	4	1148	7/81
H. B. Robinson 2	PWR	W	3	3	665	3/71
Edwin I. Hatch 1	BWR 4	GE	–	–	786	12/75
Peach Bottom 2	BWR 4	GE	–	–	1065	7/74
Peach Bottom 3	BWR 4	GE	–	–	1065	12/74
Browns Ferry 1	BWR 4	GE	–	–	1067	8/74
Browns Ferry 2	BWR 4	GE	–	–	1067	3/75
Browns Ferry 3	BWR 4	GE	–	–	1067	3/77

*The information in this table was obtained from "World List of Nuclear Power Plants," *Nuclear News* (August 1981) and "Power Reactors '77," *Nuclear Engineering International—April 1977 supplement*, 22 No. 258 (April 1977).

†Data contaminated by electrical pickup.

Table 3 presents an overview of neutron noise recordings, including nominal plant power and flow at the time of data acquisition, date of noise recording, and type of neutron noise recorded (i.e., in-core, ex-core, etc.).

Table 3. Overview of neutron noise recordings in the ORNL library

Plant	Power level (% of full power)	Flow (% of full flow)	Dates of recording	Neutron signals recorded
Calvert Cliffs 1	100	100	1/30/79	Total signal from 6 ex-core detectors
Calvert Cliffs 2	100	100	1/30/79	Total signal from 4 ex-core detectors
ANO 1	100	100	3/27/80	Total signal from 4 ex-core detectors
ANO 2	100	100	3/27/80	Total signal from 3 ex-core detectors
Trojan	100	100	10/21/80	Total signal from 4 ex-core detectors
H. B. Robinson 2	100	100	12/5-6/79	Upper and lower signals from 4 ex-core detectors
Sequoyah 1	0, 3, 100	100	4/81-2/83	4 lower ex-core and 1-total signal
Hatch 1	50-80	37-80	5/75, 6/75 11/75, 1/76	LPRM,[a] TIP[b]
Peach Bottom 2	50-100	50-100	7/75	LPRM
Peach Bottom 3	50-100	50-100	5/75, 6/75	LPRM
Browns Ferry 1	100	100	1/77	LPRM
Browns Ferry 2	0-100	33-100	8-9/74, 2/75, 1/77	LPRM, TIP
Browns Ferry 3	100	100	1/77	LPRM, APRM[c]

[a] Local power-range monitor.

[b] Traversing in-core probe.

[c] Average power-range monitor.

The neutron noise recordings obtained in PWRs were mainly from ex-core detectors; therefore, PWR neutron noise referred to in this report generally means ex-core unless in-core is specifically stated. Conversely, BWRs in the U.S. do not have ex-core neutron detectors, and therefore neutron noise in BWRs is that measured with the in-core fission detectors.

For completeness the measurements made at ANO 2 are listed in Table 2, but the signals were so heavily contaminated with electrical noise pickup that the results are not included in this report.

Raw neutron noise signals are stored on FM magnetic tape together with recording logs containing documentation of the recordings. Where available, plant descriptions and plant computer logs (documenting the conditions at the time of the measurement) are filed with the tape logs.

Most plants were visited on only one or two occasions, thus the recordings represent only a "snapshot" of the neutron noise. However, in one plant (Sequoyah 1) neutron noise was monitored continuously over the first fuel cycle and over ~2 months of the second cycle using an on-line surveillance system.[16] The surveillance system monitored the PSD of four lower ex-core detectors and two average signals made up of the sum of upper and lower detectors (see Fig. 6). In addition, FM magnetic tape recordings were made at periodic intervals throughout the fuel cycle to allow more detailed analysis of the noise behavior. The Sequoyah 1 neutron noise measurements presented in this report were obtained from the periodic FM tape recordings acquired throughout the fuel cycle.

6. DATA REDUCTION AND ERROR ESTIMATION

6.1 REDUCTION OF NOISE RECORDINGS

The analog recordings of neutron noise were reduced to frequency spectra using digital computers and the fast Fourier transform (FFT) to compute the Fourier coefficients corresponding to the frequency range of interest (generally 0.1 to 50 Hz for LWR neutron noise). The Fourier coefficients were then used to compute the power spectral density (PSD) of individual signals and the cross power spectral density (CPSD), phase, and coherence of signal pairs. The reader should refer to Bendat[15] or Thie[3] for a more detailed explanation of frequency domain noise analysis.

With FFT data reduction, the noise analyst has control over the sampling rate (R--samples/s), the data block size (B--number of samples/block), and the number of data blocks (N) averaged in a given FFT analysis. Once these variables are selected, the analysis bandwidth is given by

$$f_{max} = R/2 \tag{7}$$

and the frequency resolution of each spectral estimate is

$$\Delta f = \frac{R}{B} \quad . \tag{8}$$

The statistical error (one standard deviation) associated with each estimate in a power spectrum, expressed as a percent of value, can be estimated as

$$E_S = \frac{100\%}{\sqrt{N}} \quad . \tag{9}$$

Since the coherence between two noise signals is often used to identify the sources of neutron noise, it is helpful to understand the uncertainties in a coherence measurement, which have both statistical and bias components as explained in the following section.

6.2 UNCERTAINTIES IN COHERENCE ESTIMATES

We have found[17] that the estimated coherence satisfies the empirical relation:

$$\hat{\gamma}^2 = \gamma^2 + \frac{(1 - \gamma^2)^2}{N} \quad , \tag{10}$$

where

γ^2 = the true coherence value,
$\hat{\gamma}^2$ = the estimated (measured) coherence value, and
N = the number of data blocks averaged in determining γ^2.

Also, the standard deviation of the measured coherence was found to satisfy the empirical relation:

$$\sigma_{\hat{\gamma}^2} = \frac{\hat{\gamma}^2(1 - \gamma^2)}{\sqrt{1 + N\gamma^2/2}} \quad . \tag{11}$$

Equation 11 also seems to be valid for all values of γ^2 so long as $N \geq 5$ (this covers most cases of practical significance). To be confident that the true coherence, γ^2 is >0, the estimated coherence, $\hat{\gamma}^2$, should be $>3/N$.

In summary, the majority of analyses presented in this report were performed with a minimum of 200 data blocks, which resulted in estimated errors of ±7% on NPSD estimates. Based on 200 data blocks, we considered any coherence value >0.015 (3/N) as being significant, i.e., indicative of a causal relationship between the two variables.

6.3 NORMALIZATION OF POWER SPECTRA

The theoretical basis of neutron noise (Sect. 2) shows that the PSD is proportional to the square of reactor power. It can also be shown[10] that the dc component of a neutron detector is proportional to the detection efficiency, detector sensitivity, and gain applied by the plant instrumentation. Therefore, it has become standard practice to normalize neutron noise PSD in volts^2/Hz by dividing by the square of the dc signal level (in volts), thus yielding NPSD in units of Hz^{-1}. All spectra presented in this report are normalized in this way.

7. PWR EX-CORE NEUTRON NOISE

7.1 OVERVIEW

Figure 9 shows an ex-core neutron noise spectrum of a PWR (Sequoyah 1) at full power. (Note that there are more apparent deviations in the NPSD estimates below ~0.07 Hz, which is due to the fact that only six data blocks were used in the low-frequency analysis: the six data blocks represented ~15 h of real-time data). The spectrum can be separated into three general regions: (1) low frequency (<0.01 Hz), (2) mid-frequency (0.01 to 1 Hz), and (3) high frequency (1 to 100 Hz), each of which has a different character. The following section discusses the probable sources of noise in these three regions.

7.2 SOURCES OF PWR EX-CORE NEUTRON NOISE

7.2.1 Low-Frequency Region

Low-frequency neutron noise in PWRs has not been extensively investigated because of the lengthy data records required to obtain reasonable statistical precision in the NPSD estimates. For example, if a frequency resolution of 10^{-4} Hz (as in Fig. 9) and a statistical precision of 10% is desired, Eqs. 8 and 9 imply that N = 100 blocks of data are required with a sample rate of ~0.1/s and a block size of 1024. To obtain 100

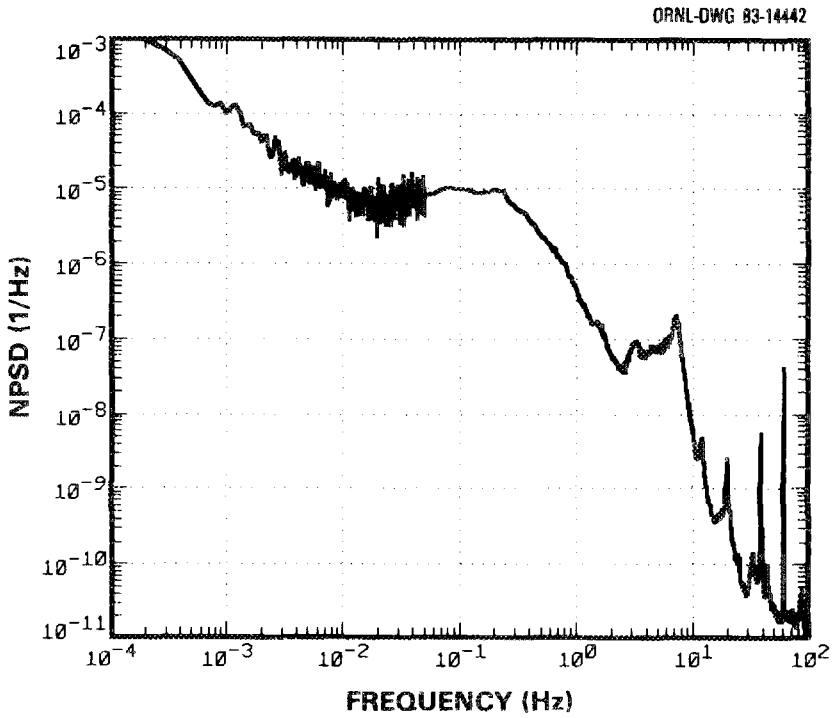

Fig. 9. Sequoyah 1 ex-core neutron noise spectrum on August 8, 1982.

blocks of such data would require sampling for 10^6 s or ~280 h. This is one reason why neutron noise is not routinely monitored at such low frequencies.

However, as part of the baseline studies, we obtained several lengthy data recordings at the Sequoyah 1 plant, and from them we can make several speculations about the sources of ex-core neutron noise at frequencies less than ~0.02 Hz. We observed that (1) the coherence between all ex-core detector signals is high, (2) the phase is ~0°, and (3) the ex-core signals are also highly coherent with most of the process signals, (i.e., steam flow, cold and hot leg temperatures, coolant flow, etc.). From this, we hypothesize that the low-frequency noise is caused by normal fluctuations in load demand and the resultant plant controller actions. Westinghouse plants have five control systems[18] -- reactor, pressurizer pressure, pressurizer level, steam dump, and feedwater -- all of which have responses on the order of 5 min. Thus they have the capability to generate fluctuations as high as 0.003 Hz in system variables. In fact, undesirable oscillations in steam and feedwater control systems were studied in the noise spectra of process variables in two PWRs.[19,20]

7.2.2 Mid-Frequency Region

Neutron noise in the frequency range between 0.01 and 1 Hz is caused in part by temperature fluctuations in the water both in the core and in the downcomer between the core and the detector. Figure 10 shows that the coherence between an ex-core neutron detector and a core exit thermocouple at Sequoyah 1 is significant in this frequency range. We therefore hypothesize that primary water temperature fluctuations in the core might be a source of neutron noise in this frequency range.

Others[21] have also concluded that a potential source of neutron noise in the 0- to 1-Hz range is coolant temperature fluctuation, which influences the neutron flux through the temperature reactivity coefficient. Also, Thie[22] suggested that temperature fluctuations in the downcomer water between the core and the ex-core neutron detector vary the attenuation of neutrons seen by the ex-core detector, thus inducing an additional noise. No doubt other sources such as flow fluctuations and perhaps pressure fluctuations contribute to neutron noise in the 0.01- to 1-Hz range, but not to the degree of temperature fluctuation.

7.2.3 High-Frequency Region

PWR neutron noise in the frequency range between 1 and 100 Hz has been studied extensively by a number of researchers. Noise analysts generally agree that the major sources of the resonances (see Fig. 9) in the spectrum of ex-core neutron noise in this frequency range are vibrations of the pressure vessel and the mechanical structures inside the vessel[23] including fuel elements, core support barrel, thermal shield, (when one is present), and control rods. (Neutron noise caused by control rod vibration is rare.) The region between 1 and 10 Hz is dominated by fuel- and core barrel-induced noise, and the region between 10 and 25

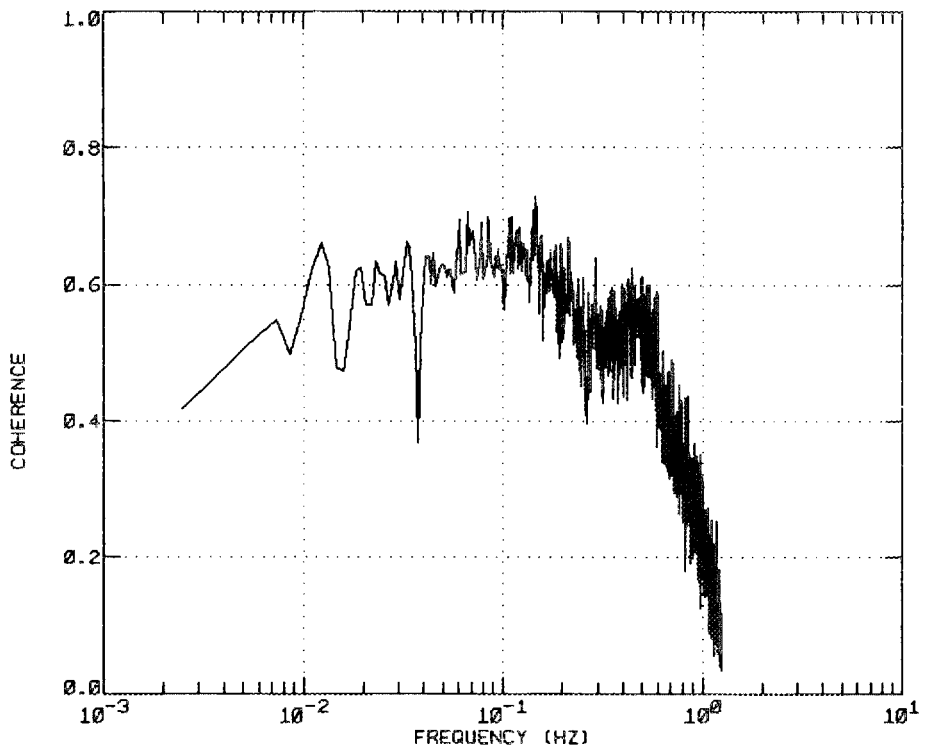

Fig. 10. Coherence between ex-core neutron noise and core exit temperature noise at Sequoyah 1.

Hz is influenced by thermal shield, pressure vessel, and higher order modes of the fuel and core barrel. Sources of noise greater than 25 Hz are not as well understood, but we have some knowledge of potential sources which will be described below.

Figure 11 shows an overall view (on a linear frequency scale) of the neutron noise signatures ORNL has obtained from six PWRs. Several observations can be made based on this overview of high-frequency PWR neutron noise. The signatures are similar in at least two ways: (1) the overall noise level has a magnitude of about 10^{-7} at low frequency, and by 50 Hz it decreases by ~4 orders of magnitude (to date noise analysts have not reported many useful applications of at-power neutron noise at frequencies greater than 50 Hz, other than possibly surveillance of the neutron detectors themselves[24,25] or wide-range measurement of power level[26]); and (2) the resonant structures are similar, particularly in the 0-25 Hz range. (More will be said about these resonances in the next section.)

There are also some notable differences in the signatures at frequencies greater than 20 Hz: (1) Trojan noise is lower in amplitude than other plants; and (2) both of the other Westinghouse (W) plants (H. B. Robinson 2 and Sequoyah 1), seem to have considerably more resonant structure. We have no explanation for the former, but the latter might be explained if the frequency response of the flux amplifiers is better in W plants. (Trojan is a W plant, but the neutron noise signals

ORNL--DWG 83-11475

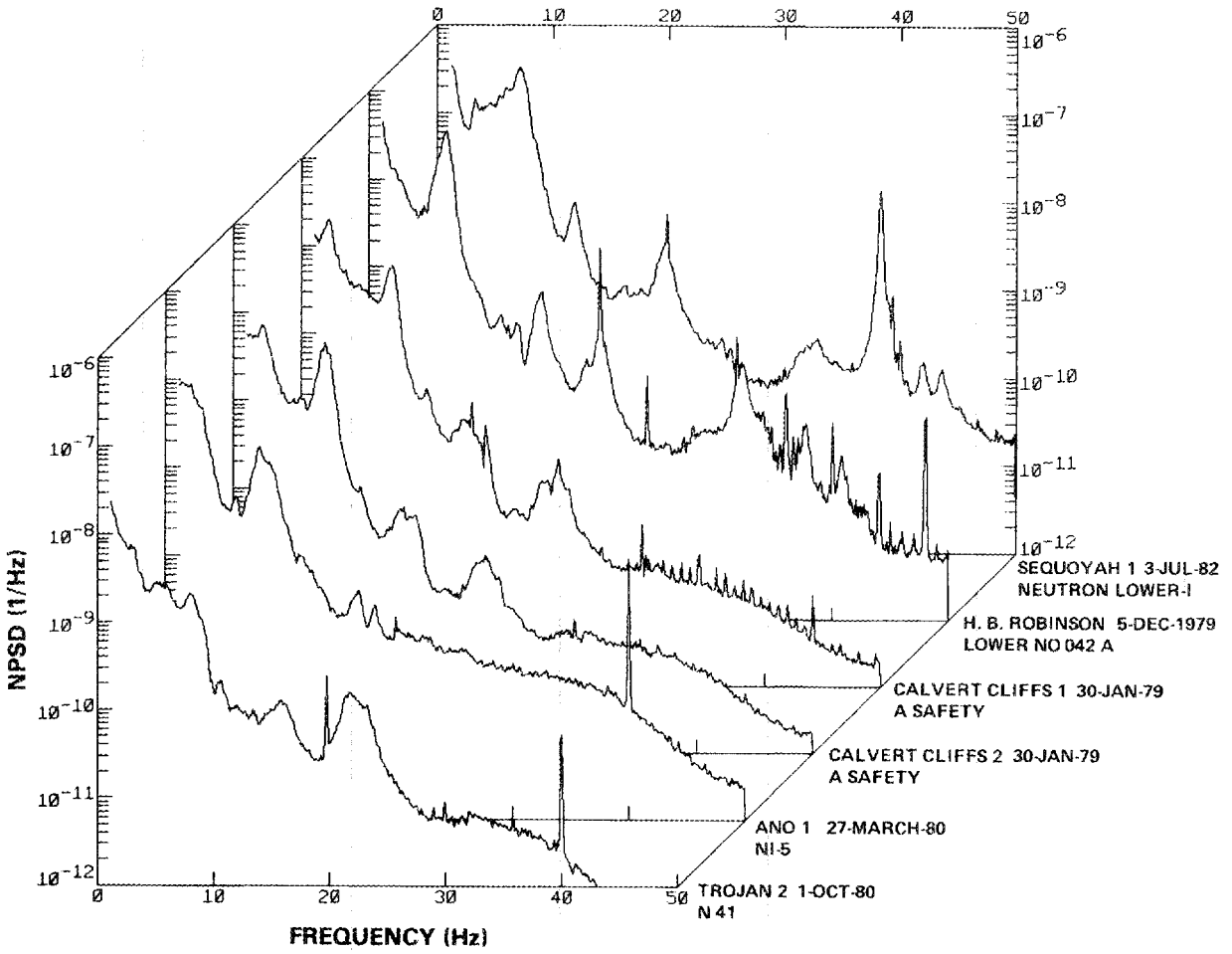

Fig. 11. Typical ex-core neutron noise signatures from six PWRs.

were obtained at the output of the vibration and loose part monitoring system signal conditioning amplifiers.) In general, noise analysts tend to discount resonances that are related to electrical line frequency or extraneous noise contamination (i.e., 40 Hz at Trojan is caused by 60 Hz aliased with respect to the 50-Hz Nyquist frequency and the small resonances between 30 and 50 Hz in Calvert Cliffs 1 which are characteristic of noise caused by a plant data logging system).

As stated previously, most PWRs have at least four ex-core neutron detectors, and in general all ex-core detectors in a plant have very similar signatures. In the next section we will demonstrate how one can utilize the relationship between the noise signals from the detectors to infer the type (mode) of vibration associated with the resonances in the signatures shown in Fig. 11.

Figures 12 to 17 show the location of ex-core neutron detectors and NPSDs for each of the six plants (detector C at Calvert Cliffs 2 was

ORNL-DWG 83-14441

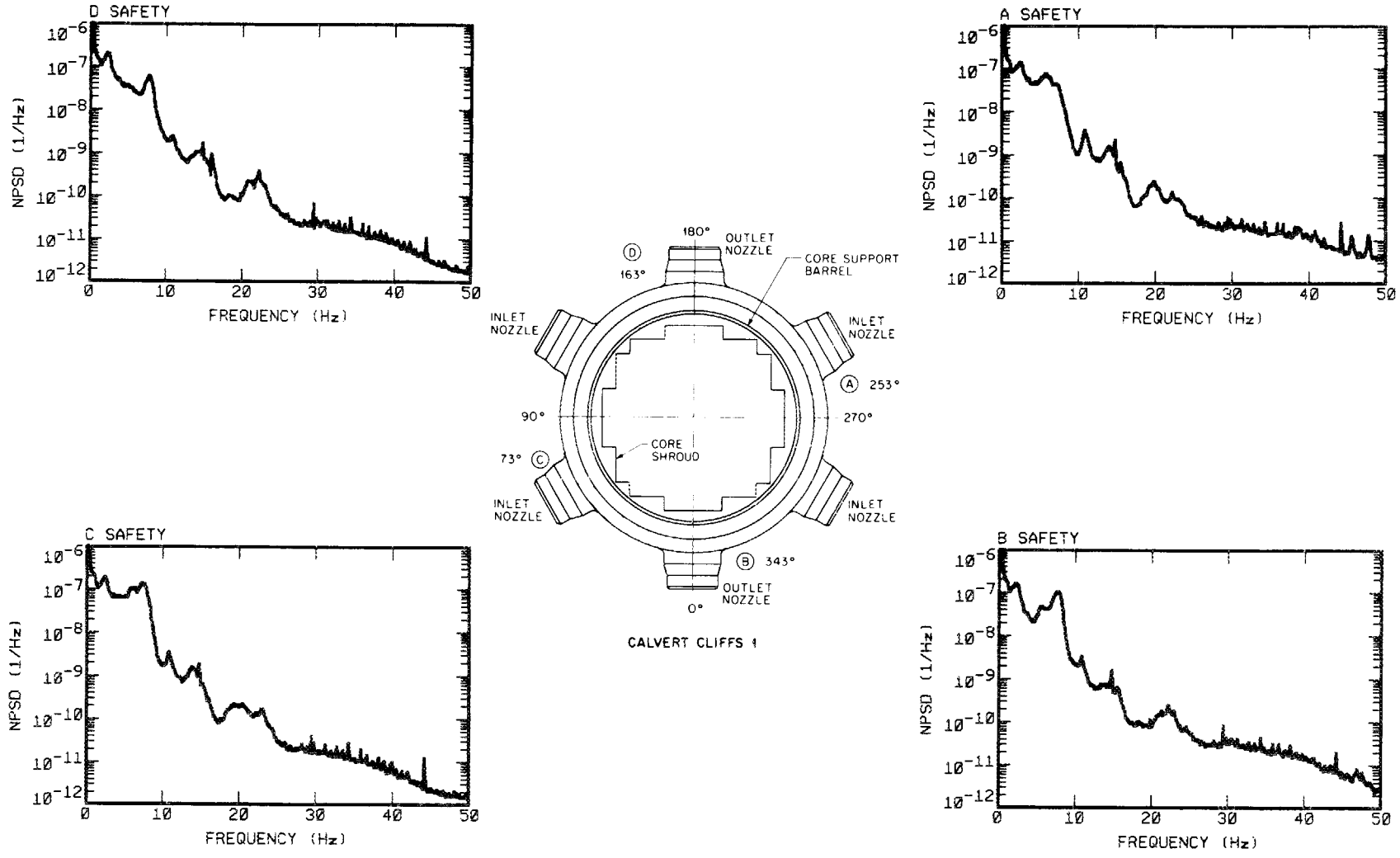

Fig. 12. Calvert Cliffs 1 ex-core neutron detector locations and their noise signatures on January 30, 1979.

ORNL-DWG 83-14440

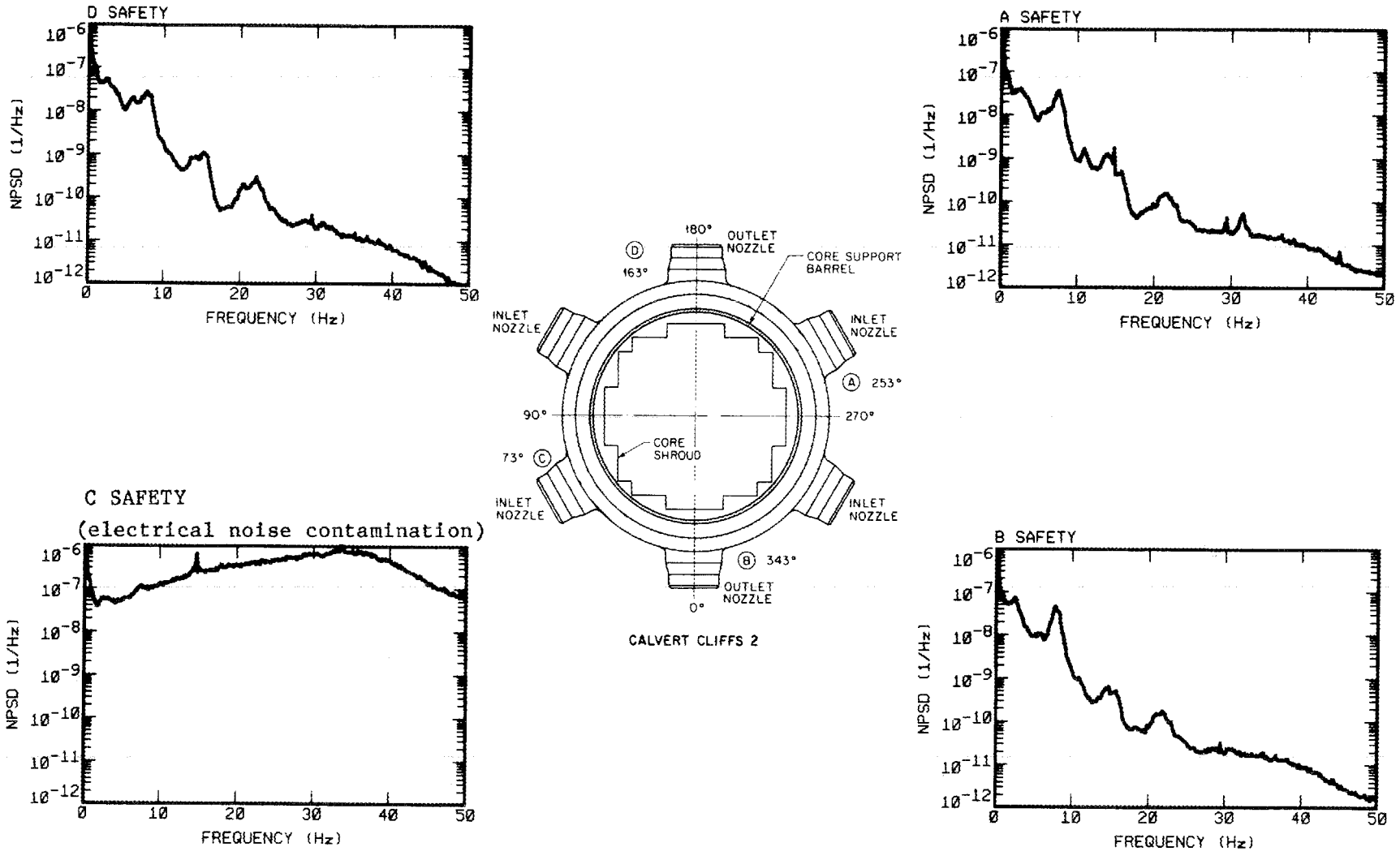

Fig. 13. Calvert Cliffs 2 ex-core neutron detector locations and their noise signatures on January 30, 1979.

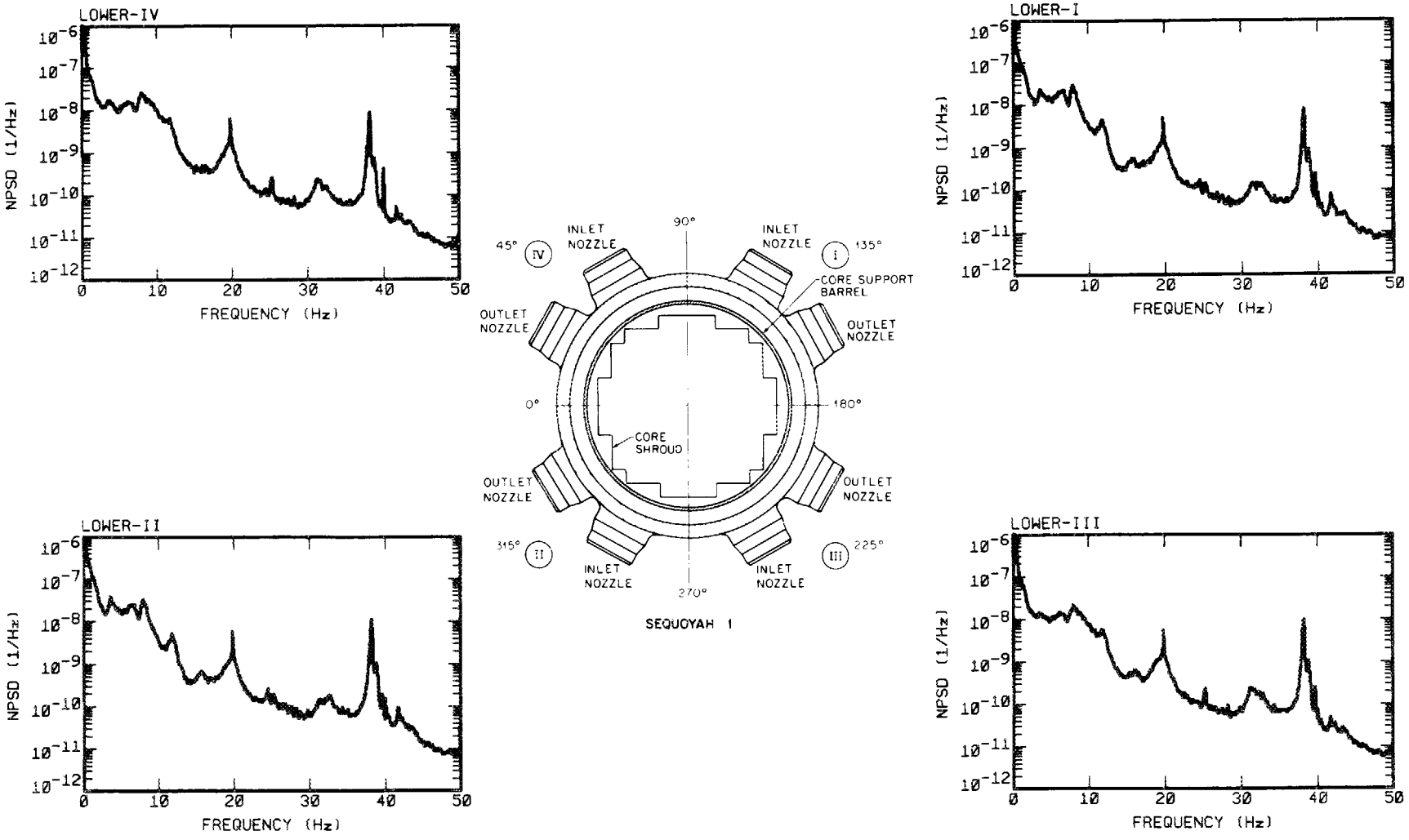

Fig. 14. Sequoyah 1 ex-core neutron detector locations and their noise signatures on April 7, 1981.

ORNL-DWG 83-14438

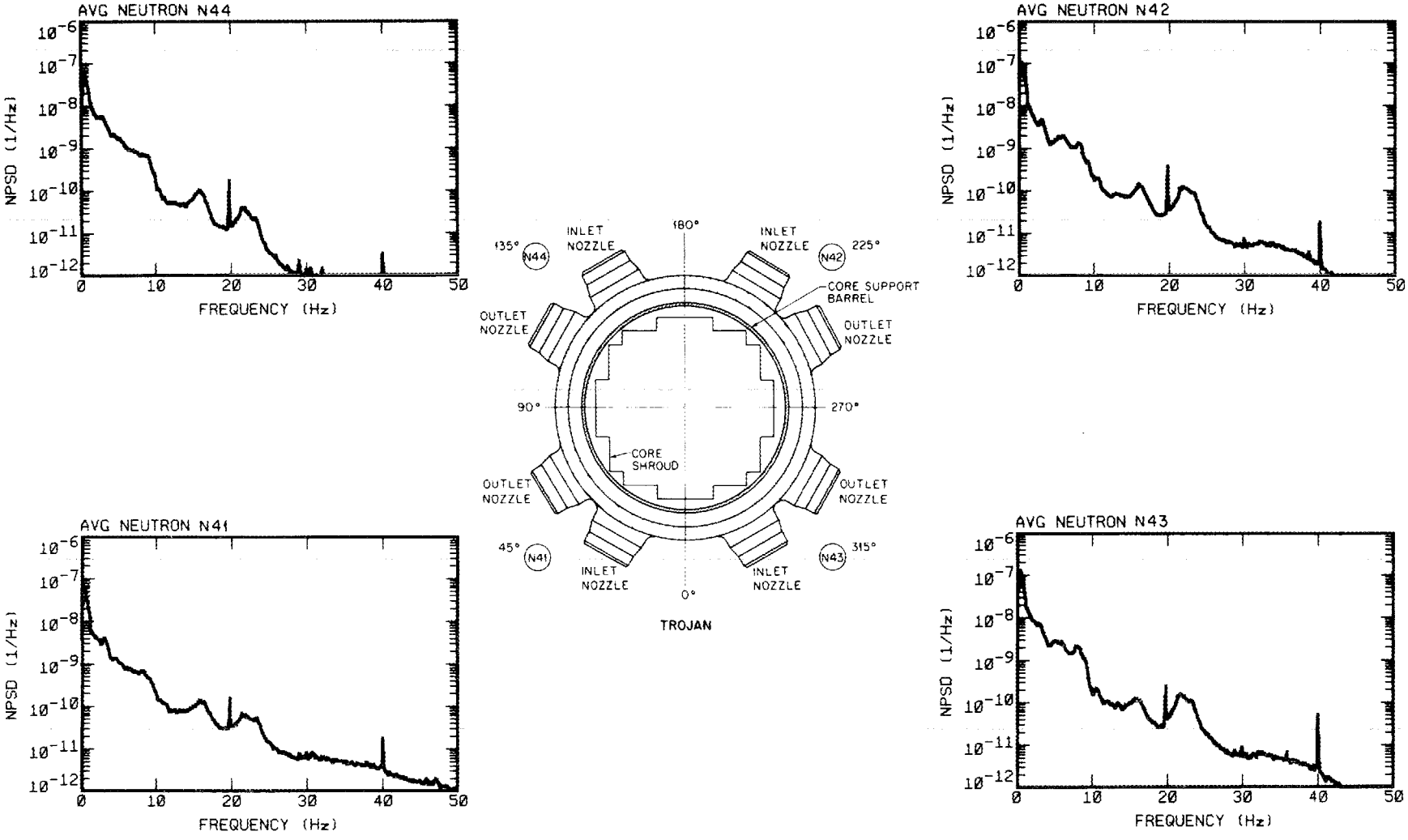

Fig. 15. Trojan ex-core neutron detector locations and their noise signatures on October 21, 1980.

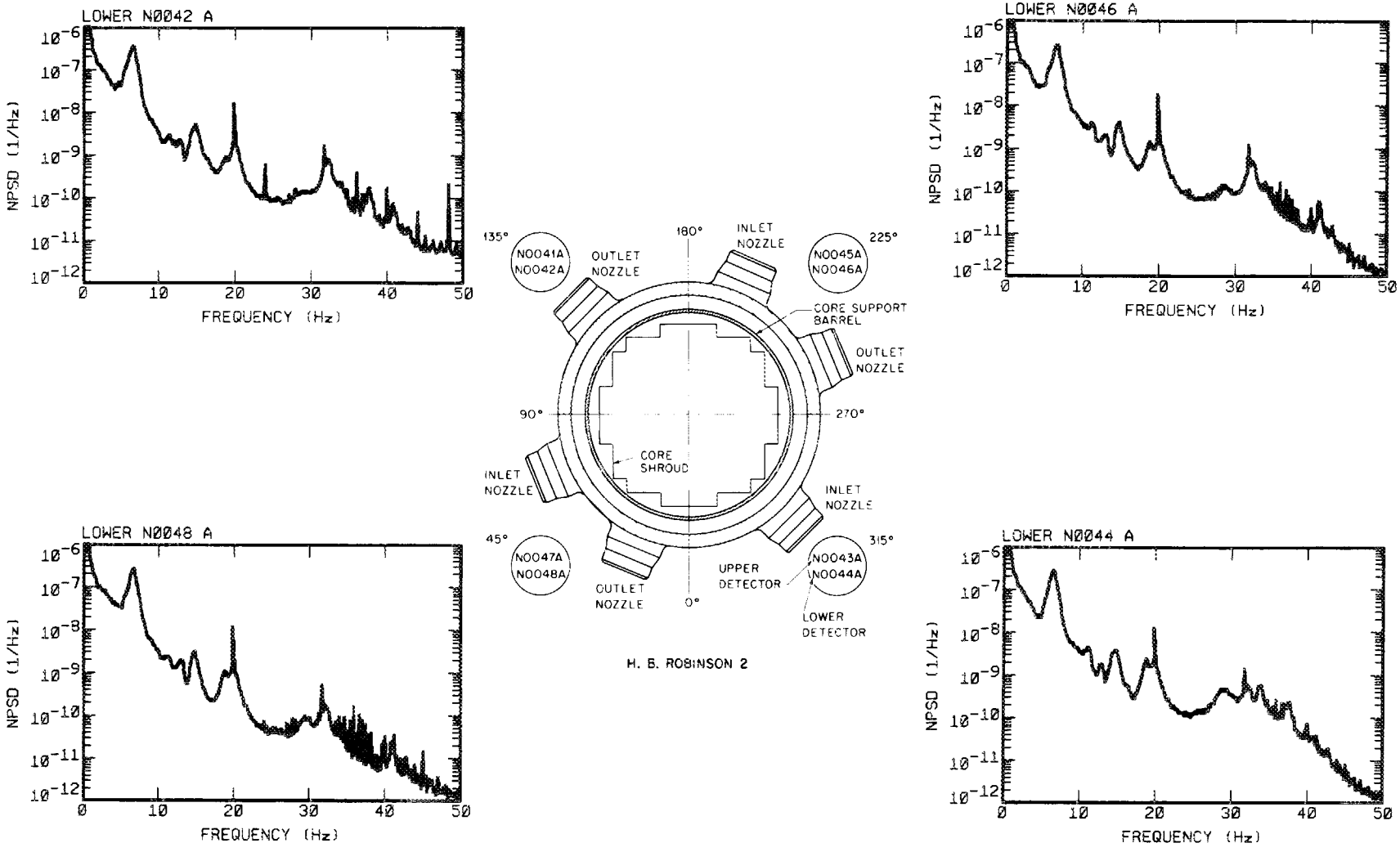

Fig. 16. H. B. Robinson 2 ex-core neutron detector locations and their noise signatures on December 5, 1979.

ORNL-DWG 83-14443

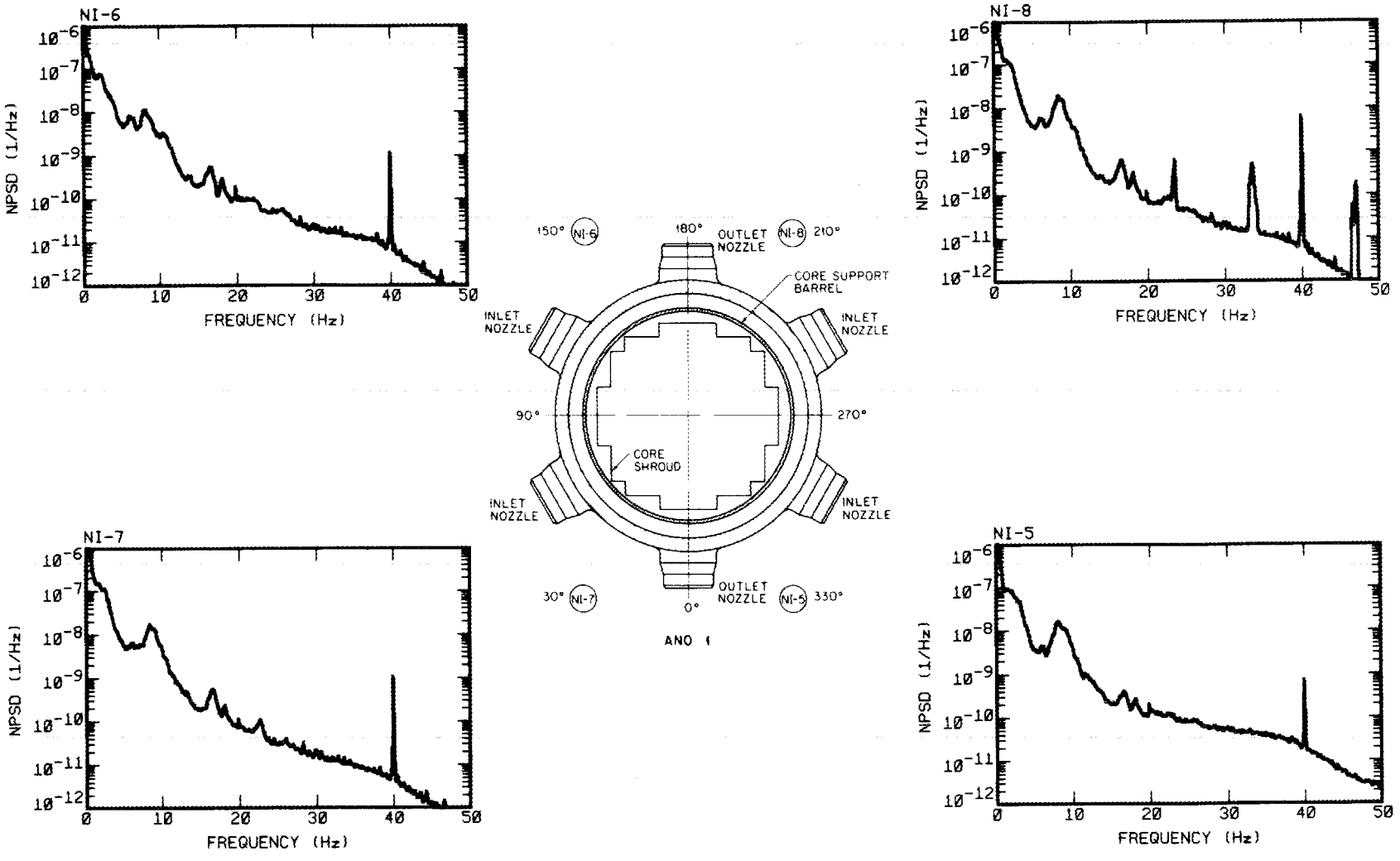

Fig. 17. ANO 1 ex-core neutron detector locations and their noise signatures on March 27, 1980.

contaminated with electrical noise when recordings where made). Note that the ex-core detectors are placed at 90° intervals around the core (except at ANO 1, where they are at 60 or 120° intervals). The fact that the detectors are spaced in this way aids the interpretation of the type of vibration as to shell mode or beam mode (see Fig. 18). For example, in the case of rigid body beam mode vibration of the core support barrel (CSB), the core (source of neutrons) moves closer to two detectors while it simultaneously moves away from the opposite two detectors. Therefore, the phase between detectors on opposite sides of the core will be ~180°, while signals from detectors at 90° can be either in phase or out of phase, depending on the preferred direction of motion. On the other hand, shell mode vibration of the CSB results in a 0° phase between opposite detectors and a 180° phase between adjacent detectors. This is an oversimplification of the complex vibrations of reactor internals, but it is presented here to introduce the reader to the methodology used by neutron noise analysts and to provide a basis for the interpretation of the baseline data in the ORNL neutron noise library.

Figures 19 to 25 show the coherence and phase relationship between ex-core detectors in each of the six plants. (The phase, of course, has no meaning if there is negligible coherence between the signals.) The phase is indeed either 0 or 180° as postulated above. A classic example is the Sequoyah 1 results of Fig. 21, which were obtained early in the first fuel cycle.

This ideal behavior of the phase has been used by noise analysts[24,27,28] to automate the separation of vibration modes by manipulating the raw time traces or frequency spectra, assuming that only a 0 or 180° phase is possible. We conclude that this type of analysis can aid the identification of neutron noise sources, but it is not a substitute for a complete cross-spectral analysis (as shown in Figs. 19 to 25), and in some cases it can be misleading if the phase is not 0 or 180° (as seen in Fig. 19) or if incoherent noise sources are present.

We have, however, implemented a visual aid to help in identifying shell and beam mode vibrations as well as in-phase noise components that might indicate reactivity type noise sources. This function is called the "phased coherence" and is based on a method suggested by Dragt.[29] Phased coherence as we define it is simply the actual coherence (which is always a positive value) to which is appended a positive or negative sign, according to whether the phase is between +90 and -90° or between -90 and -270° respectively.

The phased coherence between ex-core detectors in the six PWRs is shown in Figs. 26 through 32. (The estimated confidence limits on the coherence are shown as lines on either side of zero.) Note that in the case of Sequoyah 1 the cross-core detectors are out of phase between ~2 and 10 Hz, indicating beam mode vibration, whereas the cross-core detectors are in phase at 20 Hz and the adjacent detectors are out of phase, which identifies an N = 2 shell mode vibration. Also note the in-phase component at ~25 Hz. The results of our analysis of all plants are summarized in Table 4. Figures 19 through 25 were used to identify the

ORNL-DWG 83-12846

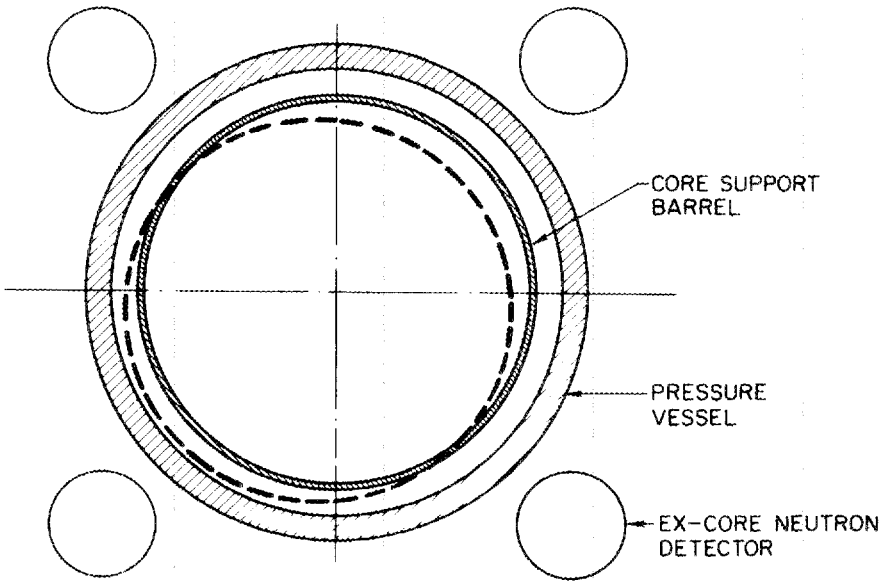

(*a*) BEAM MODE VIBRATION

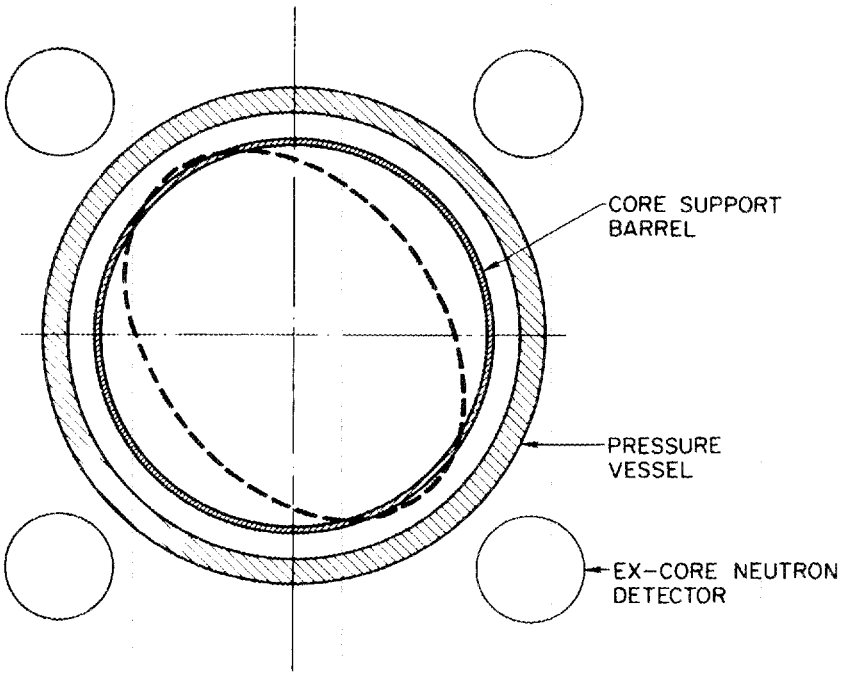

(*b*) SHELL MODE VIBRATION

Fig. 18. Shell and beam mode vibration of a PWR core barrel.

ORNL-DWG 83-14444

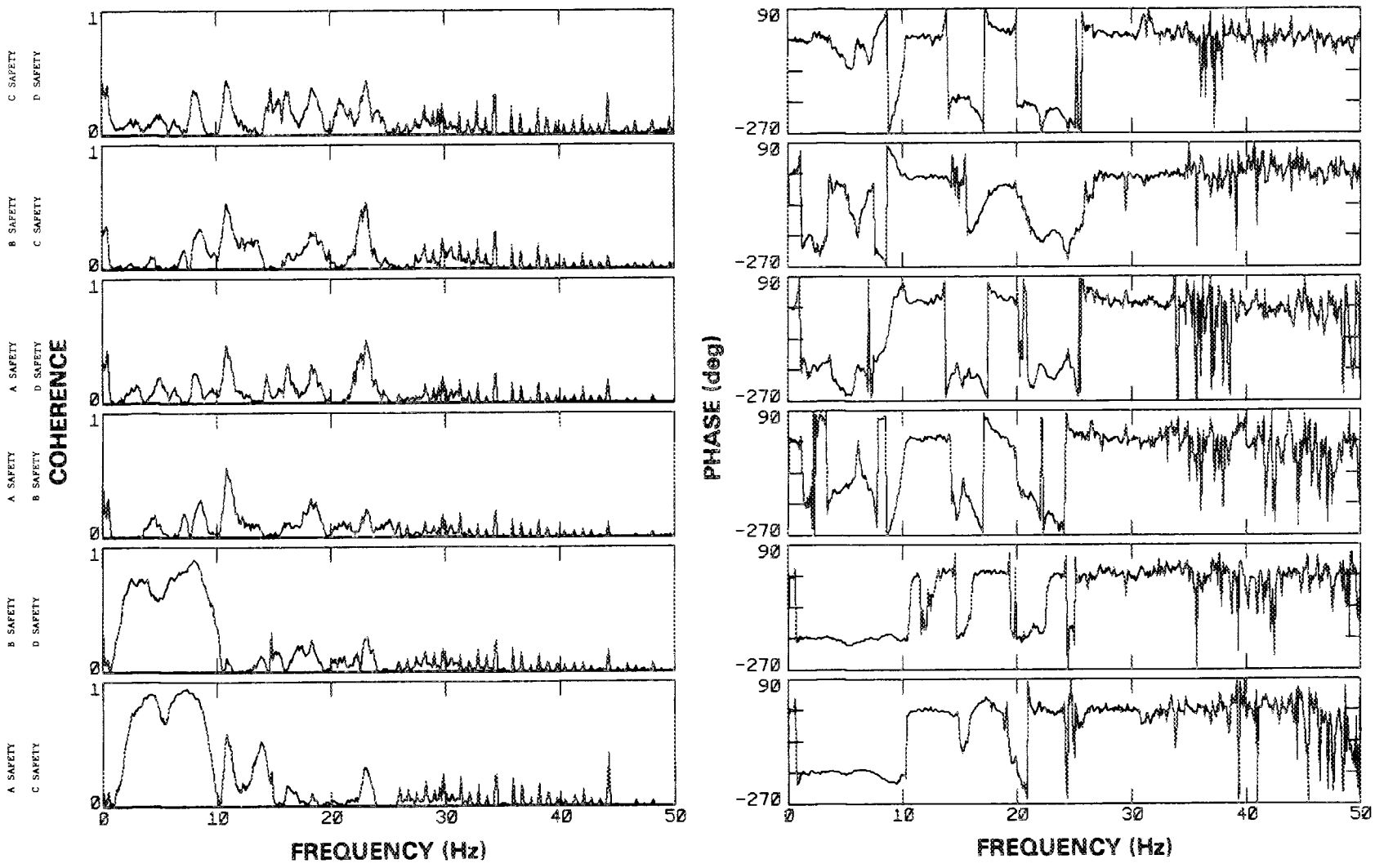

(a) COHERENCE (b) PHASE

Fig. 19. Calvert Cliffs 1 coherence and phase between ex-core neutron detectors, January 30, 1979.

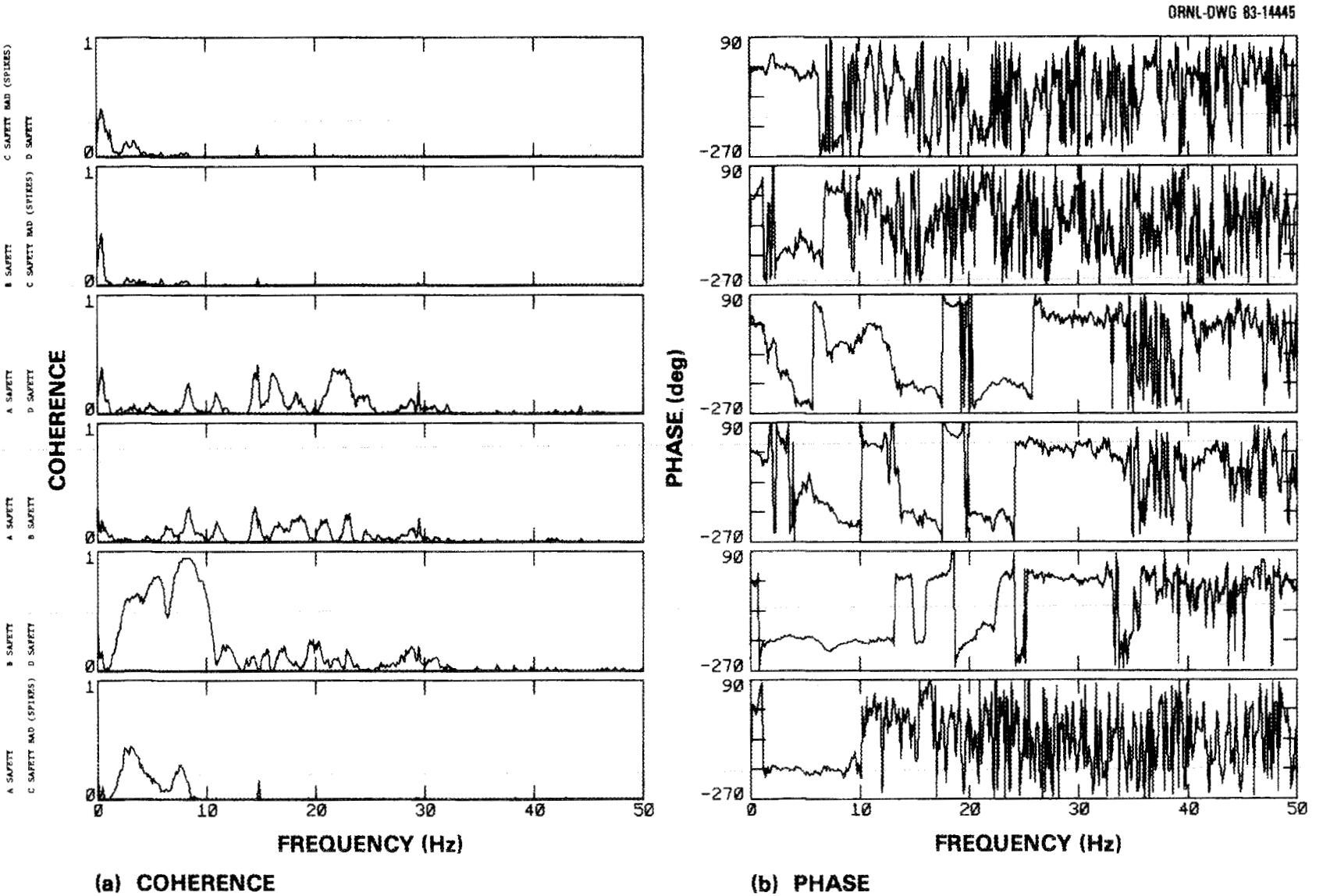

(a) COHERENCE (b) PHASE

Fig. 20. Calvert Cliffs 2 coherence and phase between ex-core neutron detectors, January 30, 1979.

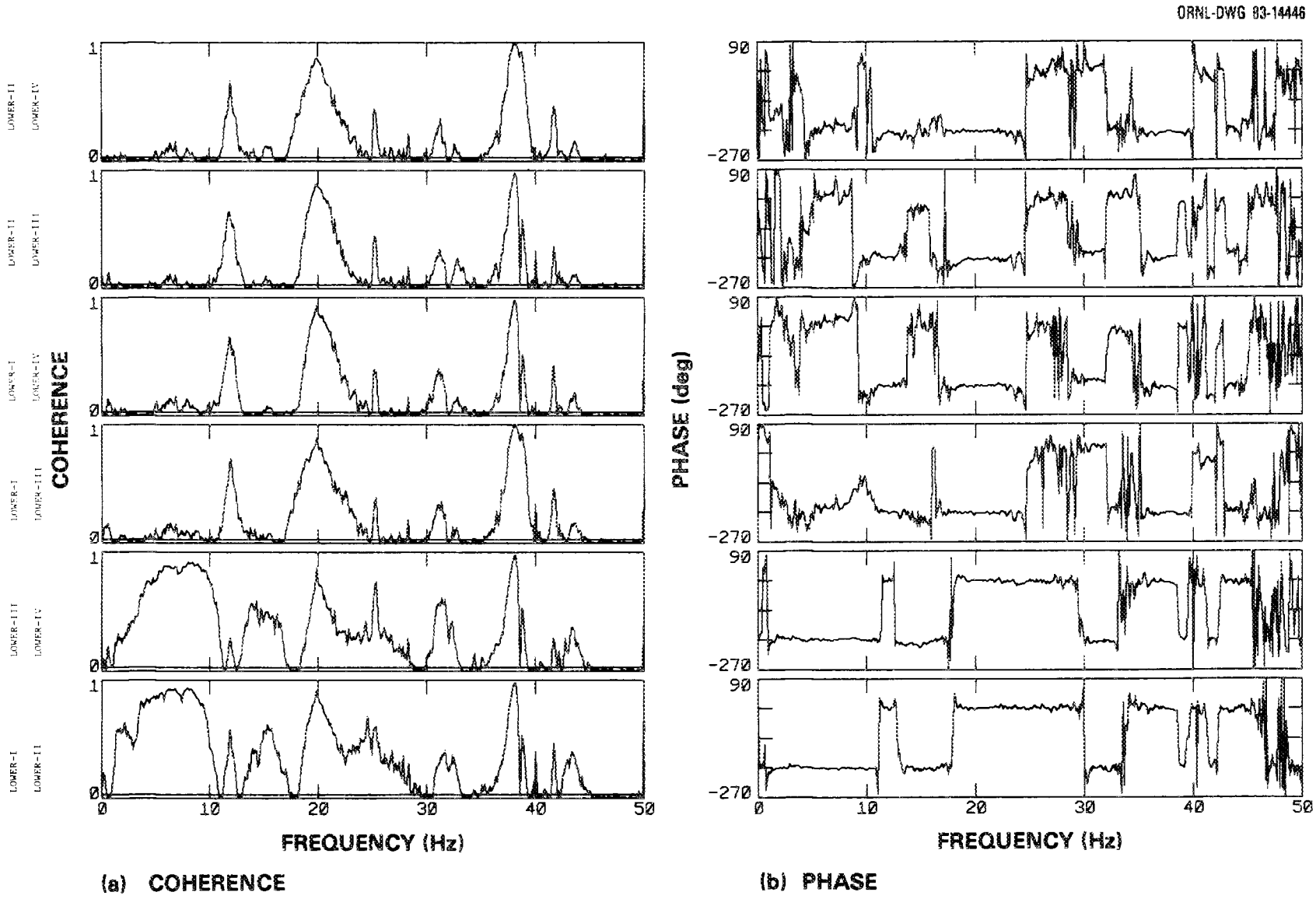

Fig. 21. Sequoyah 1 coherence and phase between ex-core neutron detectors, April 7, 1981.

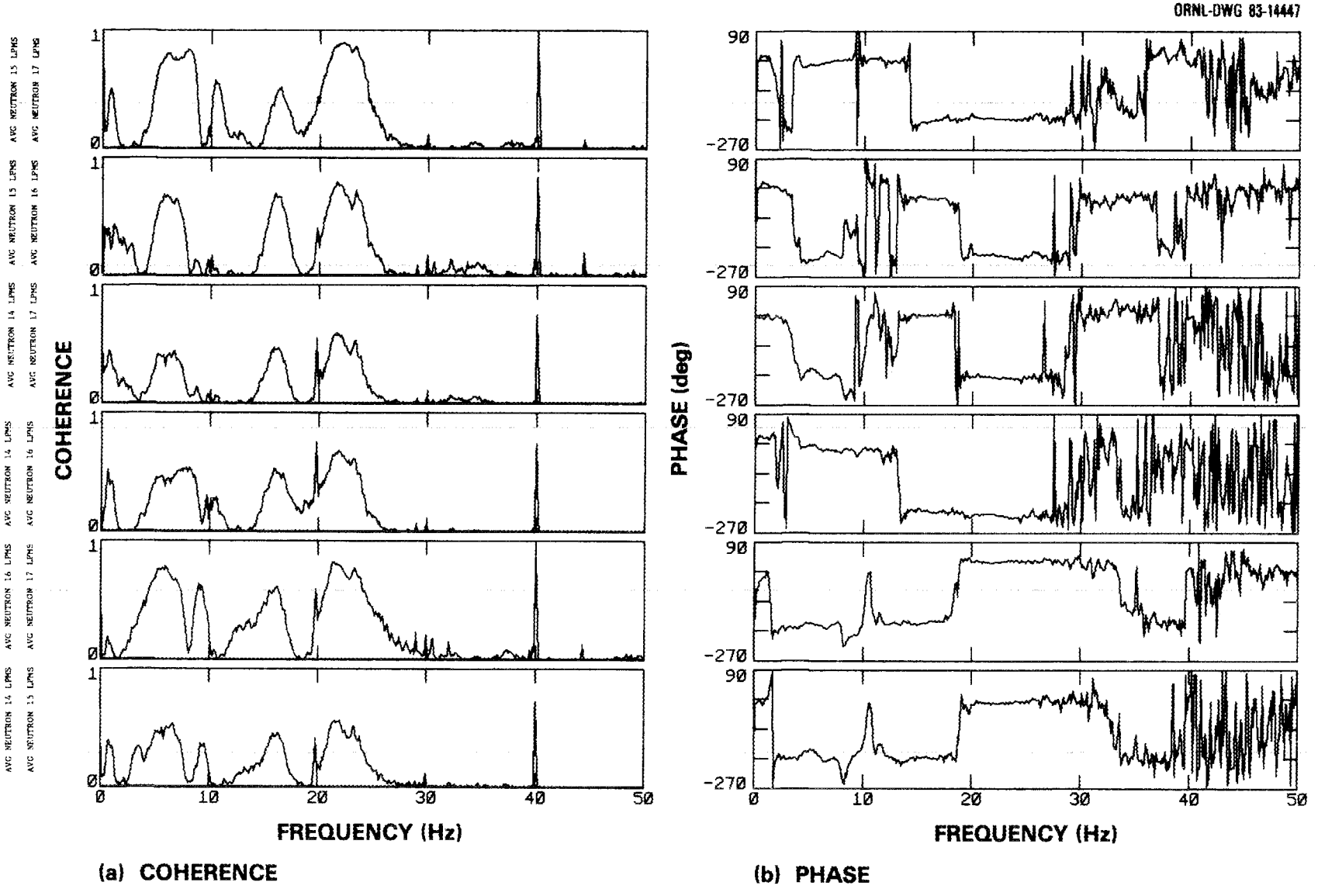

(a) COHERENCE (b) PHASE

Fig. 22. Trojan coherence and phase between ex-core neutron detectors, October 21, 1980.

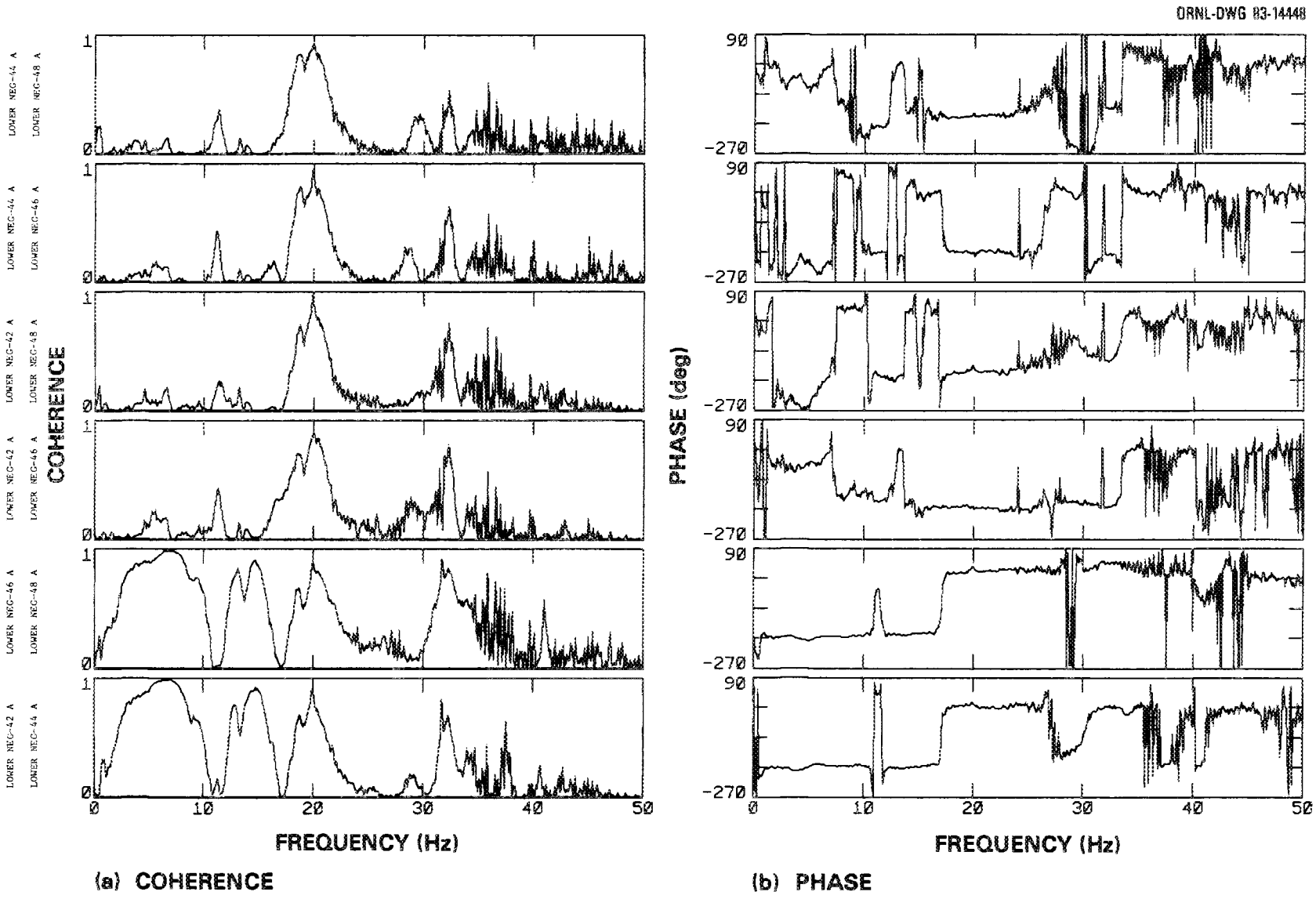

Fig. 23. H. B. Robinson 2 coherence and phase between lower ex-core neutron detectors, December 5, 1979.

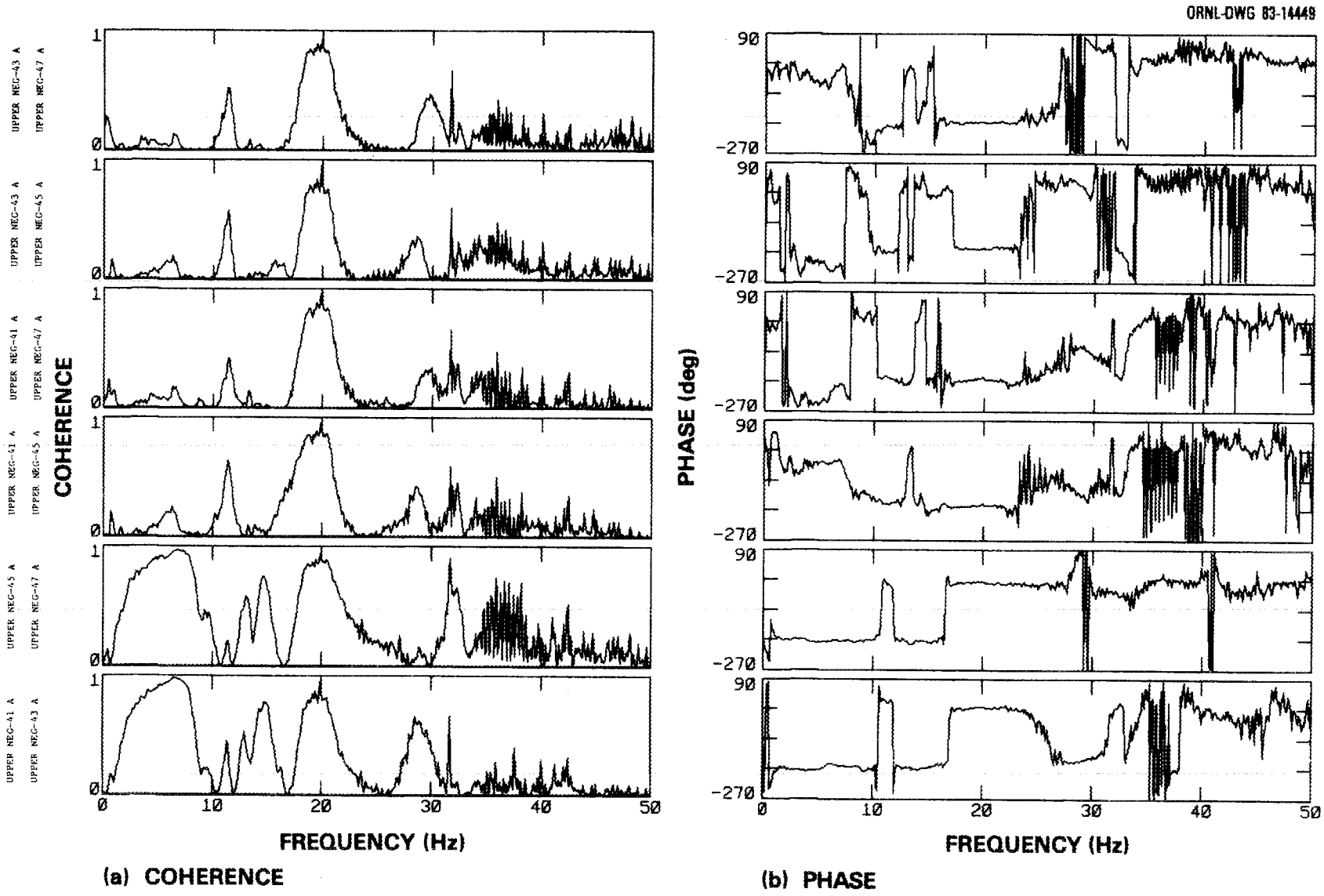

Fig. 24. H. B. Robinson 2 coherence and phase between upper ex-core neutron detectors, December 5, 1979.

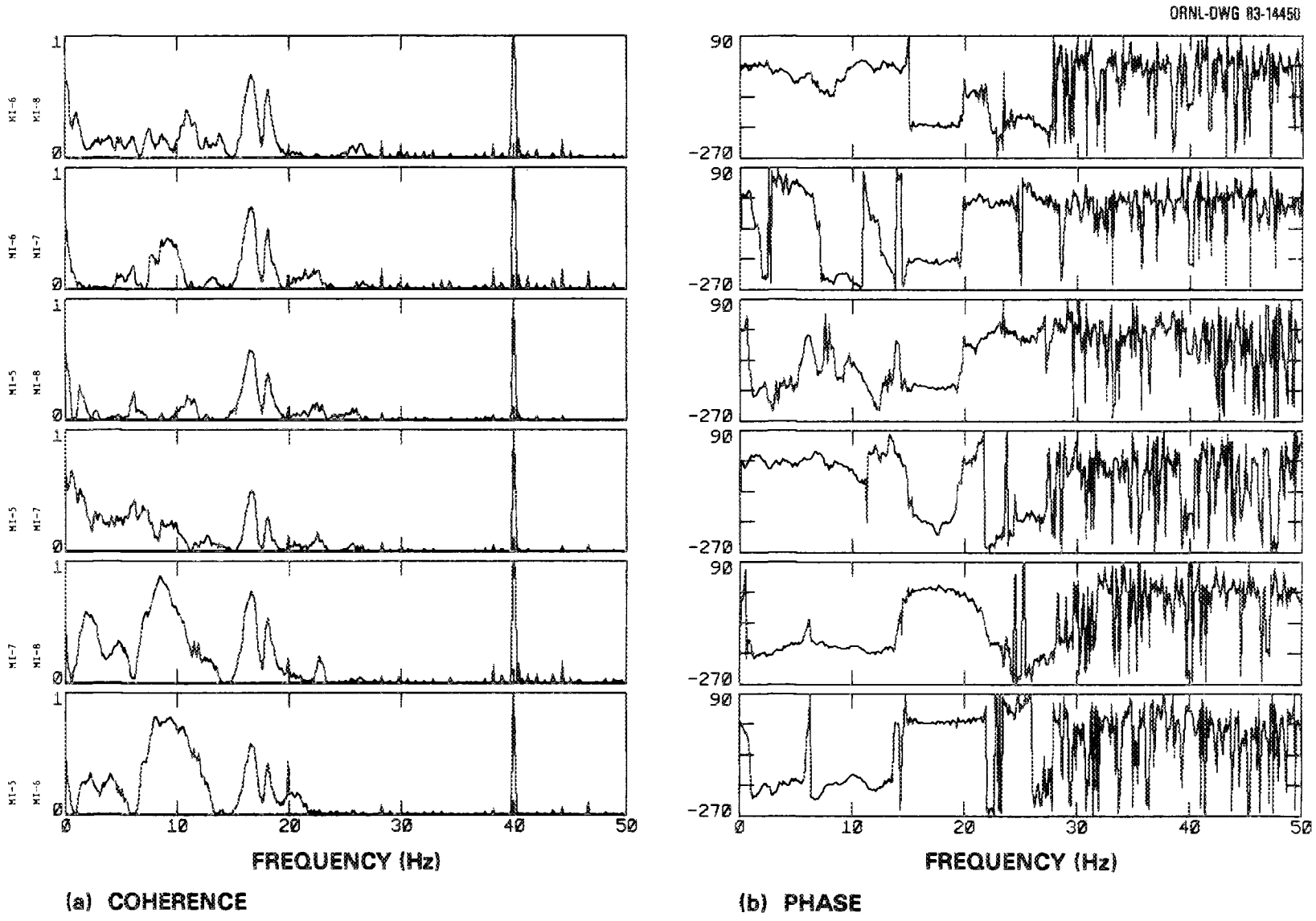

Fig. 25. ANO 1 coherence and phase between ex-core neutron detectors, March 27, 1980.

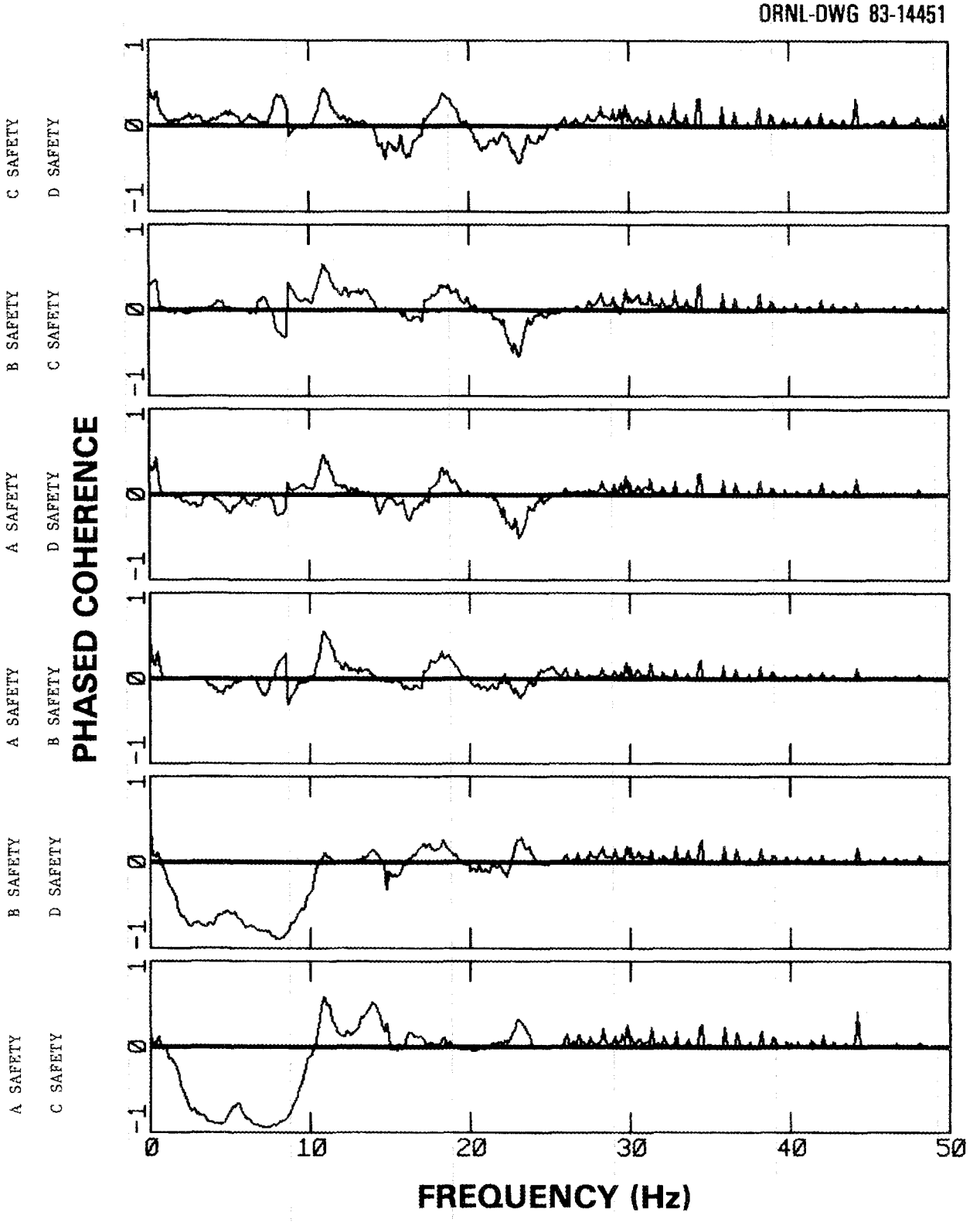

Fig. 26. Calvert Cliffs 1 phased coherence between ex-core neutron detectors, January 30, 1979.

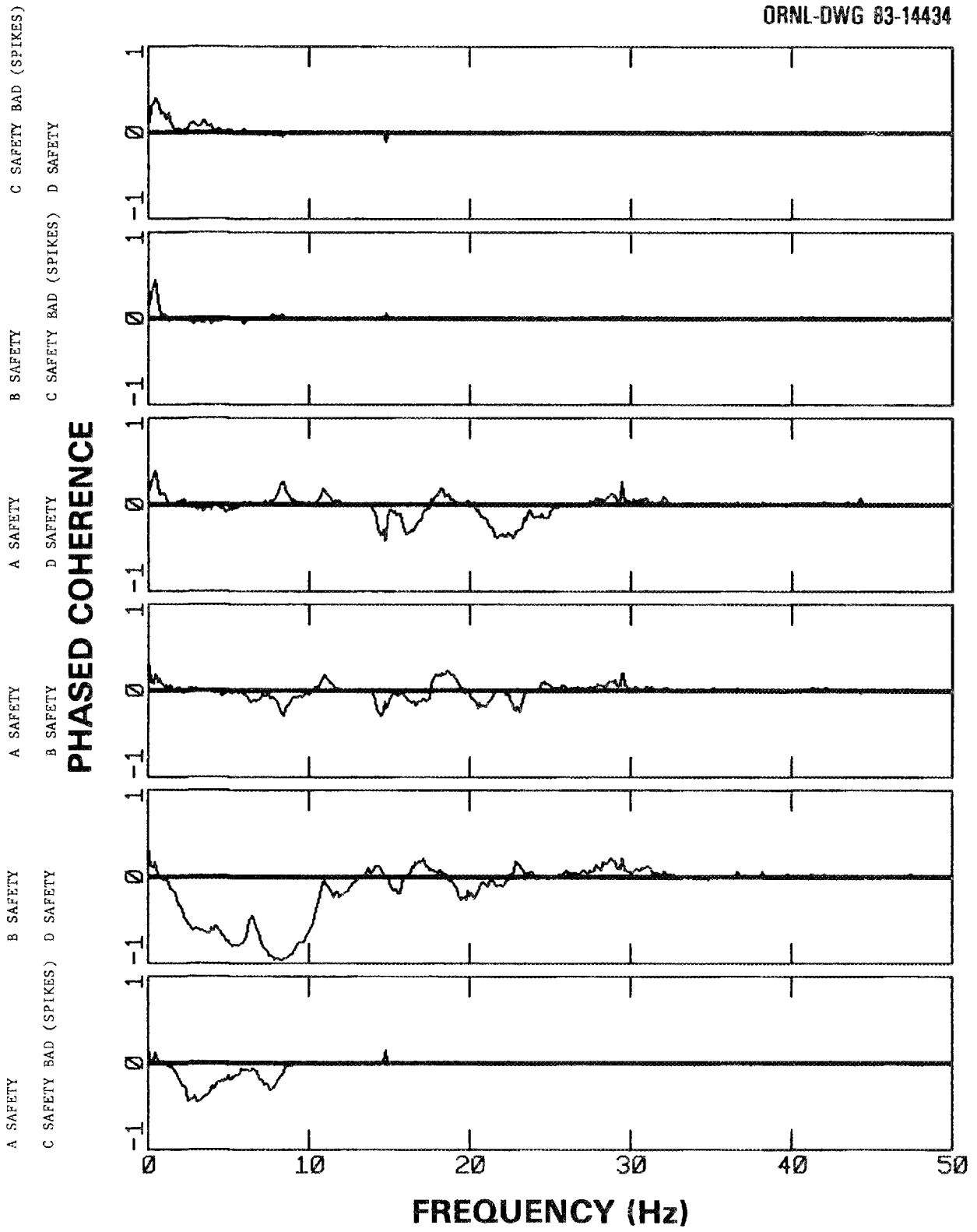

Fig. 27. Calvert Cliffs 2 phased coherence between ex-core neutron detectors, January 30, 1979.

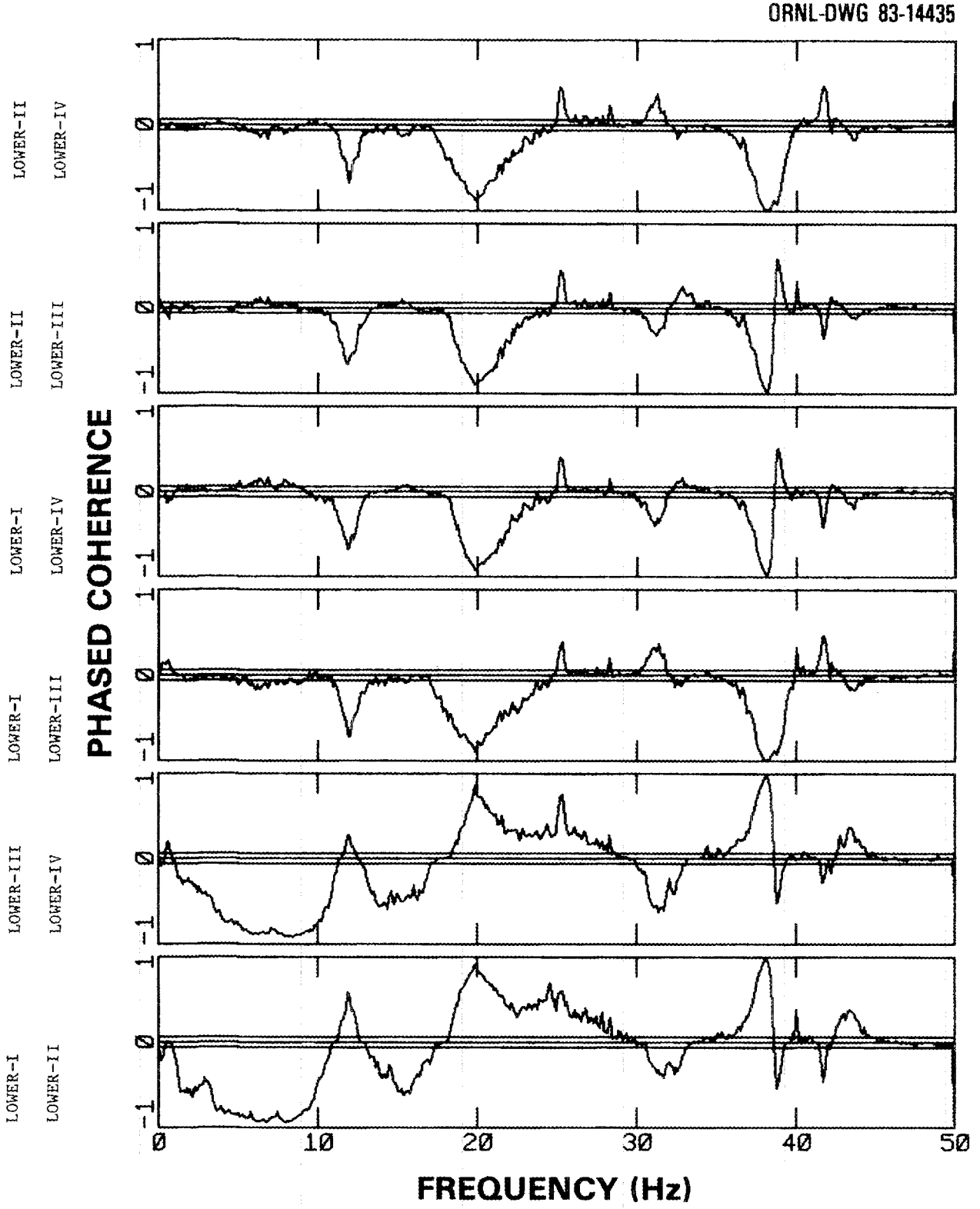

Fig. 28. Sequoyah 1 phased coherence between lower ex-core neutron detectors, April 7, 1981.

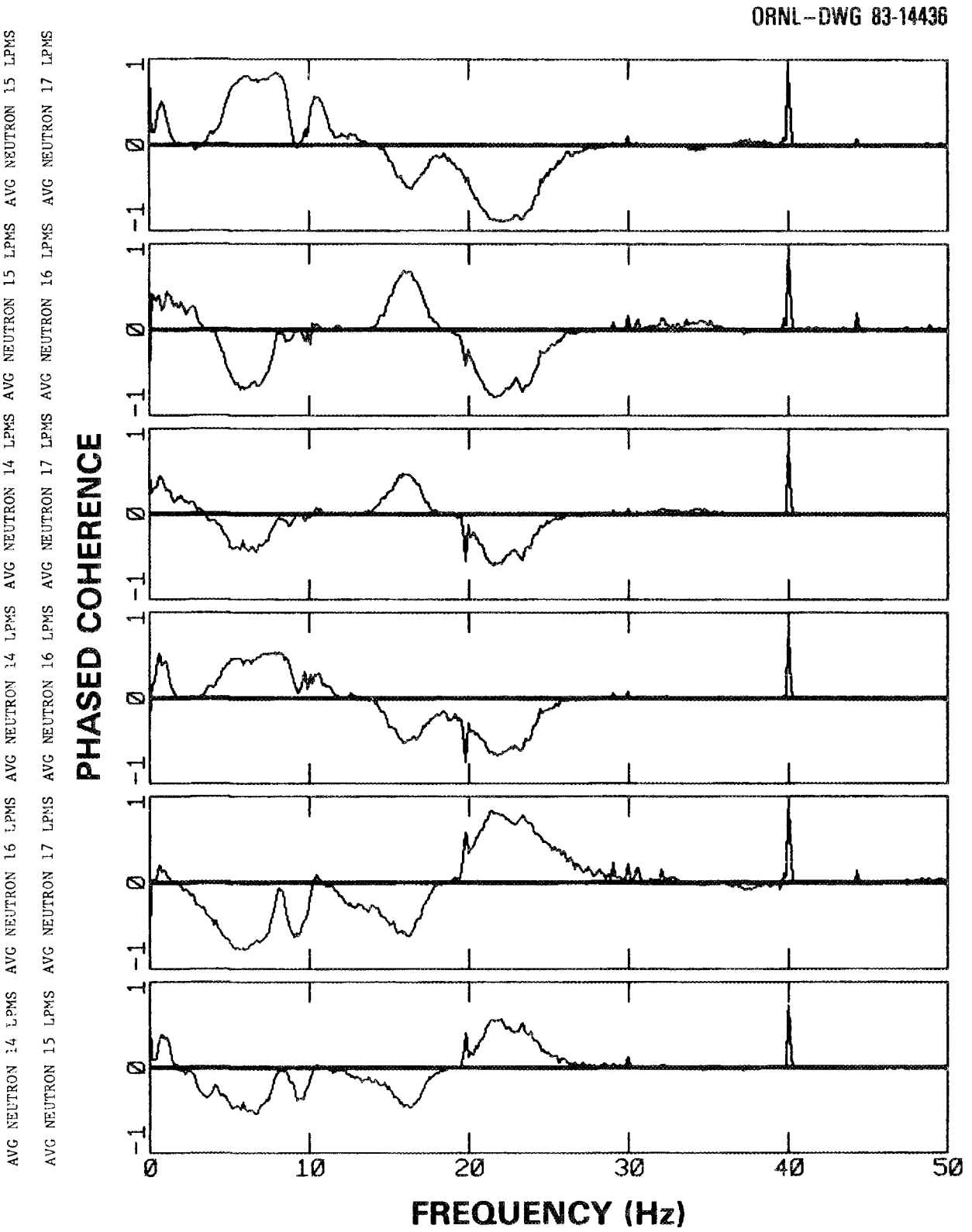

Fig. 29. Trojan phased coherence between ex-core neutron detectors, October 21, 1980.

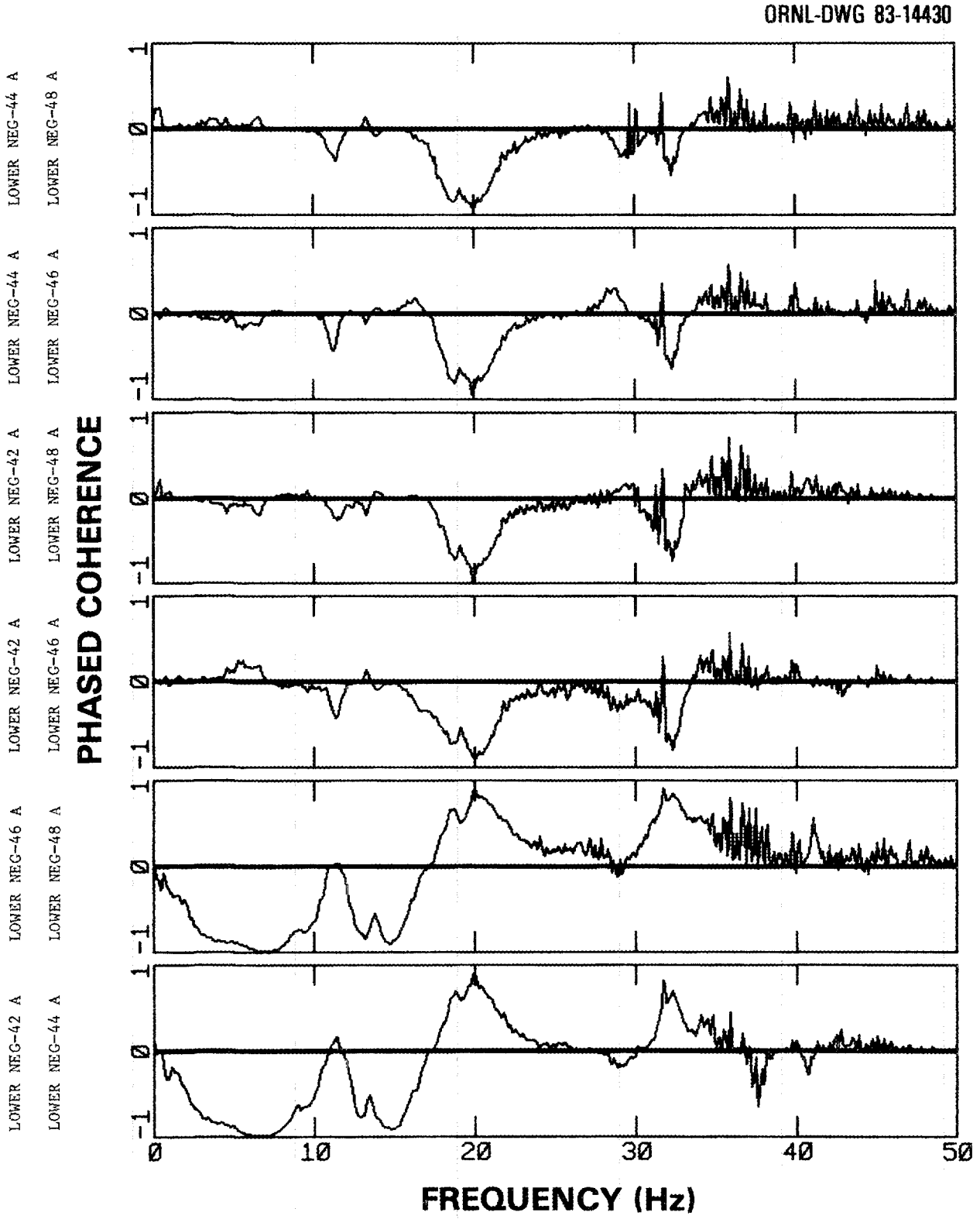

Fig. 30. H. B. Robinson 2 phased coherence between lower ex-core neutron detectors, December 5, 1979.

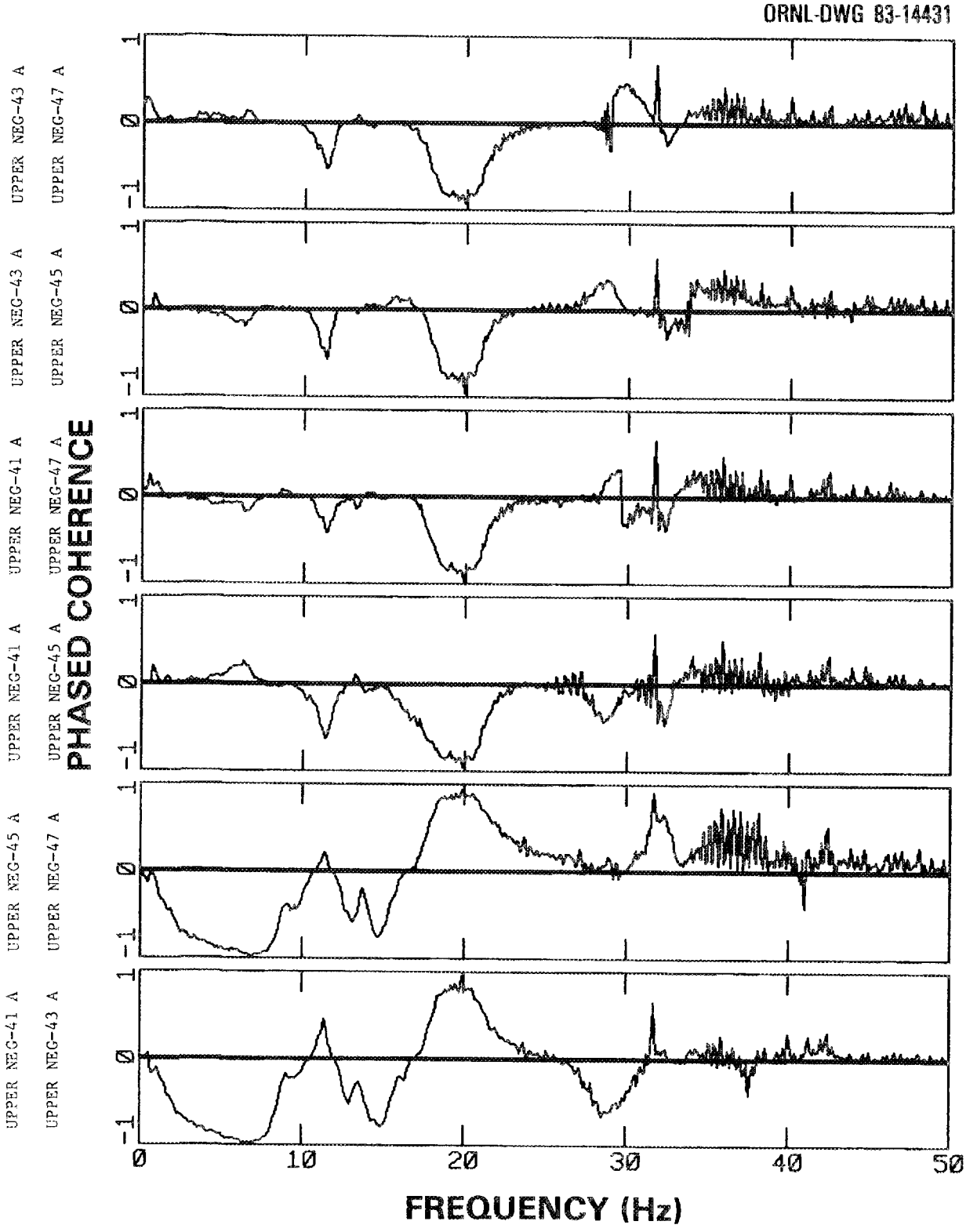

Fig. 31. H. B. Robinson 2 phased coherence between upper ex-core neutron detectors, December 5, 1979.

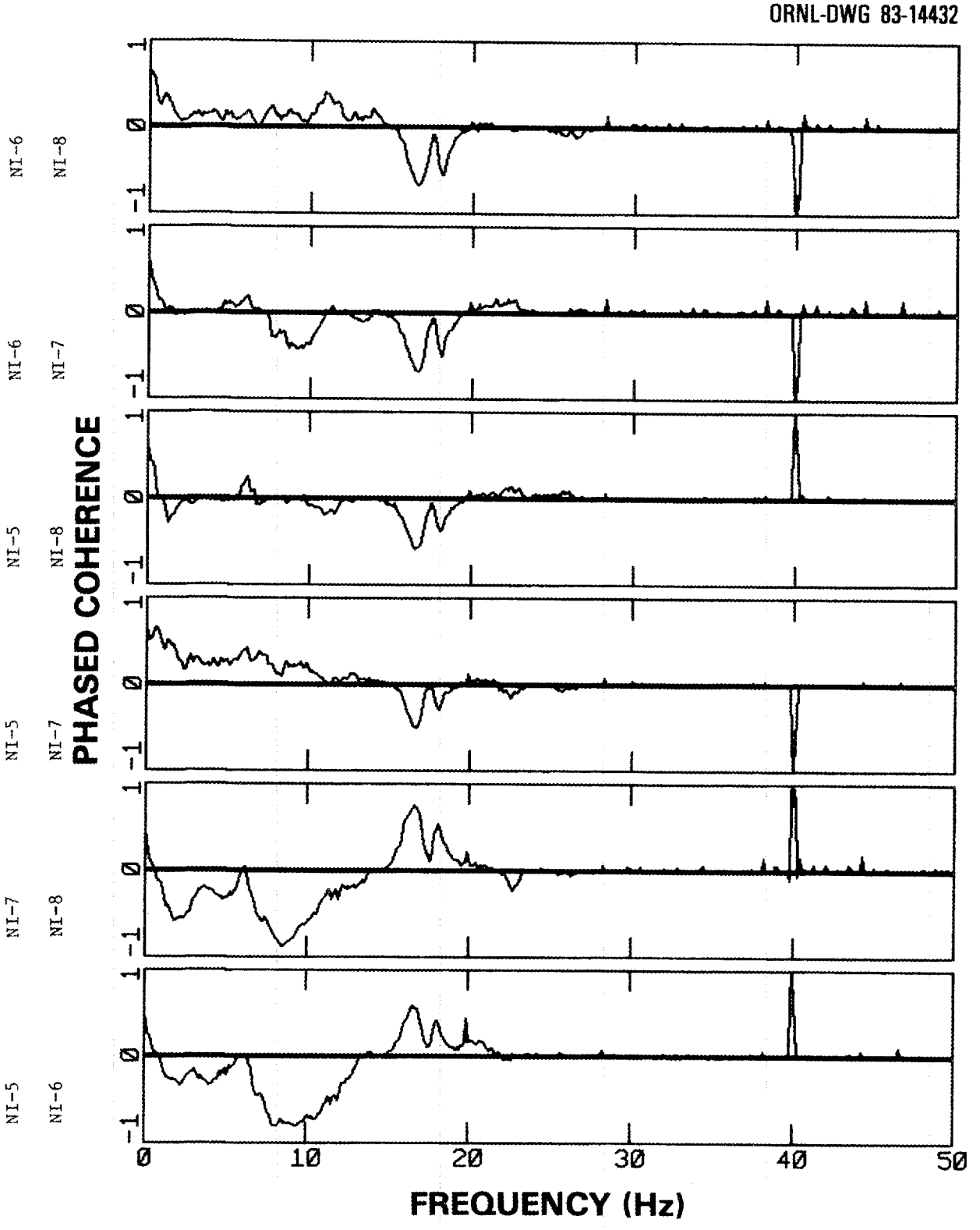

Fig. 32. ANO 1 phased coherence between ex-core neutron detectors, March 27, 1980.

Table 4. Resonances in ex-core neutron noise signatures at six PWRs*

Plant	Resonances (Hz) 1-10	Resonances (Hz) 10-20	Resonances (Hz) 20-50
Trojan	1, 3, 6, 8, 9	10.5, 16, *20*	*22*, *23*, 34, 37.5
ANO 1	1, 2, 4, 6, 7.5, 8, 9	11, 13, *17*, *18*	22.5, 27
Calvert Cliffs 2	1, 2.5, 5, 6,	11, 14, 16, 17, 18, 20	21, 22.5, 28, 31
Calvert Cliffs 1	1, 2.5, 4, 6, 7.5, 8	11, 13, 16, 18	*22.5*
H. B. Robinson (lower)	1, 3, 7, 9	*12*, 13, 15, *18*, *20*	28, 29, *32*, 41
H. B. Robinson (upper)	1, 7	*12*, 13, *20*	28, 29, *32*, 42
Sequoyah 1	1, 2, 7, 8	*12*, 14, 15, *20*	25, 31, 32.5, *38*, 42, *43*

*Frequencies are approximate based on visual analysis of the coherence plots in Figs. 19 to 25. Italics indicate a shell mode vibration, normal print is beam mode, in-phase noise is indicated by a circle, and an underline means that the mode of vibration is unknown.

†C-detector signal contaminated with electrical noise at frequencies greater than 10 Hz.

frequencies, and Figs. 26 through 32 were used to identify the mode of vibration at each frequency where possible.

Several general observations can be made from Table 4: (1) beam mode vibrations dominate the 1- to 10-Hz range with no shell mode being identified; (2) all plants have a shell mode between 18 and 22 Hz; and (3) Calvert Cliffs 1 has several in-phase components in the 10- to 20-Hz range not found in other plants. We cannot state the cause of the resonances because U.S. reactor manufacturers consider the calculated and measured vibration frequencies of reactor components to be proprietary information (which has greatly impeded the development and application of neutron noise analysis in the U.S.). Therefore, we have taken an indirect approach by reviewing the available literature on noise analysis for information regarding the identification of neutron noise sources in the 1- to 50-Hz range.

Table 5 summarizes some of the vibration frequencies of PWR components identified in the open literature. (Note that this is not an exhaustive list but does attempt to include most of the normal resonances observed when there is no anomaly present.) There are similarities between the resonances observed in our measurements (Table 4) and the sources of vibration frequencies identified in Table 5. Therefore, by association one could speculate on the specific sources of each resonance in our baseline data. However, since the purpose of our study is not to perform a diagnosis of each plant but instead to assess the generic value of neutron noise analysis for core internal vibration diagnosis, we will not make such speculations.

On the other hand, the combination of information in Tables 4 and 5 allows one to make some generic observations about the sources of neutron noise with regard to vibration of pressure vessel internals. Resonances in neutron noise in the range of 2 to 5 Hz are most likely caused by fuel element vibration stimulated by a combination of flow turbulence and the beam mode vibration of the core barrel. Resonances in the noise spectrum between 5 and 10 Hz can be caused by either core barrel vibration or the N = 2 vibration mode of the fuel assemblies. At frequencies above 10 Hz it is more difficult to identify generic causes of neutron noise. The frequencies associated with thermal shield pressure vessel and core barrel shell mode tend to be plant specific and more difficult to identify than fuel and core barrel motion. It appears that observed shell mode type neutron noise in the range 10 to 15 Hz might be due to the thermal shield and shell modes between 15 and 25 Hz are more likely the core barrel. As seen in Table 5, very little experience is reported in the literature for neutron noise above 25 Hz. However, it is clear that neutron noise does contain a great deal of information about the vibration of the pressure vessel and the mechanical structures inside it, and that research throughout the world is increasing our knowledge regarding the causes of neutron noise in PWRs.

7.3 VARIATION OF PWR EX-CORE NEUTRON NOISE OVER A FUEL CYCLE AT SEQUOYAH 1

A knowledge of the variation in neutron noise during normal plant operation can aid noise analysts in establishing criteria for detection

Table 5. Identification of resonant frequencies of PWR pressure vessels and vessel internals found in literature

Plant	Ref.	Fuel (N = 1)	Fuel (N = 2)	Resonant frequency (Hz): Core support barrel (Beam mode)	Core support barrel (Shell mode)	Thermal shield (Shell mode)	Control rod guide tube	Pressure vessel	Secondary core support
St. Lucie (CE-2 loop)	30			6, 8					
Calvert Cliffs (CE-2 loop)	21	2.3	4.6	6.8, 7.4					
Oconee 1 (B&W-2 loop)	31			7.7, 9.1, 10.7, 12.6, 13.7	16.7, 19.9				
Ringhals 2 (W-3 loop)	28	3.5		8	12, 33				
Tricastin 1[a] (FRA-3 loop)	32	3.2	6.0	8.2	20				
Bugey 5[b] (FRA-3 loop)	33			7		11, 14.6, 15.1		17	
Bugey 2[b] (FRA-3 loop)	34	3.2	7.4	6, 7.8	38.2[c]	11.1		14.8	
Stade (KWU-4 loop)	35							13, 20.5, 36.5	37.5
Fessienheim 1 & 2[b] (FRA-3 loop)	36			7	20	11-12		13.5	
Neckarwestheim (KWU-3 loop)	37	1.8, 5	11.2, 17.5	10	23.5, 25				
Unidentified (W-3 loop)	38,39			6.5			25-28		
Borssele (KWU/RDM-2 loop)	24			12, 15					
Unidentified									
(MHI-2 loop)	40			15.5				14.3	
(MHI-3 loop)	40	2.8	6.6	14.3					
(MHI-4 loop)	40			13.6					

[a] Partial thermal shield.
[b] Cylindrical thermal shield.
[c] Accelerometer at bottom of CSB.

Legend: CE = Combustion Engineering
W = Westinghouse
F = Framatome
M = Mitsubishi Heavy Industries
KMU/RDM = Kraftwerk Union/Rotterdamse Droogdok Madtschappij
B&W = Babcock & Wilcox

of abnormal behavior. Therefore, ex-core neutron noise was measured at the Sequoyah 1 plant from initial startup through the first fuel cycle and for ~2 months at the beginning of the second fuel cycle. Figure 33 shows spectra at the beginning and end of the first fuel cycle and after refueling. Note that the major change over the fuel cycle occurs around 7 Hz, which is normally associated with CSB vibration (see Table 5). However, after refueling the spectrum was nearly the same as at the beginning of the previous fuel cycle. Others[33,36] have also reported variation in the amplitude and frequency of the noise associated with CSB motion and have attributed the changes to the existence or non-existence of contact or interference between the CSB and the vessel, mainly at the radial keys or the outlet nozzle. During refueling the reactor vessel head, which clamps the core barrel in place, is removed and then replaced in its original position. The data suggest that at the beginning of the fuel cycle at Sequoyah 1 the CSB may have been clamped in a way that allowed interference with other vessel internals, thus reducing the amplitude of vibration. We hypothesize that during the fuel cycle some of the clamping force was reduced such that the barrel was at a position that allowed a natural, free-swinging motion. (Note in Fig. 33 that the resonant frequency at ~7 Hz also shifted to a slightly lower frequency, which is consistent with a relaxation of the clamping force.)

Figure 33 also shows some change at ~3 and 7 Hz; these frequencies are associated with the first and second modes of fuel assembly vibration (see Table 5 and ref. 33). Stokes and King[41] showed that the beginning-of-life fuel assembly's natural frequency is 5 to 10% greater than at the

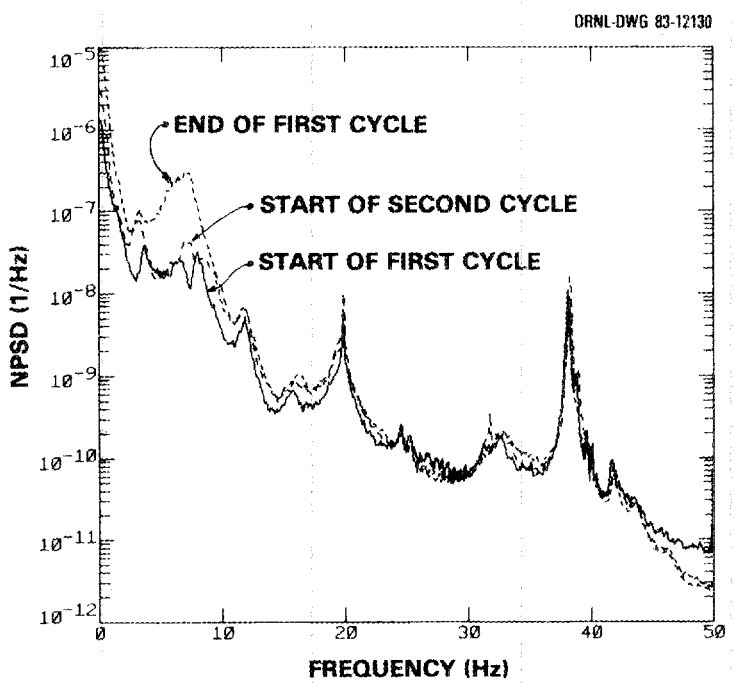

Fig. 33. Sequoyah 1 ex-core neutron noise spectrum at the start of the first and second fuel cycles and at the end of the first cycle.

end of life because the stiffness of the assembly decreases during its life. This may account for the decrease in the resonant frequency shown in Fig. 33.

Another important implication of this observation is that a significant amount of the suspected increase in Sequoyah CSB vibration mentioned above may actually be due to the ex-core neutron noise contribution of the second mode of fuel assembly vibration, which has been shown to increase over the fuel cycle due to changes in the scale factor (see Sect. 7.4.3). Therefore, it may be difficult to isolate changes in CSB vibration as suggested in Sect. 7.4.1. (Note that a caution to this effect was previously mentioned in Sect. 2 with respect to the difficulty of separating the contributions of individual noise sources if there is overlap in the resonant frequencies of separate sources.)

We also studied the effect of boron concentration, fuel burnup, and burnable poison assemblies on the ex-core neutron noise caused by fuel assembly vibration.[12] These studies showed that the ex-core noise caused by a fixed amplitude of vibration increases with fuel burnup and decreasing boron concentration. Although this result would explain the increase in noise during the first fuel cycle, we cannot explain why the noise did not return to its original amplitude at the beginning of the second cycle. However, we do know that new fuel assemblies were installed on the core periphery during the refueling, which could change the neutronic effect of fuel assembly vibration. We plan to continue these studies by performing calculations of ex-core noise for the second cycle core conditions.

Day-to-day and long-term variations in neutron noise are to be expected due to normal changes in a number of factors that cause vibrations. We have attempted to quantify these normal changes by plotting the maximum of the normalized power spectral density (NPSD) versus time for selected frequency ranges in the Sequoyah 1 spectrum (the frequency ranges were selected to encompass prominent resonances of the spectrum). Figure 34 shows that not all noise bands vary the same with time.* We have already discussed the possible causes of changes in noise associated with fuel vibration (3 to 4 Hz) and CSB (5.5 to 9 Hz). By association with the research of others[33,34,36] on similar design plants (Table 5), we infer that the resonance at ~11 Hz is likely a result of thermal shield vibration, the resonance at ~15 Hz is related to a beam mode of the pressure vessel, and the resonance at 20 Hz may be attributable to shell mode vibration of the CSB (driven by the shaft rotation of the primary coolant pumps). The sources of higher frequency resonances at ~31, ~38, and ~41 Hz are not known at this time.

As mentioned above, all the resonances vary differently with time. If we assume these to be representative of normal variations with no anomalous vibration, criteria could be established to alert plant engineers if the noise exceeds the baseline level. If the anomalous trend persists, the suspect internal component could be examined at the next refueling. However, we want to point out that the full range of

---

*The variations in neutron noise shown in Fig. 34 were obtained from ~1-h data records obtained at periodic intervals throughout the first fuel cycle and after the first refueling.

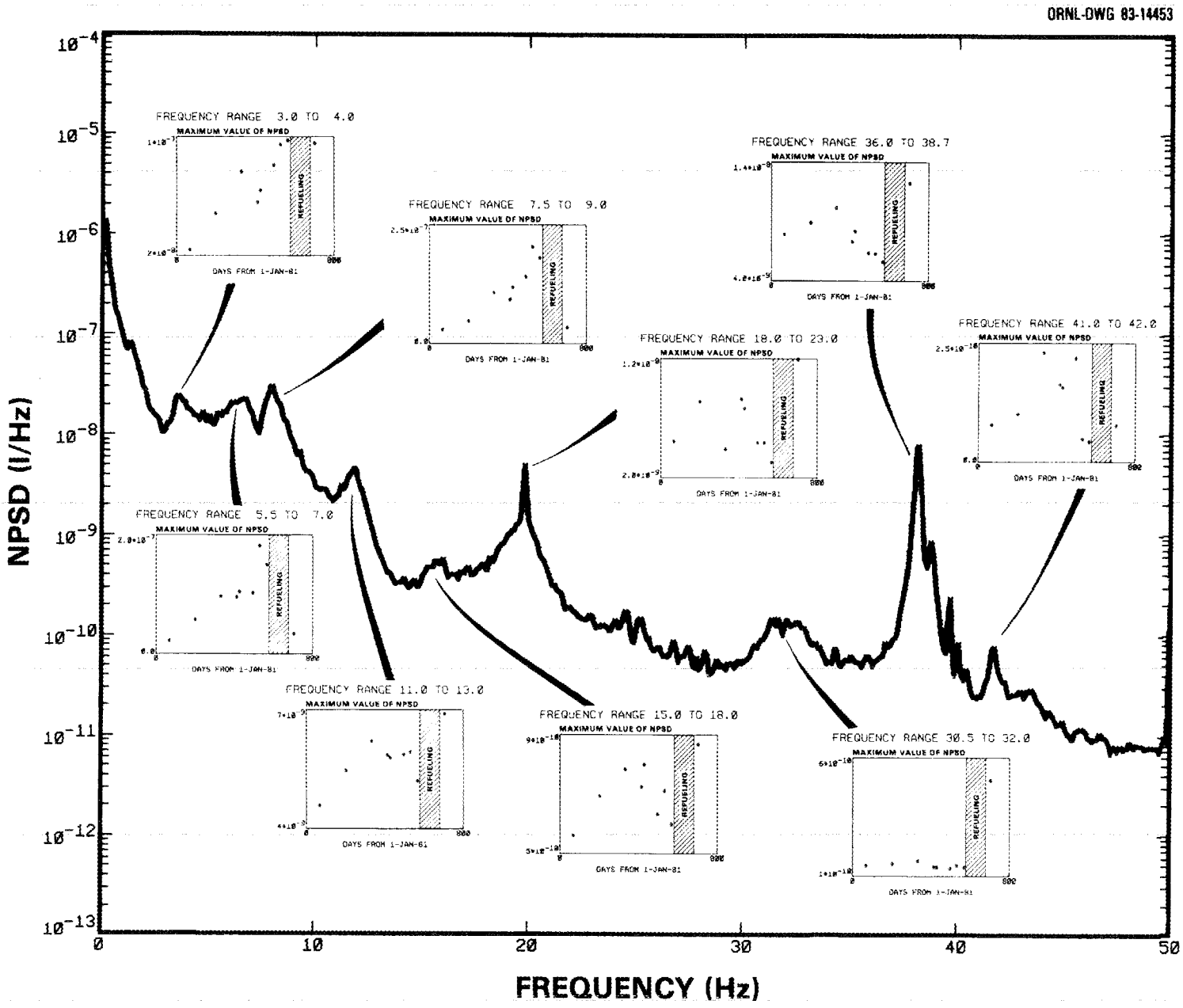

Fig. 34. Long-term variation in the amplitude of resonances in the Sequoyah 1 ex-core neutron noise spectrum.

variation in the noise may not be established until at least the end of the first equilibrium core (usually the third fuel cycle). Also, new fuel management schemes to increase burnup and to reduce pressure vessel fluence are continuing to change the definition of the equilibrium core. Therefore, only a long-term monitoring program such as those implemented in the Netherlands,[42] France,[32] the Federal Republic of Germany,[43] and Japan[40] will completely define the long- as well as short-term behavior of ex-core neutron noise.

7.4 APPLICATION OF NEUTRON NOISE IN PWRs

Thie[3] provides an excellent summary and bibliography of the application of neutron noise analysis for the diagnosis of anomalies in PWRs, including such things as excessive core barrel motion and loose thermal shields. A recent application[44] involved analysis of neutron noise measured with in-core detectors to diagnose abnormal vibrations of peripheral fuel assemblies caused by water jetting through openings between the baffle plates. In the following sections we will describe some applications of neutron noise analysis evaluated by ORNL.

7.4.1 Measurement of Core Barrel Motion

Noise analysts have used neutron noise to routinely monitor CSB motion ever since neutron noise was used to aid in the diagnosis of excessive and damaging flow-induced core barrel motion in two PWRs in the early 1970s.[45-47]

At the Palisades nuclear plant neutron noise was used to identify core barrel motion as the source of large random fluctuations observed in the ex-core detector signals (see Fig. 35). In this case, the barrel was loose because of wear on the pressure vessel and vessel head where the barrel is clamped in place (see Fig. 36), and consequently it was "rocking" rather than vibrating like a rigid body at the expected resonant frequency.

Due to the core barrel motion the ex-core noise spectrum at Palisades (Fig. 37) showed considerably more noise than the in-core signals at frequencies below 1 Hz. Also note the difference in the amplitude of normal ex-core noise at other PWRs (Figs. 9 and 12-17) relative to the abnormal noise at Palisades, which illustrates that by monitoring neutron noise it should not be difficult to detect major problems such as existed at Palisades. The American Society of Mechanical Engineers (ASME) has issued a standard[48] for monitoring core barrel motion using neutron noise. The ASME standard is based on experience in monitoring core barrel motion with ex-core neutron detectors.

The amplitude of core barrel vibration can be estimated using a scale factor that relates a change in ex-core neutron flux to a displacement of the core barrel. Others have computed[33,47,49] and measured[50]

ORNL-DWG 73-12353R

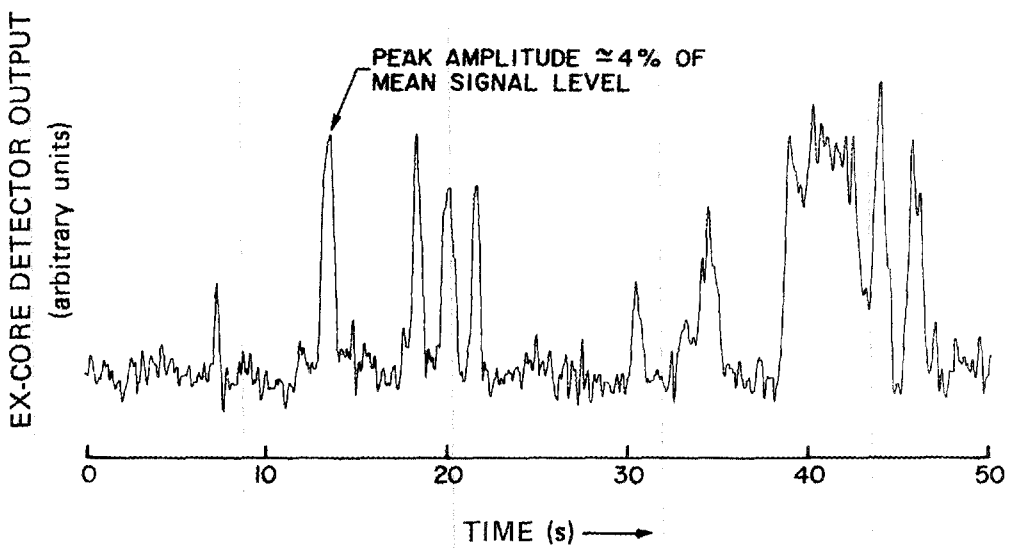

Fig. 35. Palisades ex-core neutron detector signal when the core barrel was loose. Most of the steady-state signal is biased out to illustrate the noise detail.

this scale factor. The scale factors obtained range from 0.02%/mil to 0.05%/mil.* ORNL is currently reviewing the scale factors associated with both CSB and thermal shield motion and will publish the results in a future report. In the meantime we assumed a value of 0.03%/mil to estimate the motion of CSB from ex-core neutron noise. By using the graph of maximum NPSD in the range 5.5 to 7.0 Hz (Fig. 34), the change in CSB motion over the fuel cycle can be estimated in the following way.

According to the graph, the NPSD is $\sim 2 \times 10^{-8}$ at the beginning of the fuel cycle and $\sim 1.8 \times 10^{-7}$ at the end. Since the NPSD is in units per hertz, one must integrate the noise over the frequency range estimated for CSB motion.

In the present example the NPSD is assumed to be constant over a 1.0-Hz range. Thus we can integrate by multiplying the NPSD by 1.0 Hz and taking the square root to obtain the percent root-mean-square noise (RMS) as 1.4×10^{-2}% and 4.2×10^{-2}% at the beginning and end of the fuel cycle respectively. Then, dividing by the nominal scale factor equal to 0.03%/mil, the RMS motion is estimated to vary from ~0.5 mil to ~1.4 mils over the fuel cycle. This of course represents only an average value of motion over the time a spectrum is averaged. If a Gaussian distribution of the neutron noise is assumed, the motion could be as much as a factor of five (assuming an arbitrary crest factor of five for the amplitude

*These scale factors do not take into account that for CSB beam mode vibration the amplitude of vibration at the lower grid is greater than an axial average motion.

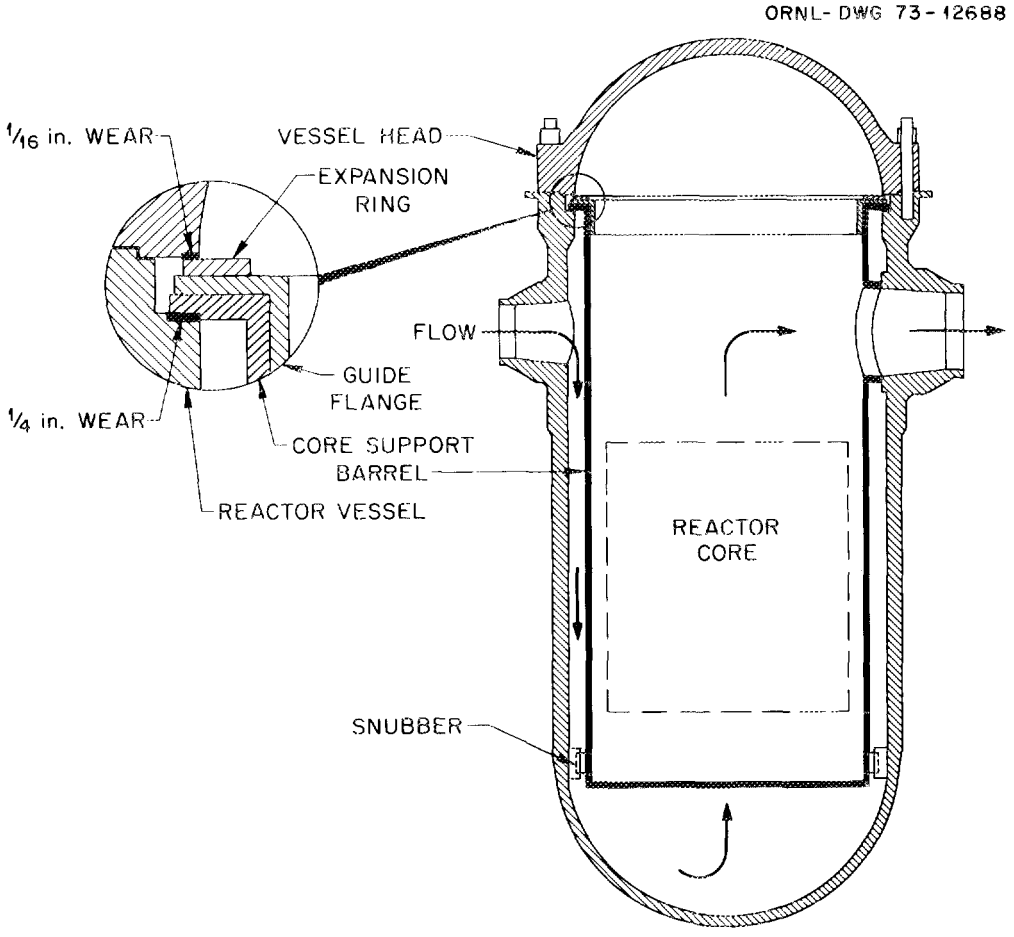

Fig. 36. Cause of abnormal core barrel motion in Palisades.

distribution) greater than the estimated values above. Also, the preferred direction of CSB motion might not be in line with the ex-core detectors used to measure the neutron noise, thus introducing another uncertainty in the estimate of motion.

Robinson et al.,[30] used the phase and magnitude of the coherence between pairs of ex-core detectors to infer the preferred direction of CSB motion. In the case of Sequoyah 1, the coherence between ex-core detectors at the CSB resonance of ~7 Hz (Fig. 21) is almost equal between cross-core detectors I-II and III-IV and much larger than between detectors at 90°. Figure 21(b) shows that noise signals from the cross-core detector combinations I-II and III-IV are out of phase (-180°), which leads us to conclude that the preferred direction of motion is either along a 0 to 180° axis or a 90 to 270° axis. Further analysis shows the phase between adjacent detectors to be -180° for II-IV and I-III and 0° for II-III and I-IV. Therefore, referring to the Sequoyah detector locations in Fig. 14, we conclude that although the barrel is moving in all directions, it has a preferred direction along the 90° to 270° axis. This is not unexpected, since the main forcing function for core barrel vibration is the hydraulic force of coolant entering the

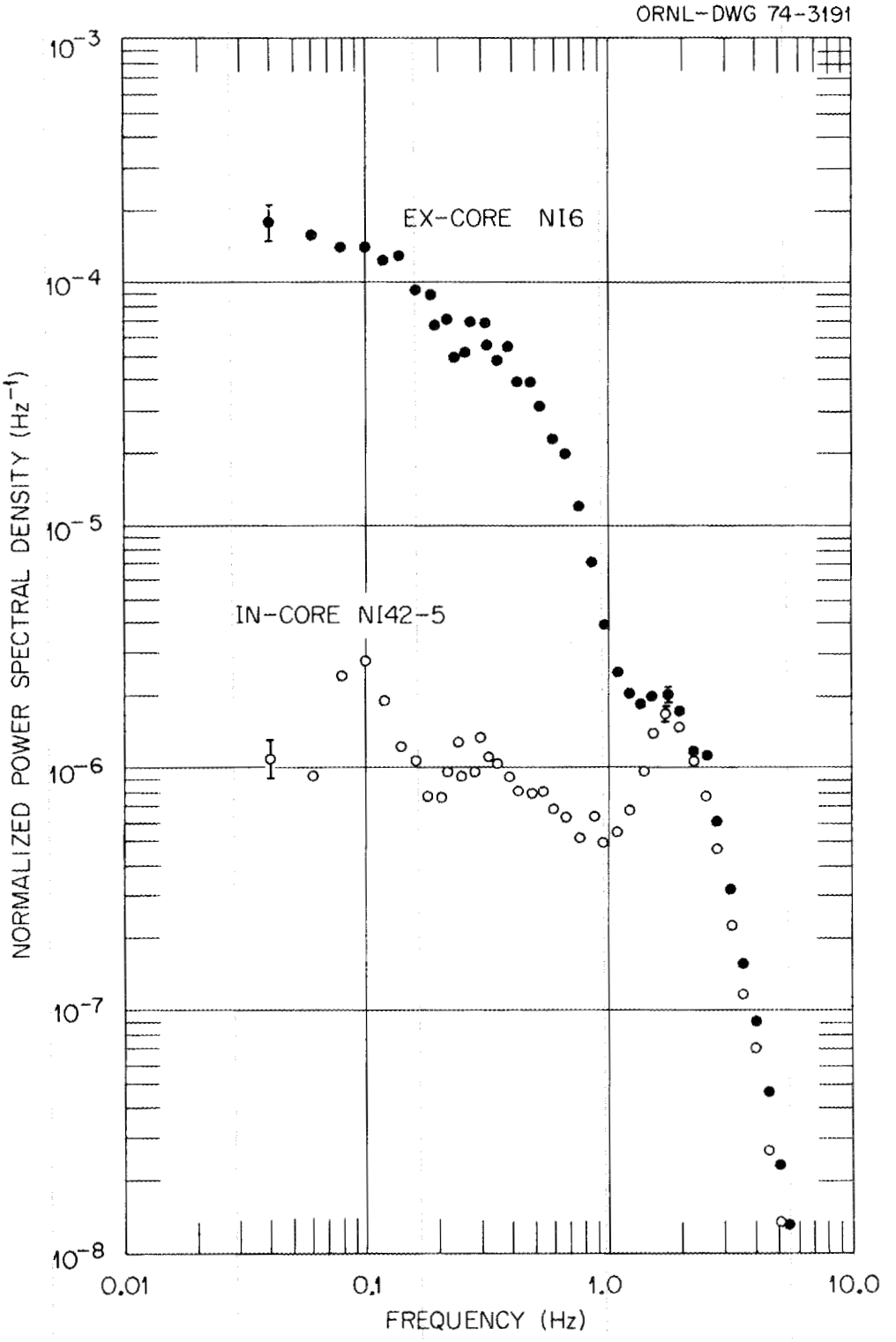

Fig. 37. Comparison of ex-core and in-core power spectra obtained at Palisades when the core barrel was loose.

downcomer. The estimation of CSB motion in the above manner yields only a qualitative value at best because of the limitations of the measurement, namely uncertainties in the scale factor, randomness of the motion, and the assumption that the CSB-induced noise can be separated from other ex-core neutron noise sources such as the fuel assembly vibration mentioned earlier.

The amplitude probability density (APD) function has also been used to monitor and evaluate PWR lateral core motion in several applications. ORNL used the single-input APD function to demonstrate the lateral constraint of core barrel motion caused by contact with the reactor vessel during operation with loss of core support assembly axial preload.[46] Mayo[27] used the joint amplitude probability density distribution between two neutron noise signals to monitor preferential direction of lateral core support assembly beam mode resonance vibrations.

Interpretation of the neutron noise APD distribution as being representative of the spatial distribution of core barrel motion requires that the analyzed signal be dominated by lateral core motion neutron noise. There is also a slightly less restrictive requirement that the core and core barrel be moving as an approximately rigid body. These conditions have been reasonably demonstrated for the large-amplitude, low-frequency motions associated with loss of core barrel axial clamping such as occurred at Palisades. Some additional restrictions apply in cases where the core support assembly has normal clamping are discussed below.

Neutron noise measurements made at a PWR operating without axial preload on the core barrel showed that the broadband neutron noise signal was dominated by the lateral motion of the core and support assembly.[46] This effect was attributed to the associated low frequency and large amplitude of lateral motion due to loss of clamping, and it resulted in essentially rigid body motion of the core and support assembly that was restricted by contact with the reactor vessel. (Plots of the neutron noise APD distribution on probability graph paper clearly indicated restriction of the internal motion.)

PWR neutron noise measurements under normal clamping conditions show that lateral core and support assembly motions typically dominate the neutron noise signal in the frequency band associated with the beam mode resonance vibration frequency of the reactor internals. This condition is indicated by high coherence and 180° phase between cross-core detector pairs. Loss of coherent, 180°-phase signals in this frequency band can be caused by change in the core barrel end support conditions, by non-rigid body motion, or by the presence of an additional noise source. Under these conditions the neutron noise signals do not have direct lateral motion interpretation. Therefore, neutron noise cross power spectral density amplitude, phase, and coherence must be used to select and verify the appropriate region of the frequency spectrum for APD measurement of lateral core motion.

The joint probability density distribution between ex-core neutron detectors has been used to monitor the spatial preference of core support assembly beam mode reasonance vibration under normal core clamping conditions. This measurement is based on an analysis which shows that the ex-core neutron detectors sense primarily internal lateral motion

along lines between the core center and the detector. Two detectors located at ninety degrees around the exterior of the core therefore sense orthogonal components of the lateral motion. Using band-pass filters to select the region of the spectrum dominated by the beam mode resonance vibration, the joint probability density distribution of these signals can provide a direct display of the spatial preference of the motion. Distinct, reproducible differences in the direction of the maximum vibration amplitudes of the core support assembly beam mode resonance have been observed by this technique. This measurement may provide useful information about the direction and magnitude of lateral core motion constraints or spatial differences in stiffness.

We do not believe that the core and support assembly will respond as a rigid body to external motion constraints at the normal core support assembly beam mode vibration frequency. For this reason APD distributions may not show a significant deviation due to small amplitude interaction with the reactor vessel guide lugs under normal core clamping conditions.

Correct interpretation of APD distribution measurements requires supporting cross power spectral density analysis to verify the quality and frequency band of lateral core motion neutron noise signals. For these reasons we conclude that probability density distribution interpretation of lateral core motion is a supplementary technique to the more general spectral analysis.

7.4.2 Measurement of In-Core Coolant Velocity

In Sect. 7.2.2 we stated that temperature fluctuations in the core coolant are a source of neutron noise in the frequency range 0.01 to 1 Hz. This suggests that a better understanding of the relationship between neutron noise and core coolant temperature fluctuations might lead to methods for diagnosing abnormalities in core thermal hydraulics.

Noise analysts[51] have noted a delay time between core-exit thermocouple and ex-core neutron noise signals, but the coolant velocity they inferred using the delay time was lower than the expected core velocity. However, recent research at The University of Tennessee[52] and ORNL[53] has indicated that PWR in-core coolant velocity can be inferred from the phase relationship between neutron noise and core-exit temperature noise provided a correction is made for the thermocouple time response. We evaluated this technique by analyzing core-exit temperature and in-core neutron noise at the Loss-of-Fluid Test (LOFT) reactor, and core-exit temperature and ex-core neutron noise at Sequoyah 1.

Figure 38 is a typical plot of the phase shift between core exit temperature and ex-core neutron noise at Sequoyah 1 before and after correction for the estimated response time of the temperature sensor (~0.7 s). Velocities at LOFT and Sequoyah 1, inferred using the relationships in Eqs. 12 and 13 (Sect. 8.2.3), are listed in Table 6 along with reference velocities measured in LOFT with a turbine flowmeter and obtained from the Sequoyah 1 design description (FSAR). The relatively

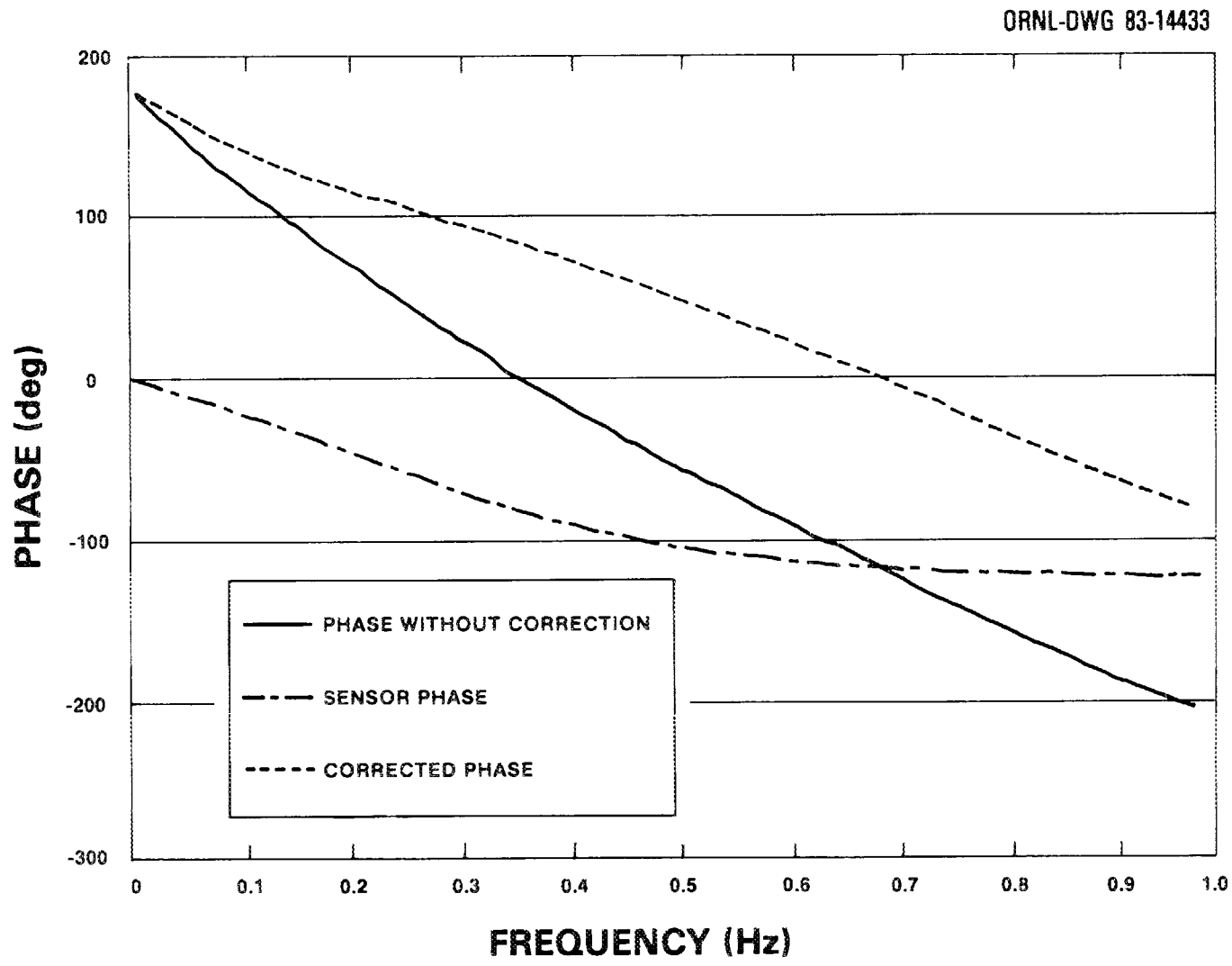

Fig. 38. Phase shift between a Sequoyah 1 ex-core neutron signal and a core-exit thermocouple before and after correction for thermocouple response time.

Table 6. In-core coolant velocities inferred from the phase relationship between core-exit temperature and neutron noise after correction for thermocouple response

Reactor	Flow (% of full flow)	Velocity: Noise analysis (ft/s)	Velocity: Reference (ft/s)
LOFT	100	12.2	12.6[a]
LOFT	65	8.7	8.4[a]
Sequoyah 1	100	15.0	15.8[b]

[a] Measured by a turbine flowmeter.

[b] From Sequoyah 1 Final Safety Analysis Report.

good agreement between the velocity inferred from noise analysis and the reference velocities suggests that noise monitoring might supply information regarding in-core thermal hydraulic anomalies if they should occur. We are continuing to evaluate these results with additional measurements at LOFT and Sequoyah 1 (in-core as well as ex-core neutron noise).

7.4.3 Measurement of Fuel Motion

Methodologies for inferring the magnitude of fuel assembly vibraions in PWRs is of great interest because excessive mechanical motion of fuel assemblies has led to fuel rod cladding failure in a number of PWRs.[54] The loose parts that might result from such failures increase the possibility of local flow blockages, which could lead to coolant boiling. Excessive fuel assembly vibrations and coolant boiling are therefore potential safety issues, since both conditions could lead to clad failure and fission product release into the primary coolant system.

Neutron noise may provide a means of monitoring fuel assembly vibration. For example, noise analysts[44] have used in-core neutron noise to detect abnormal fuel assembly vibrations caused by water jetting through clearances in the baffle plates. ORNL has studied[12] the sensitivity of detecting fuel assembly vibrations in a PWR by calculating the scale factors, which relates the amplitude of fuel assembly vibrations to ex-core neutron noise amplitude. The results indicate that, in the frequency range 2 to 4 Hz associated with the first mode of fuel assembly vibration, the scale factor varies as a function of burnup and boron concentration. Table 7, (ref. 12) presents the variation in the scale factors over a fuel cycle under the assumptions of driving forces which are spatially correlated (as might result from fuel assembly vibrations induced by core barrel motion) or uncorrelated (as might result from flow-induced fuel assembly vibrations). All fuel assemblies were assumed to vibrate with equal amplitude and with random direction.

Table 7. Calculated ex-core detector scale factors for fuel assembly vibrations in a Westinghouse PWR

	Total scale factors*					
	Beginning of cycle		End of cycle		% increase	
	BPR†	NBPR	BPR	NBPR	BPR	NBPR
Correlated	6.0	5.1	9.5	9.0	58	76
Uncorrelated	0.7	0.6	1.1	1.0	57	67

*Units are NRMS per cm of fuel assembly vibration normalized to the mean detector response. All fuel assemblies are assumed to vibrate with the same amplitude.

†BPR--burnable poison rods; NBPR--no burnable poison rods.

These scale factors were used to infer an average amplitude of vibration at the beginning and end of the first fuel cycle at Sequoyah 1. Note in Fig. 34 that the NPSD of ex-core neutron noise associated with fuel vibration (3-4 Hz) at Sequoyah 1 increased over the fuel cycle. However, when the change in scale factor due to burnup and boron concentration is taken into account the actual fuel vibration inferred from the neutron noise remained approximately constant (see Table 8). Further study is required to explain why the ex-core noise did not return to the beginning-of-cycle amplitude at the start of the second fuel cycle. We hypothesize, as mentioned in Sect. 7.3, that a new baseline level may have been established when new fuel was added around the core periphery during refueling, or that the scale factor is more sensitive to burnup than to boron concentration.

Table 8. Fuel assembly vibrational amplitudes inferred from measured ex-core detector neutron noise at Sequoyah 1

	Inferred amplitudes ($\times 10^{-4}$ cm RMS)	
	Beginning of cycle	End of cycle
Correlated	0.37	0.36
Uncorrelated	3.1	3.1

*All fuel assemblies are assumed to vibrate with the same amplitude. Scale factors for BPR cases (Table 7) were utilized.

8. BWR NEUTRON NOISE

As mentioned in Sect. 5, the BWR noise recordings in the ORNL library were obtained several years ago as a part of our assessment of abnormal instrument tube vibrations, and therefore our discussion of baseline noise in BWRs must be somewhat limited in scope. Nevertheless, we hope to introduce the reader to BWR neutron noise and discuss several applications. A detailed analysis of BWR baseline noise will be completed and reported after we obtain additional data from a BWR.

Figure 39 shows that the signatures of individual LPRM detectors at the four axial positions are considerably different from each other and from the APRM signal, which is the average of a number of LPRM signals. We also note from Fig. 40 that the signatures at a given axial level (B) can be different depending on the radial location of the detector.

Figure 41 shows the low-frequency spectrum of a typical APRM signal in a BWR (Browns Ferry 3). The slight resonance at ~0.5 Hz and the rapid decrease in noise above ~0.6 Hz are the major features of the spectrum. (The sharp decrease in noise above 4 Hz is due to the anti-aliasing filter used in analyzing the noise.) It is generally believed that the 0.5-Hz resonance is related to the stability of the core. This will be discussed in more detail in the Sect. 8.2.4 on application of neutron noise in BWRs.

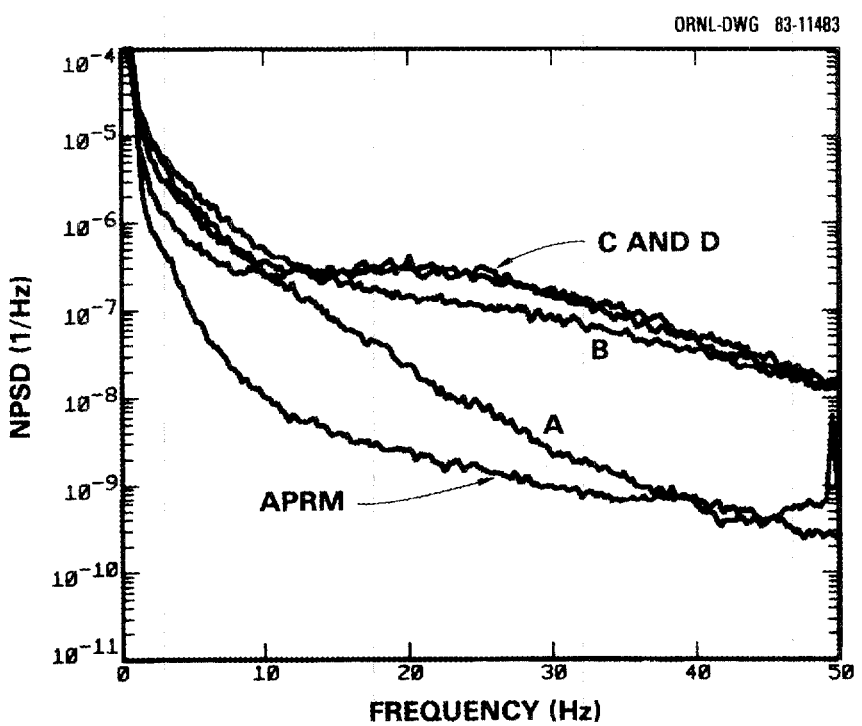

Fig. 39. NPSDs for the APRM and the four detectors in LPRM string 08-33 (Browns Ferry 3 on January 17, 1977).

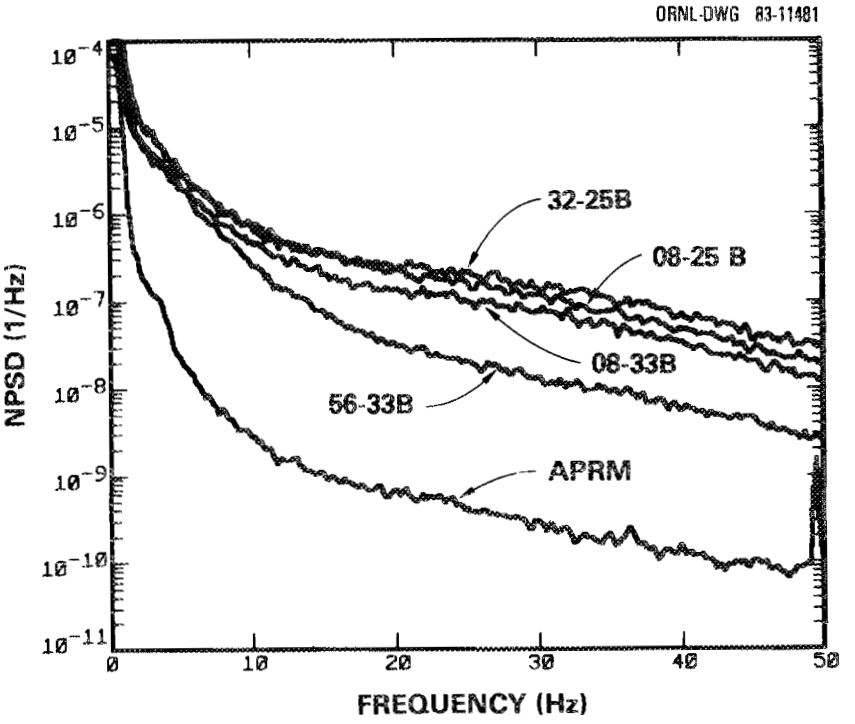

Fig. 40. NPSDs for the APRM and the B-level detectors in four LPRM strings (Browns Ferry 3 on January 17, 1977).

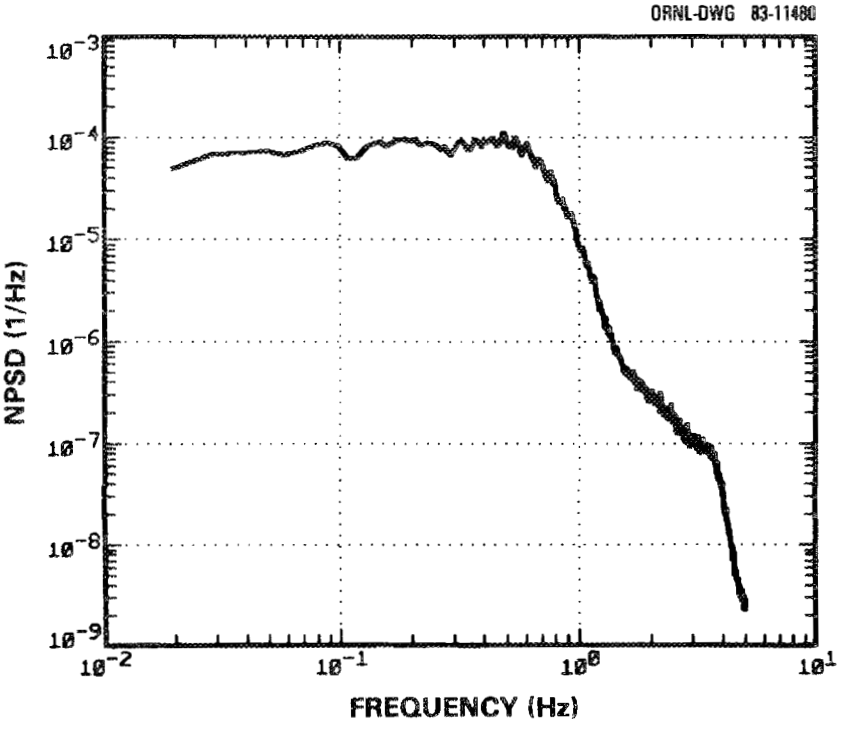

Fig. 41. NPSD of a typical APRM signal in a BWR at full power (Browns Ferry 3 on January 18, 1977).

8.1 SOURCES OF BWR NEUTRON NOISE

A great deal of research has been and is being performed worldwide on understanding the sources of BWR neutron noise. A very good starting place for the reader interested in BWR noise is a 1981 book by Thie.[3] That work, together with recent updates provided by the proceedings of the 1981 International Meeting of Reactor Noise Specialists[7] and an excellent contribution by Difilippo,[55] provides a good overview of the current understanding of BWR neutron noise. We will not attempt to review all of the previous work here, but only summarize some of the present knowledge and point out a few diagnostic applications of BWR neutron noise.

The major source of normal BWR neutron noise is the formation, collapse, and transport of steam voids in the reactor core. The voids modify neutron absorption and thermalization, thereby introducing perturbations in cross sections and thus in the neutron density as seen by the in-core fission detectors.[14,56] The APRM signature is a measure of the radially correlated sources of neutron noise in the core, whereas the difference between APRM and LPRM noise is an indication of the uncorrelated noise at a given detector location. Because the APRM signal is made up of the sum of 20 to 30 LPRM signals, any portion of the individual signals that is uncorrelated will tend to be reduced in the total signal by a factor of approximately one over the square root of the number of signals in the sum. The overall fluctuations in core voids introduce a feedback to the core dynamics which, when coupled with the thermal-hydraulic behavior, causes spatially correlated low-frequency fluctuations. This is believed to be the source of the resonance at ~0.5 Hz in the APRM signature shown in Fig. 41.

The major source of radially uncorrelated noise is the perturbations in neutron flux caused by voids in the vicinity of the neutron detectors. This generally accounts for the increased noise "seen" by the LPRM detectors at frequencies above 1.0 Hz. Note that the detectors near the top of the core (detectors C and D in Fig. 39) see more radially uncorrelated noise (presumably because there are more voids) than those near the bottom. Differences in local void fraction may also account for the differences in noise on the B-level detectors in Fig. 40. These interpretations of the sources of BWR neutron noise suggest several diagnostic applications.

8.2 APPLICATION OF NEUTRON NOISE IN BWRs

Behringer and Crowe[57] provide a good summary of several applications of neutron noise in BWRs, including instrument tube vibration monitoring, detection of bypass coolant boiling, and investigation of two-phase flow characteristics in BWR fuel assemblies.

The following sections summarize our evaluation of these applications--and an additional one, stability monitoring--in order to provide guidance on the use of neutron noise for diagnosis in BWRs.

8.2.1 Vibration Monitoring

It was originally thought that void-induced noise would mask the neutron noise caused by in-core vibrations in BWRs. However, in at least one case, instrument tube vibration, noise analysis was instrumental in identifying the problem and confirming that the solution offered by the reactor manufacturer cured the problem.[58,59]

The nature of the problem is illustrated in Fig. 42. In order to improve cooling in the vicinity of the in-core instrument tube, up to four coolant bypass holes (as needed) were drilled through the lower core support plate near each instrument tube penetration. While the holes improved the cooling, they also created a flow along the tubes that induced tube vibrations of sufficient amplitude that some of the instrument tubes contacted the corners of adjacent fuel channel boxes with sufficient force and rapidity to cause wear of the boxes. The vibration of instrument tubes caused the neutron detectors contained therein to move in a flux gradient, thus creating fluctuations in the detector output. Cheng and Diamond[60] calculated the amount of signal fluctuation caused by vibration and concluded that wear on the corners of channel boxes caused by impacting would allow higher amplitude vibration and thus more neutron noise. However, this technique required that the channel boxes be damaged before an increase in noise could be observed.

On the other hand, ORNL noise analysts and their consultants from the University of Tennessee used the neutron noise from LPRM detectors to detect when the instrument tubes were impacting the fuel box, thus providing a means of preventing damage to the boxes.

Figure 43 shows the flow dependence of the normalized* cross power spectral density (NCPSD) of the upper two LPRM detectors (C and D) in a vibrating instrument tube. NCPSD was used in order to enhance the vibration-induced signature by eliminating some of the uncorrelated noise caused by local voids near the detectors. Note that the resonance in the 1- to 3-Hz frequency range (due to the instrument tube's natural frequency) did not disappear at 50% flow. However, the broader resonance in the vicinity of 5 Hz diminished as the flow was reduced. We concluded that impacts of the instrument tube on the fuel channel box excited the box's natural resonant frequency (~5 Hz). The motion involved is similar to a cantilevered beam attached to the lower core support plate, with the largest amplitude in the upper region of the core (thus the use of detectors C and D for maximum sensitivity of diagnosis). This motion caused perturbations in the neutron flux that were coherent along the tube axis. Until a solution to the problem could be implemented, noise analysis was used by the USNRC and the BWR operators to establish an operating condition (~50% flow and 60% power) where fuel channel box damage would not occur.

Neutron noise (NCPSD) analysis was also used to determine the degree to which plugging the preexisting bypass cooling holes in the core sup-

---

*The magnitude of CPSD was normalized by dividing by the product of the dc signal levels of detectors C and D.

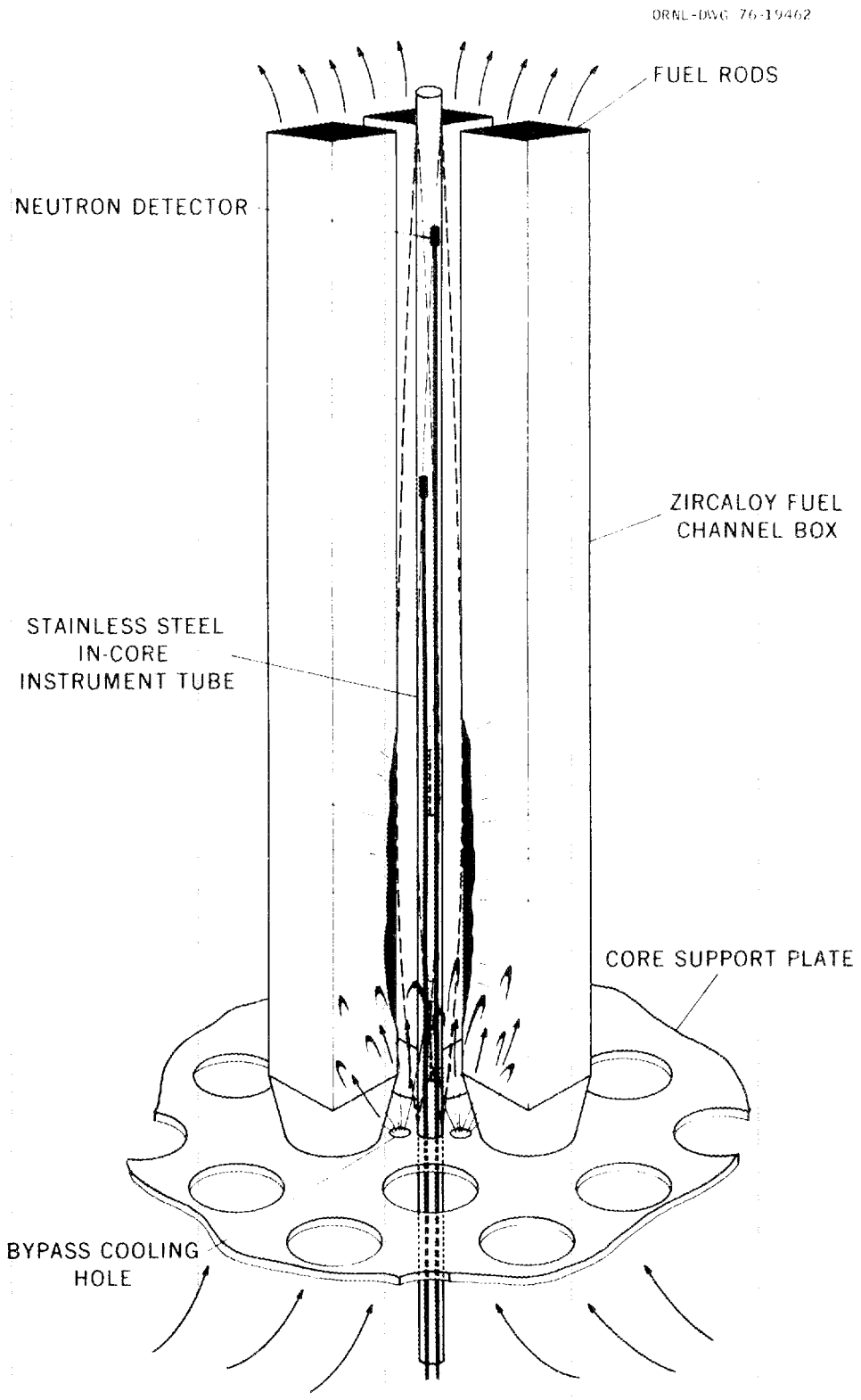

Fig. 42. Bypass flow which caused in-core instrument tubes to vibrate in BWR-4s.

ORNL-DWG 76-9892R

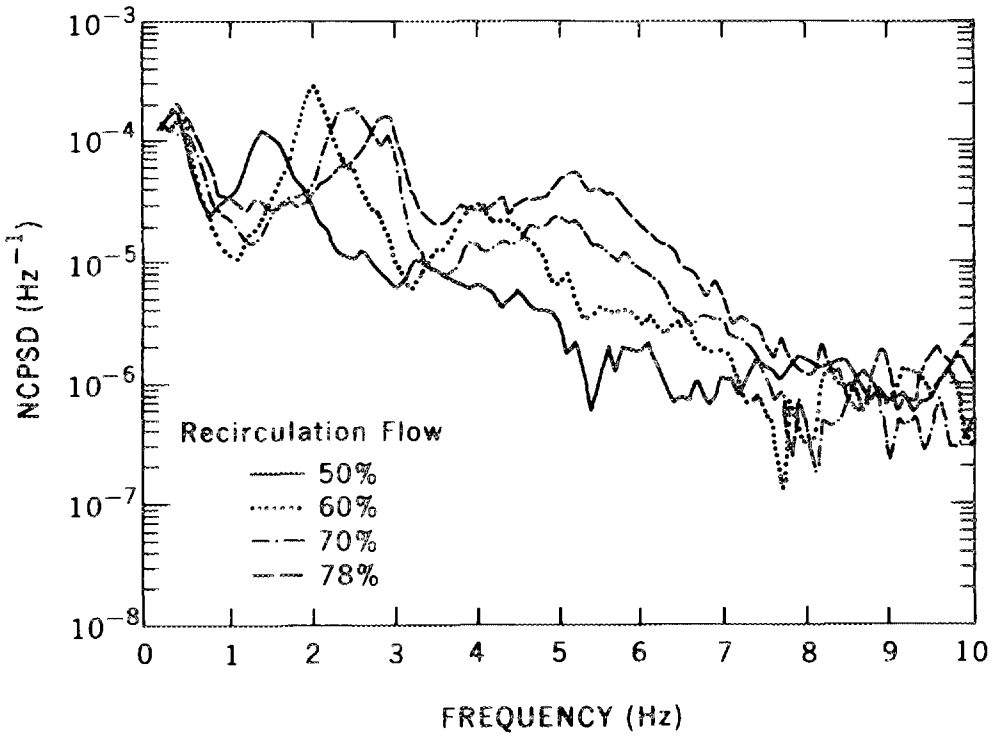

Fig. 43. Flow dependence of NCPSD between C and D detectors when instrument tubes were vibrating.

port plate (an interim solution) eliminated instrument tube vibrations and impacts. The NCPSD measurements were made at a BWR-4 plant before and after the coolant holes were plugged, utilizing an on-line minicomputer-based noise analysis system developed by ORNL.

Figure 44 shows spectra obtained before and after plugging. Note that the NCPSD measurement confirmed that plugging the cooling holes eliminated the vibrations and impacting. Furthermore, the coherence between C and D detectors (Fig. 45) is negligible in the 3.5- to 6-Hz range after plugging, which supports the conjecture that channel box motion caused by impacting results in neutron flux perturbations which are coherent along the tube axis. Figure 46 compares the neutron noise signatures from 31 instrument tubes in a core that was modified by plugging the bypass cooling holes and a typical signature obtained before the holes were plugged. Since some BWR-4s were derated in power after bypass cooling holes were plugged, this technique was considered to be at best an interim solution.

A more permanent solution, developed by General Electric, consisted of plugging all bypass coolant holes in the core support plate and drilling two 1.43-cm-diam holes in the lower tie plate of each fuel assembly

ORNL DWG 76-17305R

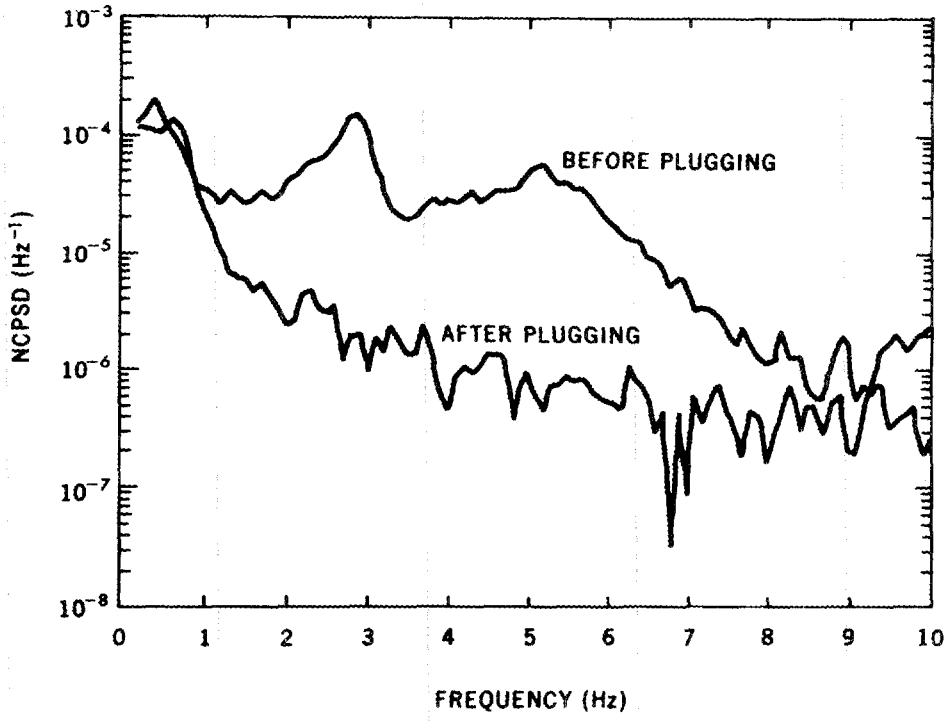

Fig. 44. NCPSD between C and D detectors before and after plugging.

to provide cooling for the instrument tubes. Figure 47 shows the signatures from 39 instrument tubes in a BWR in which this permanent solution was implemented. There is no evidence of instrument tube vibration or, more importantly, impacts on the fuel channel boxes.

This example illustrates how neutron noise analysis aided the assessment of an abnormal vibration condition in a BWR core. However, the interim solution to the instrument tube vibration problem--plugging the bypass cooling holes--introduced another potential problem, that of boiling in the bypass region around the instrument tube due to insufficient bypass region cooling. Noise analysis was also used by ORNL to assess bypass boiling, as discussed in the following section.

8.2.2 Bypass Boiling Detection

If boiling occurs in the region immediately adjacent to the neutron detectors it can produce errors in the flux readings and therefore the power monitoring of a BWR core, which is important to plant operation and safety. We hypothesized that if bypass boiling occurs, for example between the C and D detectors, additional neutron noise in the downstream detector (D) signals caused by the bypass voids will not be correlated to the upstream detector signal (C), thereby decreasing the coherence between the two signals.[61]

ORNL-DWG 76-8622R

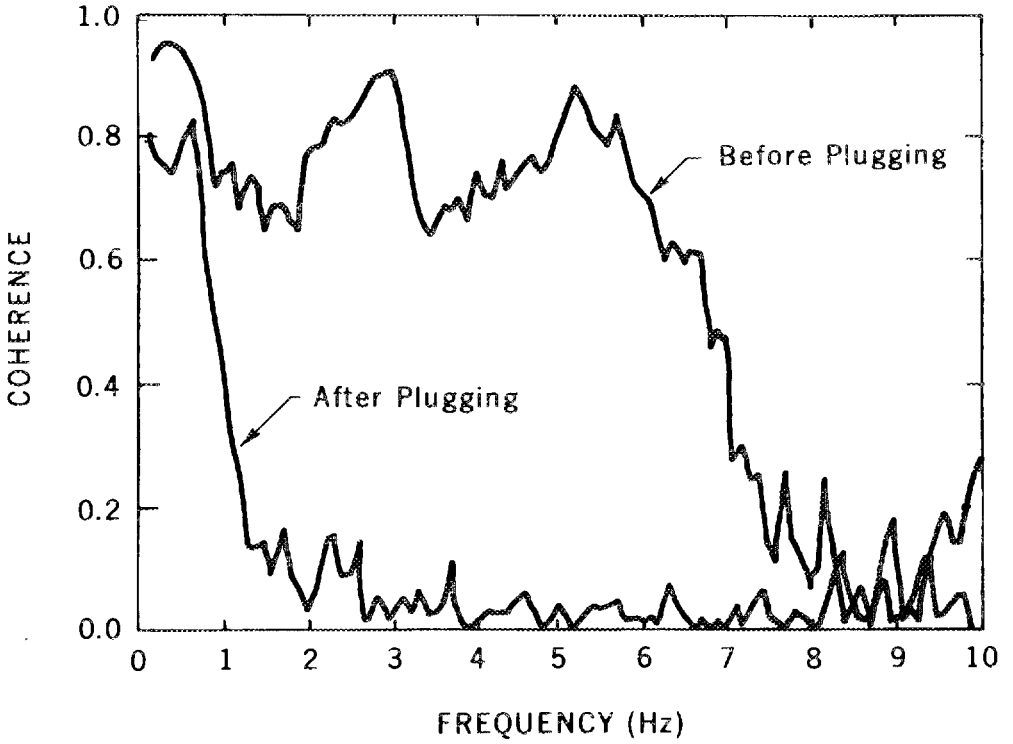

Fig. 45. Coherence between C and D detectors before and after plugging.

To establish the validity of this hypothesis, we analyzed noise recordings from plants with plugged coolant bypass holes (bypass flow only 6 to 8% of total core flow) and from plants with coolant bypass holes drilled in the lower tie plates of the fuel bundle (10 to 12% bypass flow). Figure 48 compares typical NPSDs of the C and D detector signals and their coherence in plants with 6 to 8% bypass flow to NPSDs and coherence typical of a plant with 10 to 12% bypass flow. With 6 to 8% bypass flow, the amplitude of the noise spectrum of the D detector from 1 to 10 Hz is almost an order of magnitude larger than that of the C detector (Fig. 48a), whereas with 10 to 12% bypass flow, the C and D detector noise spectra are similar in the same frequency range (Fig. 48b).

Normally, the major contributors to neutron noise in the frequency region above ~1 Hz are steam voids in the channel boxes. Most of these voids are formed below the C and D detectors such that both detectors detect some of the same voids. Therefore, the C and D detector signals are highly coherent, as in the case of the plant with 10 to 12% bypass flow (Fig. 48c). On the other hand, the added noise at the D detector location (presumably due to void formation in the bypass region between the C and D detectors) in plants with 6 to 8% bypass flow is not correlated with the C detector signal, thus resulting in a low coherence between

ORNL-DWG 76-8619R

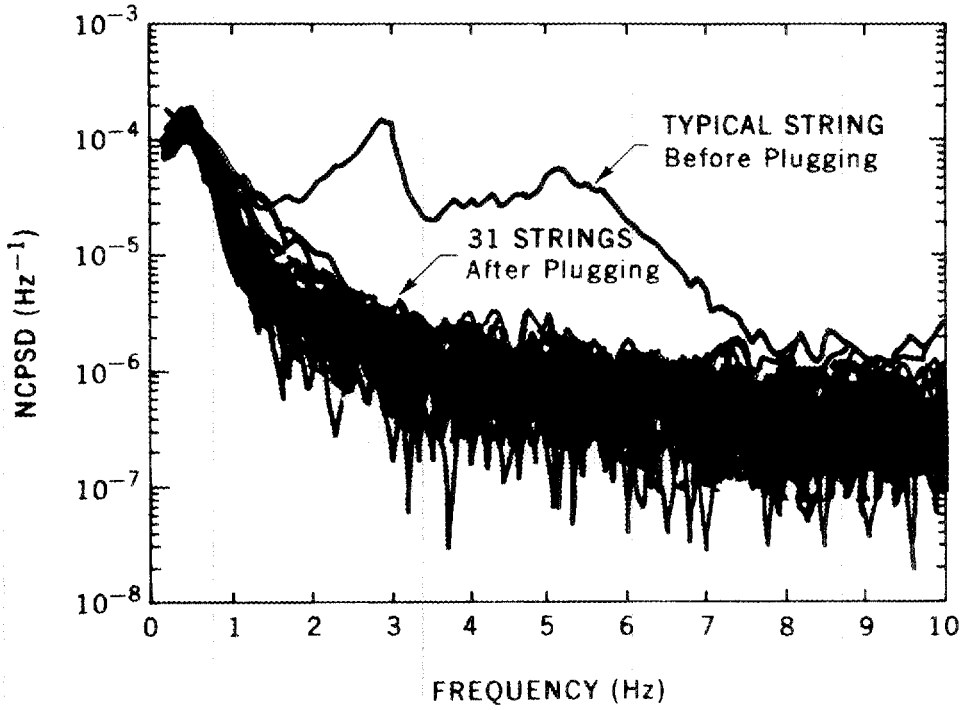

Fig. 46. Comparison of a typical impact signature (C and D NCPSD) before plugging with signatures from 31 strings after bypass cooling holes were plugged.

the C and D detector signals (Fig. 48c). (As will be discussed in the next section, noise analysts also use these correlated neutron noise signals to infer the steam-void velocity and void fraction in the channel boxes in operating BWRs.)

To support the above interpretations, we performed a thermal-hydraulic calculation to estimate the elevation at which bypass boiling occurs as a function of the bypass flow rate. The fuel bundle coolant temperature was calculated using a code developed by Mills,[62] along with a typical normalized traversing in-core probe (TIP) trace to provide the power shape. The fuel bundle temperature and flow rates, together with the bypass flow rates and inlet conditions, were used to calculate the amount of heat conducted from the fuel bundle coolant through the fuel box wall to the bypass coolant. The heat contribution from fast-neutron moderation in the bypass coolant was also included, based on work by Carlson.[63] From these heat sources we estimated the temperature of the bypass coolant as a function of elevation and bypass flow. Figure 49 shows that for 6 to 8% bypass flow the average bypass coolant temperature is predicted to reach saturation (bulk boiling) at ~100 to 126 in. elevation (between the C and D detectors). For bypass flows greater than ~9%, the saturation temperature is not attained in the bypass region at elevations below the core outlet.

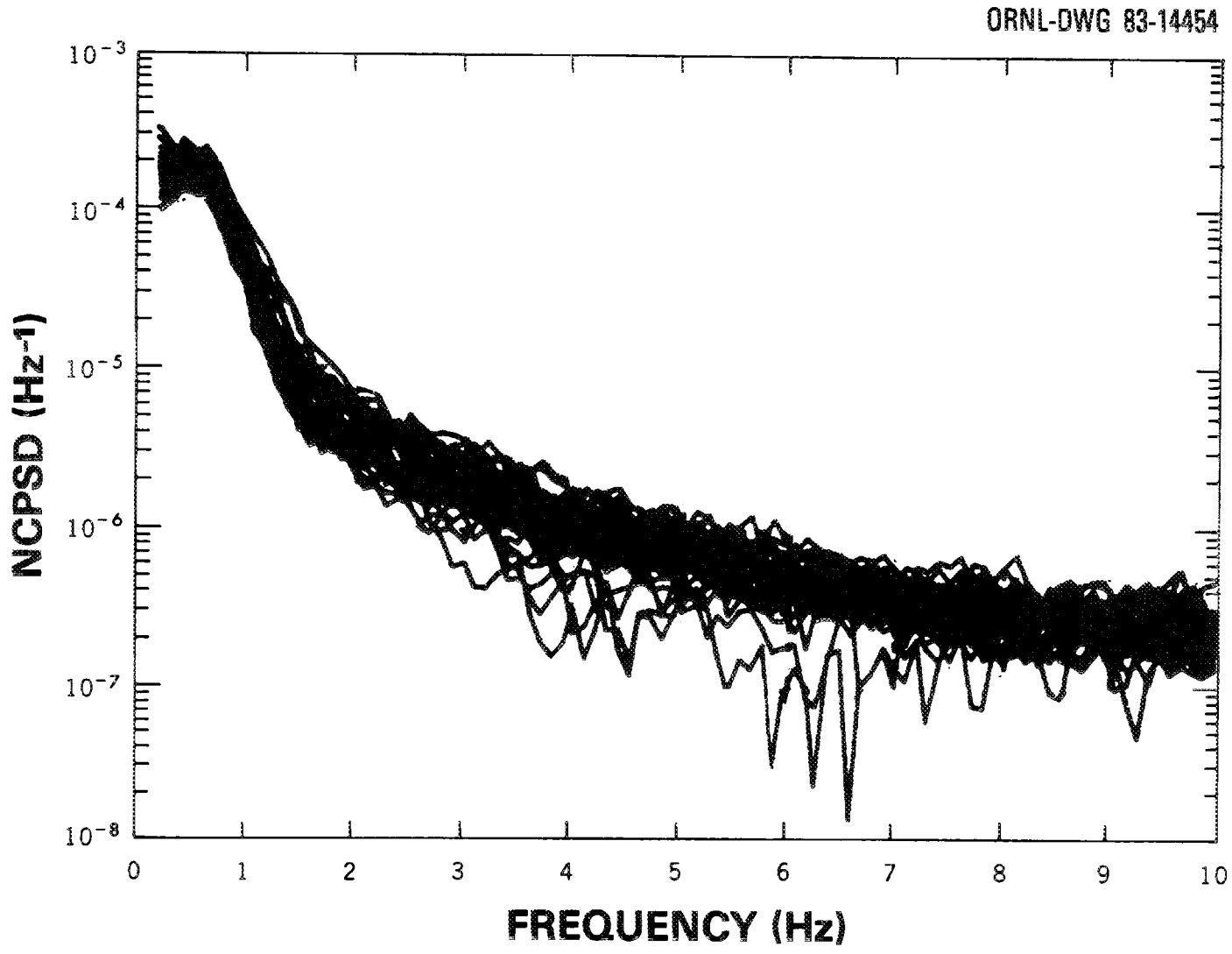

Fig. 47. NCPSD between C and D detectors for a BWR-4 following tie plate modifications.

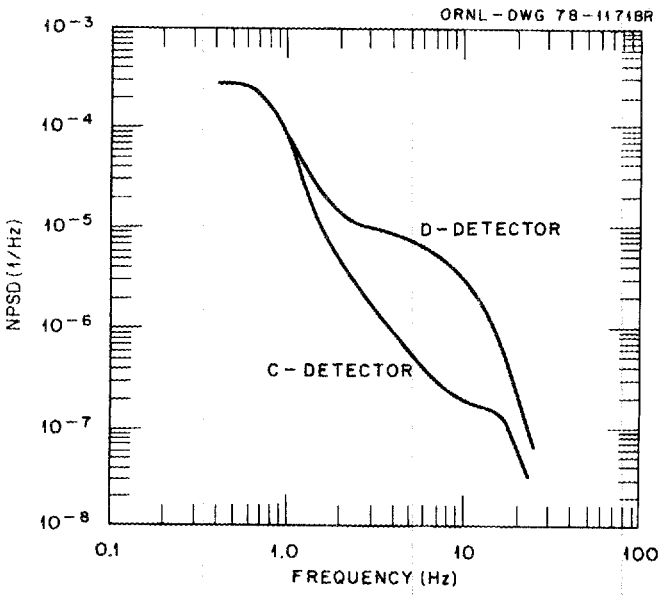

(a) Power spectrum for bypass flow of 6-8%.

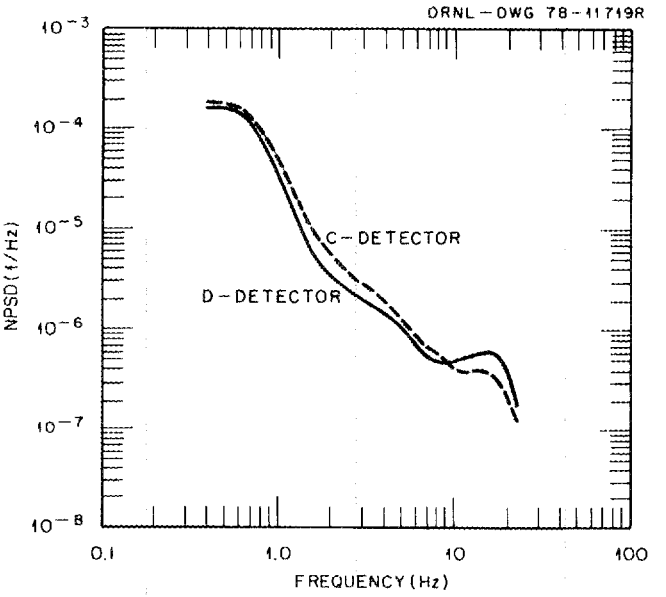

(b) Power spectrum for bypass flow of 10-12%.

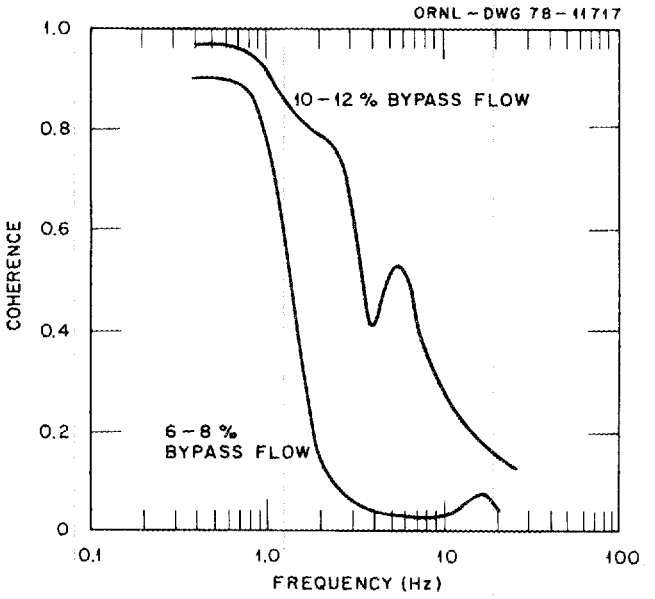

(c) C-D detector coherence spectra for different bypass flows.

Fig. 48. BWR in-core neutron noise as a function of bypass flow.

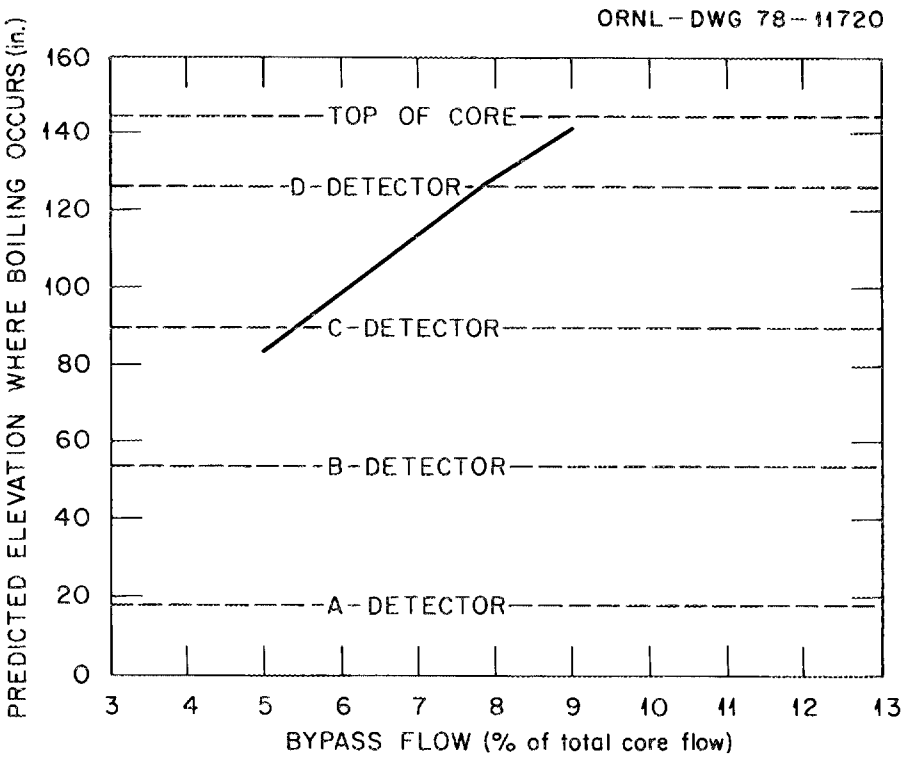

Fig. 49. Core elevation where bypass coolant bulk boiling is predicted to occur.

These results suggest that the axial location at which bypass boiling occurs might be determined with the aid of TIPs, and that with additional measurements and more refined thermal-hydraulic calculations it might be possible to infer the bypass void fraction, which is of interest in the safety evaluation of BWRs.

8.2.3 Two-Phase Flow Measurement

We will not attempt to summarize the considerable research that has been conducted throughout the world since Seifritz and Cioli[64] first reported the use of neutron noise for investigation of two-phase flow in BWRs. Our intent here is to introduce the subject and summarize some methods used by ORNL to infer in-core steam velocity and void fraction using LPRM noise signals.

It is postulated that LPRM noise above 1 Hz is dominated by neutron density fluctuations caused by the formation and transport of steam voids. As steam bubbles are formed they are carried by the flowing water from the point of formation to the top of the core (if they survive), thereby perturbing the local neutron field with their passage. If the signal from one LPRM detector is delayed τ seconds with respect to another axially separated detector (in the same LPRM string), the phase angle between the signals is expected to be a linear function of frequency as shown in Fig. 50. The time delay, τ, between axially

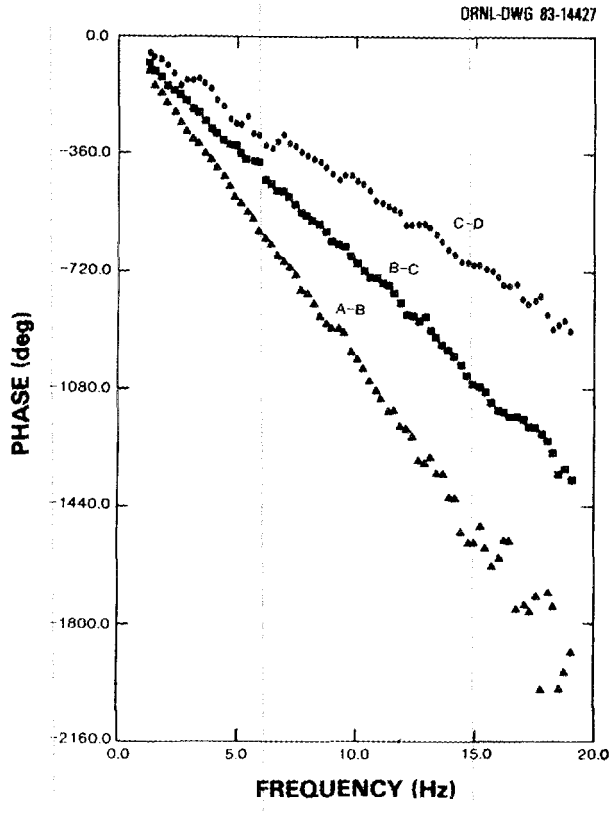

Fig. 50. Phase versus frequency for A-B, B-C, and C-D detector pairs in LPRM string 20-37 at Hatch 1 on January 14, 1976.

separated LPRMs can be inferred from the phase angle versus frequency plot using the relationship

$$\tau = \frac{-\Delta\Theta}{\Delta f \cdot 360}, \tag{12}$$

where $\Delta\Theta/\Delta f$ is the slope of the phase angle versus frequency (deg/Hz). If the delay between LPRMs is the result of void transport, an average velocity can be inferred over an interval Z_1 to Z_2 by knowing the distance between the detectors:

$$V_{1,2} = |Z_2 - Z_1|/\tau_{1,2} \tag{13}$$

where $V_{1,2}$ is the average velocity over the interval from Z_1 to Z_2.

Several factors are important to such an inference of velocity from the phase angle of axially separated LPRMs: (a) the frequency range of phase measurements, (b) the spatial sensitivity of void detection by the neutron detectors (detector "field of view"), (c) the response of the reactor neutron dynamics and the detectors to void formation and propagation, and (d) the stochastics of void propagation and formation. A strong note of caution in the measurement of delay time between detectors is in order: The frequency response of the LPRM flux amplifiers must be taken into account because it can vary depending on the amplifier gain (see Sect. 4).

As part of another project[65] we performed both a deterministic thermal-hydraulic analysis and a stochastic space-, frequency-, and energy-dependent neutron kinetics analysis. In the latter analysis the reactor system was treated as steady-state, but the stochastic analysis considered the small fluctuations (noise) that occur in a BWR and their space-energy statistical correlation. The analysis was performed over a frequency range of 2 to 10 Hz based on observations that other noise processes (such as reactivity feedback from voids and temperature) influence the neutron noise below 2 Hz and that flux amplifier frequency response and neutron kinetics can affect the phase measurement at frequencies above 10 Hz. From the deterministic analysis we concluded that the velocity obtained using noise analysis is closely related to the steam velocity occurring within the bundles (except at the top and bottom of the core) but that the agreement between predicted and measured velocities is highly dependent on the two-phase flow correlations employed in the thermal hydraulic analysis. Uncertainties in the bundle flow rate, power, and heat flux distribution, as well as the inherent inaccuracies of subchannel analysis codes, suggest caution in relating the inferred velocities to specific thermal-hydraulic conditions in the fuel bundles.

The conclusions drawn from the stochastic analysis yielded some insight into the LPRM detector field of view:

1. The axial and radial detector fields of view are highly peaked at the detector location.

2. The detector fields of view are independent of frequency in the range 2 to 10 Hz.

3. The detector field of view varies with axial detector location.

The stochastic studies also showed that the LPRM is sensitive to more of the fuel bundle in the radial direction at the top of the core than at the bottom. While additional work needs to be done to study the effects of control rod position, burnup, and bypass boiling, we conclude that the LPRM spatial field of view is an important factor and must be considered in any interpretation of inferred velocities using noise analysis.

We have also evaluated the feasibility of using the inferred velocities to determine the average void fraction in the four fuel bundles that surround an in-core detector string.[66] The velocity, together with the measured power distribution and mass flow rate, was used to obtain the void fraction as a function of axial position using

$$\alpha(Z) = \frac{W\chi(Z)}{A\rho_g V_g(Z)} \tag{14}$$

where W is the mass flow rate in the channel, χ the local quality, A the flow area, ρ_g the steam density, and V_g the steam velocity inferred from neutron noise.

Figure 51 shows the steam velocity inferred from neutron noise as a function of axial position. These measurements were made at the Hatch 1 plant using the TIP together with the fixed LPRM detectors to measure velocity at seven axial positions. Also shown is the void fraction obtained from the measured steam velocity compared with an analytical calculation of void fraction using a semi-empirical correlation recommended by Zuber et al.[67] These results suggest that neutron noise analysis may provide a measure of void fraction in BWRs. However, considerable research in this area is still being conducted both in the U.S.[68] and other countries,[69] to better understand the limitations of the method.

8.2.4 Stability Monitoring

Three different types of instabilities are widely recognized as being possible in commercial BWRs:[70,71] (a) total plant instability, which is related to the reactor control systems; (b) channel thermal-hydraulic instability, which is related to flow oscillations in single fuel channels; and (c) reactivity instability, which results from the interactions between the reactor neutronics and the thermal-hydraulic feedback loops. This last type of instability is of major concern with respect to BWR operation at low recirculation flow rates.

A major characteristic of the low-frequency part of the BWR neutron noise spectrum is a resonance in the frequency range between 0.3 and 0.7 Hz. BWR stability experiments[72-74] have shown that this resonance is

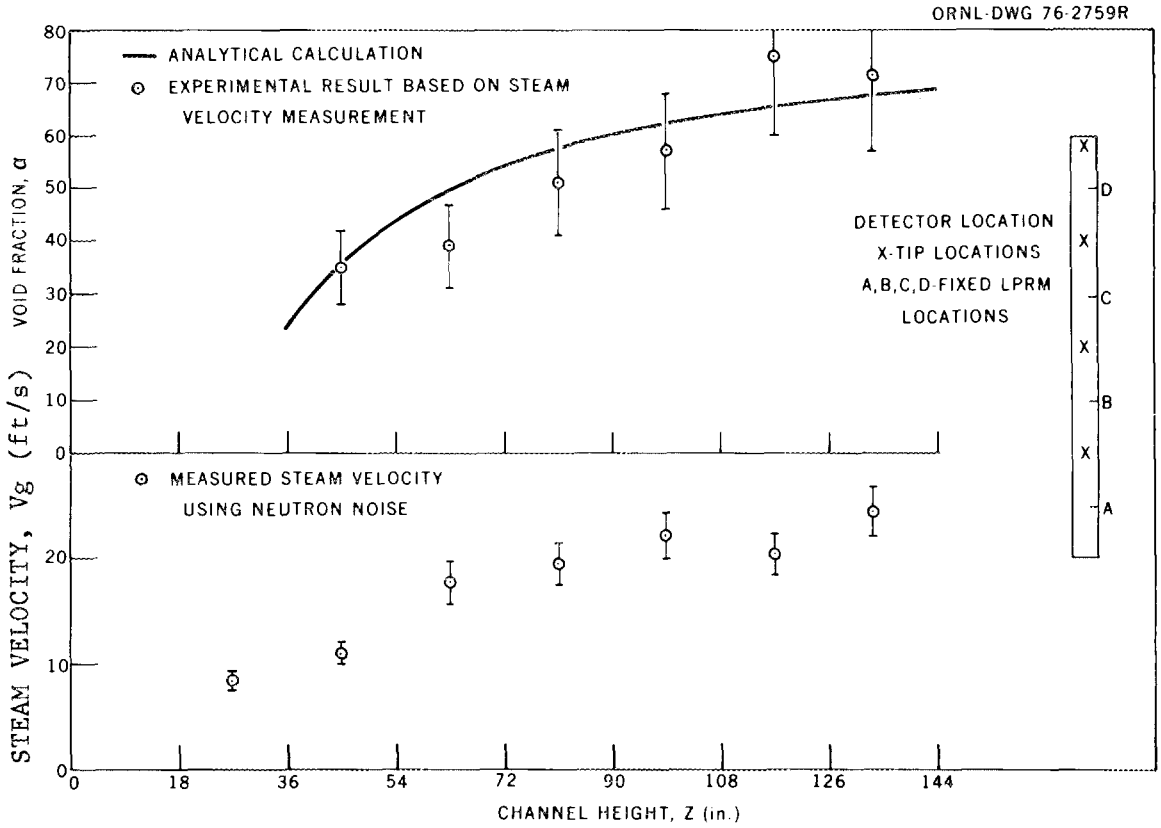

Fig. 51. Steam velocity and void fraction as a function of the channel height Z.

due to the reactivity-to-power closed-loop transfer function, and thus is related to the reactivity stability.

Stability is usually quantified in terms of a decay ratio; however, several definitions of decay ratio can be found in the literature. We have determined that only the "asymptotic" decay ratio correctly specifies the absolute reactor stability. The asymptotic decay ratio is defined as the limit of the sequence formed by the ratios between every two consecutive peaks in either the impulse response or the autocorrelation function; it can also be determined from the position of the most unstable pair of complex conjugate poles in the reactor transfer function using the relation

$$DR = e^{-\frac{2\pi\sigma}{\omega}} \tag{15}$$

where σ and ω are, respectively, the real and imaginary parts of the pole.

Three different methods of estimating the asymptotic decay ratio were evaluated at ORNL:

(a) Correlation function: The asymptotic decay ratio is obtained directly from the measured autocorrelation function of the neutron noise (an APRM signal should be used to minimize the radially uncorrelated noise caused by perturbations in the neutron flux near the detector).

(b) NPSD fit: The NPSD is fitted to a functional form containing only poles and zeros. The asymptotic decay ratio can then be obtained from the position of the most unstable complex pole, which should correspond to the 0.3- to 0.7-Hz peak in the PSD.

(c) Autoregressive (AR) model: A univariate AR model of the form

$$x(t) = \sum_{k=1}^{N} A_k \, x(t-k\Delta t) + V(t) \tag{16}$$

is fitted to an APRM signal, x(t). The model order is chosen so as to minimize Akaike's information criterion as described in ref. 75. The impulse response can be estimated from the model as

$$h(t) = \sum_{k=1}^{N} A_k \, h(t-k\Delta t) \tag{17}$$

with $h(0) = 1$ and $h(-k\Delta t) = 0$. The asymptotic decay ratio is then obtained directly from h(t).

Our evaluation of these methods showed that the correlation technique is the most accurate method because it does not require any model fitting that could introduce bias error; however, unless the decay ratio is close to unity, extremely large amounts of data are needed for the autocorrelation function to converge at large time lags. The PSD fit method proved to be the least reliable of the three: when a second-order model (2-poles) was fitted, the errors in the calculated decay ratio were large, and most of the time the estimates were non-conservative; higher order fits yielded better results, but the fitting procedure was lengthy and difficult. The AR model technique gave the best results, even for limited amounts of data, and hence we recommend it for BWR stability measurements with noise analysis.

As an example, the AR technique has been applied to the APRM-B signal from Browns Ferry 3 operating at full rated power. Figure 52 shows a comparison between the NPSD using fast Fourier transform (FFT) analysis (crosses) and the NPSD predicted by the optimal AR model of order 30 (solid line). This figure shows that the AR fit can be highly accurate if enough data (in this case 2 h) and a sufficiently high-order model are used. The impulse response corresponding to this model is represented in Fig. 53; from it a decay ratio estimate of 0.12 ± 0.04 was

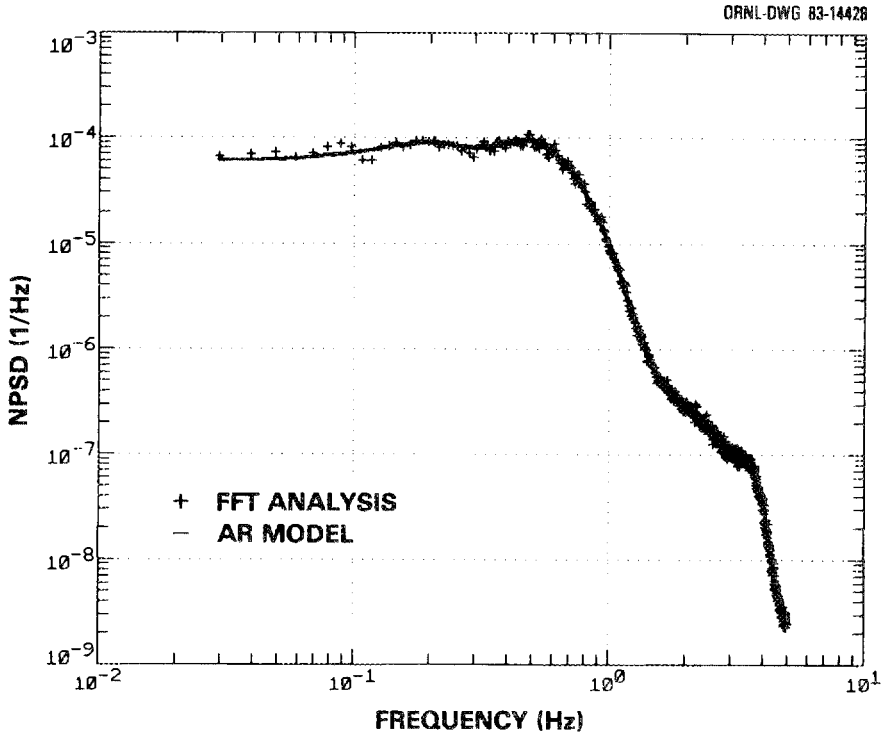

Fig. 52. Comparison of Browns Ferry 3 NPSDs obtained by using Fast Fourier Transform (FFT) and by using the optimal autoregressive (AR) model.

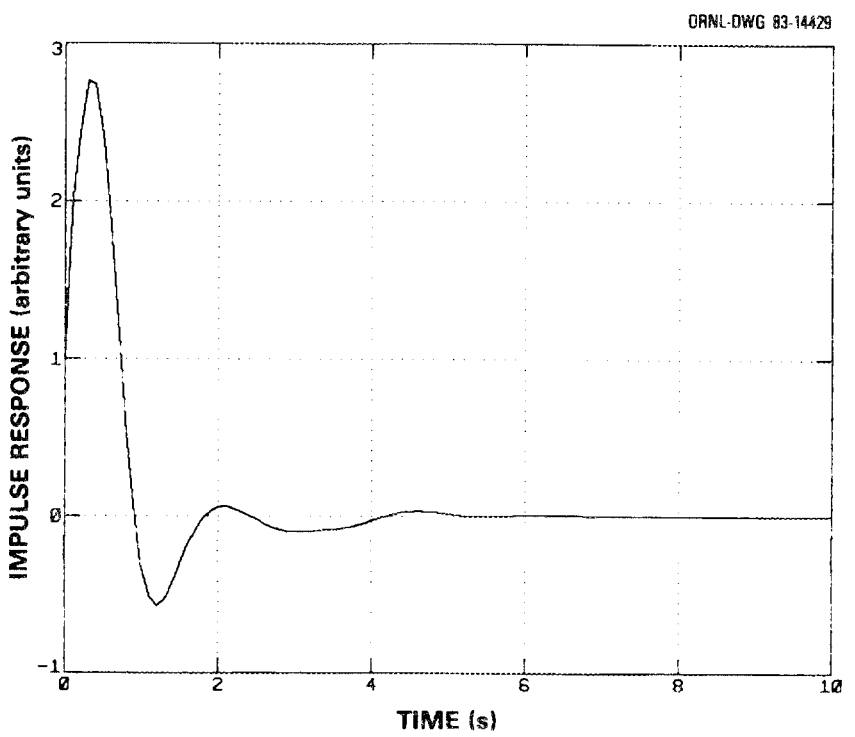

Fig. 53. Impulse response obtained from the optimal AR model fit to the Browns Ferry 3 APRM signal.

obtained. The error estimate is based on the statistical uncertainty of the measured NPSD, which in turn depends on the amount of data used. The error in estimating decay ratios can be very large (in this case, with a 2-h measurement, the error was 33%) fortunately, the error decreases as the decay ratio approaches unity (the stability limit). In fact, 5 min of data yield an error of only 2% when the decay ratio is 0.95.

9. SUMMARY AND CONCLUSIONS

The value of neutron noise analysis for diagnosis of in-vessel anomalies in LWRs was assessed by:

(1) analyzing ex-core neutron noise from seven PWRs to determine the degree of similarity in the noise signatures and the sources of ex-core neutron noise;

(2) measuring changes in ex-core neutron noise over an entire fuel cycle at a commercial PWR;

(3) applying PWR neutron noise analysis to diagnose a loose core barrel, to infer in-core coolant velocity, and to infer fuel assembly motion; and

(4) applying BWR neutron noise analysis to diagnose in-core instrument tube vibrations and bypass coolant boiling, to infer in-core, two-phase flow velocity and void fraction, and to infer stability associated with reactivity feedback.

We conclude that ex-core neutron noise can be used to monitor in-vessel structural component vibrations in PWRs, providing the contribution of individual structures can be separated from the total noise spectrum. A better understanding of the scale factors used to infer the amplitude of vibration is needed, especially the variation of these scale factors over the fuel cycle. The use of neutron noise coupled with core exit temperature noise shows promise as a method of monitoring for inadequate core cooling (through measurement of coolant velocity), provided core-exit thermocouples have adequate time response. The results of additional research in the U.S. and abroad should confirm the sensitivity and limitations of neutron noise analysis for inferring in-core coolant velocity.

A great deal of similarity was found in the PWR noise signatures we obtained and also in the resonant frequencies reported for structural components in PWRs. However, we conclude that to obtain the maximum benefits from neutron noise monitoring, each plant should maintain its own file of baseline signatures.

We conclude that although BWR neutron noise was used to diagnose abnormal vibration of instrument tubes and fuel boxes, we cannot generalize that other vibrations could be detected in the presence of the large background noise caused by boiling. We are also confident that the stability associated with reactivity feedback in BWRs can be quantitatively measured by performing noise analysis of the APRM signal. Additional research needs to be performed to reduce uncertainties associated with the interpretation of BWR noise for inferring bypass coolant boiling or two-phase flow parameters.

10. RECOMMENDATIONS

In view of the research still being conducted world-wide, we hesitate to make specific recommendations regarding the use of neutron noise for anomaly detection, and this will be the case for some years into the future. However, for the present we believe that the maximum benefit of neutron noise analysis can be realized only if each plant has a program to perform either continuous or periodic measurements to establish baseline signatures and their normal variations. If a generic problem should then surface for that type of plant, the data on file could be used by all affected licensees and the USNRC to verify the condition of the component associated with the problem in other similar plants without a necessity for costly shutdowns. Of course, uniform methods of neutron noise measurement and results presentation should be used to avoid confusion in comparing measurements among plants.

At its present state of development we don't see neutron noise analysis as a real-time operating aid for use by control room operators to make decisions regarding day-to-day operations or for use by the plant protection system.

On the other hand, the develoment status of noise data reduction hardware and software techniques no longer places a limitation on the in-plant use of noise analysis. In fact, ORNL has demonstrated a noise monitoring system that automatically screens noise signatures and retains only those that differ statistically from the established baseline condition. This screening greatly reduces the amount of data requiring evaluation by a noise analyst.

Since the evidence presented in this report and in the literature indicates that there is a large potential value of neutron noise analysis for in-vessel component vibration monitoring in PWRs, we suggest an optimum noise monitoring program containing the following elements:

(1) Identification of the natural resonant frequencies of pressure vessel internal structures from hot functional accelerometer measurements, on a plant-specific basis if possible.

(2) Comparison of results from in-plant accelerometer measurements with calculations of resonant frequencies and measurements in reactor manufacturers' test facilities.

(3) Monitoring of neutron noise from a minimum of four ex-core detectors (and several in-core locations for more ambitious programs) at startup, just prior to refueling shutdowns, and periodically throughout each fuel cycle.

(4) Identification of in-vessel component vibration frequencies in the neutron noise by comparison with mechanical analysis and out-of-reactor measurements.

The value of routine neutron noise monitoring in BWRs is still being evaluated, but it appears that potential benefits could be gained by:

(1) measuring the decay ratio using the APRM signal, especially during single-loop operation or when introducing new fuel designs; and

(2) utilizing LPRM and APRM signals to establish baseline signatures for various normal operating conditions for use in future assessments of possible anomalies.

Finally, we strongly recommend that reactor owners' groups, the Electric Power Research Institute, or the Institute of Nuclear Power Operations conduct periodic workshops for utility representatives to share experiences in the interpretation and application of neutron noise for diagnosis of nuclear power plant problems.

REFERENCES

1. R. E. Uhrig, *Random Noise Techniques in Nuclear Reactor Systems*, New York: Ronald Press Co. (1970).

2. M. M. R. Williams, *Random Processes in Nuclear Reactors*, Oxford, England: Pergamon Press, Ltd. (1974).

3. J. A. Thie, *Power Reactor Noise*, La Grange Park, Ill: American Nuclear Society (1981).

4. G. Kosály, "Noise Investigations in Boiling-Water and Pressurized-Water Reactors," *Prog. Nucl. Energy* 5, 145-199 (1980).

5. "Proceedings of the European-American Committee on Reactor Physics Specialist Meeting on Reactor Noise: From Critical Assemblies to Power Reactors, Rome, 21-25 October 1974," *Ann. Nucl. Energy* 2, Pergamon Press (1975).

6. M. M. R. Williams and R. Sher, "Reactor Noise-SMORN II," *Prog. Nucl. Energy* 1, Pergamon Press (1977).

7. M. M. R. Williams, "Reactor Noise-SMORN III," *Prog. Nucl. Energy* 9, Pergamon Press (1982).

8. D. N. Fry, R. C. Kryter, and J. C. Robinson, "Analysis of Neutron-Density Oscillations Resulting from Core Barrel Motion in the Palisades Nuclear Power Plant," Oak Ridge National Laboratory Report ORNL/TM-4570 (1974).

9. D. N. Fry, R. C. Kryter, M. V. Mathis, J. E. Mott, and J. C. Robinson, "Summary of ORNL Investigation of In-Core Vibrations in BWR-4s," Oak Ridge National Laboratory Report ORNL/NUREG/TM-101 (1977).

10. J. C. Robinson, "Analysis of Neutron Fluctuation Spectra in the Oak Ridge Research Reactor and the High Flux Isotope Reactor," Oak Ridge National Laboratory Report ORNL-4149 (1967).

11. C. E. Cohn, "A Simplified Theory of Pile Noise," *Nucl. Sci. Eng.* 7, 472-475 (1960).

12. F. J. Sweeney and J. P. Renier, "Sensitivity of Detecting In-Core Vibrations and Boiling In Pressurized Water Reactors Using Ex-Core Neutron Detectors," Oak Ridge National Laboratory Report NUREG/CR-2996, ORNL/TM-8549 (1983).

13. J. P. Renier and F. J. Sweeney, "A Method to Calculate Detector Kinetic Sensitivities to In- and Ex-Core Perturbations of Power Reactors," Topical Meeting on Advances in Reactor Computations, Salt Lake City, Utah, March 28-31 (1983).

14. F. J. Sweeney, "A Theoretical Model of Boiling Water Reactor Neutron Noise," Ph.D. dissertation, The University of Tennessee, Knoxville, Tennessee (1980).

15. J. S. Bendat and A. G. Piersol, *Random Data: Analysis and Measurement Procedures*, New York: Wiley-Interscience (1971).

16. C. M. Smith and F. J. Sweeney, "Demonstration of an Automated On-Line Surveillance System at a Commercial Nuclear Power Plant," *Proc. Fifth Power Plant Dynamics, Control, and Testing Symposium*, Knoxville, Tennessee (March 1983).

17. W. T. King, "The Convergence of the Coherence Function," internal ORNL Application note (February 1980).

18. A. J. Spurgin, "Some Aspects of the Process Control and Protection Systems of a Westinghouse PWR," *IEEE Trans. Nucl. Sci.* 17, 599-607 (February 1970).

19. K. J. Serdula, "Canadian Experience in the Area of Reactor Noise," *Ann. Nucl. Energy* 2, 287 (1975).

20. J. C. Robinson et al., "Noise Analysis Investigation at the Oconee Nuclear Power Plant," *Trans. Am. Nucl. Soc.* 19, 383 (1974).

21. J. H. Steelman and B. T. Lubin, "Analysis of Changes with Operating Time in the Calvert Cliffs Unit 1 Neutron Noise," *Prog. Nucl. Energy* 1, 389 (1977).

22. J. A. Thie, "Neutron Noise Sources in PWRs," *Prog. Nucl. Energy* 1, 284 (1977).

23. D. Wach and R. Sunder, "Improved PWR Neutron Noise Interpretation Based on Detailed Vibration Analysis," *Prog. Nucl. Energy* 1, (1977), p. 320.

24. J. B. Dragt and E. Turkcan, "Borssele PWR Noise: Measurements, Analysis and Interpretation," *Prog. Nucl. Energy* 1, 293-307 (1977).

25. J. P. Niessel, W. K. Green, and Y. Dayal, "Method and Apparatus for Monitoring the Output of a Neutron Detector," U.S. Patent No. 4,103,1066 (July 25, 1978).

26. J. F. Boland, *Nuclear Reactor Instrumentation (In-Core)*. New York: Gordon and Breach (1970).

27. C. W. Mayo, "Detailed Neutron Noise Analysis of Pressurized Water Reactor Internal Vibrations," *Atomkernenergie* 29, 9-13 (1977).

28. F. Åkerhielm, R. Espefalt, and J. Lorenzen, "Surveillance of Vibrations in PWR," *Prog. Nucl. Energy* 9, 453-464 (1982).

29. J. B. Dragt, "Partial and Multiple Coherence in Nuclear Reactor Noise," *Prog. Nucl. Energy* 9, 131 (1982).

30. J. C. Robinson, J. W. Hardy, G. R. Shamblin, and C. L. Wolff, "Monitoring of Core Support Barrel Motion in PWRs Using Ex-Core Detectors," *Prog. Nucl. Energy* 1, 369-378, (1977).

31. W. G. Pettus and R. L. Currie, "Monitoring Oconee 1 Internals with Neutron Noise Analysis," Babcock and Wilcox Report TP-74-31 (December 1974).

32. C. Puyal, A. Fernandes, and C. Vincent, "Primary System Surveillance and Diagnostics of PWR Power Plants in France," presented at the Fifth Power Plant Dynamics Control and Testing Symposium, Knoxville, Tennessee (March 1983). (Note: The full manuscript may be obtained from C. Puyal or from the authors of this report).

33. P. Bernard, C. Messainguiral, J. C. Carre, A. Epstein, R. Assedo, and G. Castello, "Quantitative Monitoring and Diagnosis of French PWRs' Internal Structures Vibrations by Ex-Core Neutron Noise and Accelerometers Analysis," *Prog. Nucl. Energy* 9, 465-492 (1982).

34. J. Marini, D. Romy, J. C. Spadi, R. Assedo, and G. Castello, "Neutron Noise Measurements on Bugey 2 PWR," *Prog. Nucl. Energy* 9, 557-568 (1982).

35. V. Bauernfeind, "Investigations on the Vibrative Excitation of PWR Pressure Vessel and Internals by Pressure Noise Analysis and Model Calculations," *Prog. Nucl. Energy* 1, 323-332 (1977).

36. A. Brillon and C. Puyal, "Mechanical Surveillance of French PWRs," Electricite De France (EDF) Report ABN-CPI/LK (July 1981).

37. D. Wach and R. Sunder, "Improved PWR Neutron Noise Interpretation Based on Detailed Vibration Analysis," *Prog. Nucl. Energy* 1, 309-322 (1977).

38. R. Gopal and W. Ciaramitaro, "Experiences with Diagnostic Instrumentation in Nuclear Plants," *Prog. Nucl. Energy* 1, 759-779 (1977).

39. D. Haensel, "Vibration Measurements in a Three-Loop Pressurized Water Reactor--Instrumentation, Analysis, and Results," *ISA Trans.* 11,(4), 299-303 (1972).

40. Y. Fujita and H. Ozaki, "Neutron Noise Monitoring of Reactor Core Internal Vibrations at PWRs in Japan," *Prog. Nucl. Energy* 9, 423-436 (1982).

41. F. E. Stokes and R. A. King, "PWR Fuel Assembly Dynamic Characteristics," *Proc. Int. Conf. Vib. in Nucl. Plant*, Keswick, UK (May 1978).

42. E. Turkcan, "Review of Borssele PWR Noise Experiments, Analysis and Instrumentation," *Prog. Nucl. Energy* 9, 437-452 (1982).

43. W. Bastl and D. Wach, "Experiences with Noise Surveillance Systems in German LWRs," *Prog. Nucl. Energy* 9, 505-516 (1982).

44. P. Bernard, J. Cloue, C. Messainguiral, R. Baeyens, P. Mathot, J. Satinet, and C. Puyal, "PWR Core Monitoring by In-Core Noise Analysis," *Prog. Nucl. Energy* 9, 541-556 (1982).

45. M. Calcagno and F. Cioli, "Trino Vercellese Nuclear Power Plant In-Service Monitoring of Core Structures and Reactor Internals by Neutron Noise Measurements," Euratom Report C3.R1/09.70, by Ente Nazionale per l'Energia Elettrica, Rome (August 1970).

46. D. N. Fry, R. C. Kryter, and J. C. Robinson, "Analysis of Neutron Density Oscillations Resulting from Core Barrel Motion in the Palisades Nuclear Power Plant," Oak Ridge National Laboratory Report ORNL/TM-4570 (1974).

47. J. A. Thie, "Theoretical Considerations and Their Application to Experimental Data in the Determination of Reactor Internals" Motion from Stochastic Signals," *Ann. Nucl. Energy* 2, 253 (1975).

48. "Inservice Monitoring of Core Support Barrel Axial Preload in Pressurized Water Reactors," ANSI/ASME OM-5 (1981).

49. J. C. Robinson, F. Shahrokhi, and R. C. Kryter, "Calculation of the Scale Factor for Inference of Pressurized Water Reactor Core Barrel Motion From Neutron Noise Spectral Density," *Nucl. Technol.* 40 (August 1978).

50. J. P. Thompson, G. R. McCoy, and B. T. Lubin, "Experimental Value of Percent Variation in Root-Mean-Square Ex-Core Detector Signal to the Core Barrel Amplitude Scale Factor," *Nucl. Technol.* 48, 121 (1980).

51. T. Katona, L. Meskó, G. Pór, and J. Valkó, "Some Aspects of the Theory of Neutron Noise Due to Propagating Disturbances," *Prog. Nucl. Energy* 9, 209-222 (1982).

52. B. R. Upadhyaya and F. J. Sweeney, "Theoretical and Experimental Stochastic Modeling Analysis of PWR Core Heat Transfer," *Proc. Fifth Power Plant Dynamics Control and Testing Symposium*, Knoxville, Tennessee (March 1983).

53. F. J. Sweeney and B. R. Upadhyaya, "Relationship of Core Exit Temperature Noise to Thermal-Hydraulic Conditions in PWRs," *Proc. Second International Topical Meeting on Nuclear Reactor Thermal-Hydraulics*, Santa Barbara, California (January 1983).

54. W. J. Bailey, K. H. Rising, and M. Tokar, "Fuel Performance Annual Report for 1980," NUREG/CR-2410 (PNL-3953) (1981).

55. F. C. Difilippo, "Neutron Wave Propagation in Hetergeneous Media and the Interpretation of Neutron Noise in Boiling Water Reactors," *Nucl. Sci. Eng.* 80, 211-217 (1982).

56. F. J. Sweeney, "Modeling the Local Component of In-Core Neutron Detector Noise in a BWR," *Trans. Am. Nucl. Soc.* 33, 854-855 (1979).

57. K. Behringer and R. Crowe, "Practical Application of Neutron Noise Analysis at Boiling Water Reactors," EIR-Bericht Nr. 385, Swiss Federal Institute for Reactor Research, Ch-5303 Wurenlingen, Switzerland (1980).

58. K. Behringer, Lj. Kostic, and W. Seifritz, "Observation of In-Core Instrument Tube Vibrations in a Boiling Water Reactor by Evaluating Reactor Noise Data," *Prog. Nucl. Eng.* 1, 183 (1977).

59. D. N. Fry, R. C. Kryter, M. V. Mathis, J. E. Mott, and J. C. Robinson, "Use of Neutron Noise to Detect BWR-4 In-Core Instrument Tube Vibrations and Impacting," *Nucl. Technol.* 43, 42-54 (1979).

60. H. S. Cheng and D. J. Diamond," A Neutronic Analysis of Boiling Water Reactor In-Core Detector Noise", *Nucl. Technol.* 45, 46 (1979).

61. D. N. Fry, E. L. Machado, and F. J. Sweeney, "Method for Detecting Bypass Coolant Boiling in Boiling Water Reactors," *Trans. Am. Nucl. Soc.* 30, 511-513 (1978).

62. L. Mills, *An Investigation of the Thermal Aspects of a Boiling Water Reactor,* M.S. thesis, The University of Tennessee, Knoxville (March 1968).

63. R. G. Carlson and D. R. Gott, "Bypass Flow Distribution in a Boiling Water Reactor," *Nucl. Technol.* 33, 161-173 (1977).

64. W. Seifritz and F. Cioli, "On-Load Monitoring of Local Steam Velocity in BWR Cores by Neutron Noise Analysis," *Trans. Am. Nucl. Soc.* 17, 451 (1973).

65. D. N. Fry, J. March-Leuba, F. J. Sweeney, W. T. King, J. A. Renier, and R. T. Wood, "In-Core Flow Velocity Profiles During the First Fuel Cycle at Hatch-1 - Inferred from Neutron Noise," EPRI Report NP-2083 (1981).

66. M. Ashraf Atta, J. E. Mott, and D. N. Fry, "Determination of Void Fraction in BWRs Using Neutron Noise Analysis," *Trans. Am. Nucl. Soc.* 23, 466 (1976).

67. N. Zuber, F. W. Staub, G. Bijwaard, and P. G. Kroeger, "Steady State and Transient Void Fraction in Two Phase Flow Systems," Vol. I, General Electric Report GEAP-5417 (1967).

68. G. Kosály and J. M. Fahley, "Investigation of Axial Void Propagation Velocity Profiles in BWR Fuel Bundles," EPRI Report NP-2401 (June 1982).

69. D. Lübbesmeyer, "Possibilities of Flow-Pattern Identification by Noise Techniques," *Prog. Nucl. Energy* 9, 13-21 (1982).

70. D. L. Fischer et al., "Stability and Dynamic Performance of the General Electric Boiling Water Reactor," NEDO-21506, 76NED89 (1977).

71. J. March-Leuba and P. J. Otaduy, "A Comparison of BWR Stability Measurements with Calculations Using the Code LAPUR-IV," NUREG/CR-2998, ORNL/TM-8546 (1983).

72. L. A. Charmichael and R. O. Niemi, "Transient and Stability Tests at Peach Bottom Atomic Power Station Unit 2 at End of Cycle 2," EPRI Report NP-564 (1978).

73. L. A. Charmichael and R. O. Niemi, "Low Flow Stability Tests at Peach Bottom Atomic Power Station Unit 2 During Cycle 3," EPRI Report NP-971, 1981.

74. N. O. Niemi and S. F. Chen, "Vermont Yankee Cycle 8 Stability and Recirculation Pump Trip Test Report," NEDE-25445 (1982).

75. B. R. Upadhyaya and M. Kitamura, "Stability Monitoring of Boiling Water Reactors by Time Series Analysis of Neutron Noise," *Nucl. Sci. Eng.* 77 480 (1981).

NUREG/CR-3303
ORNL/TM-8774
NRC Dist. Category R-1

INTERNAL DISTRIBUTION

1. M. E. Buchanan
2-11. D. N. Fry
12. R. C. Gonzalez
13. T. L. King
14. W. T. King
15. R. C. Kryter
16. J. V. Leeds, Jr. (Advisor)
17. A. P. Malinauskas
18-27. J. March-Leuba
28. C. A. McKay (Advisor)
29. J. A. Mullens
30. P. W. Murrill (Advisor)
31. F. R. Mynatt
32. L. C. Oakes
33. B. M. Oliver (Advisor)
34. R. B. Perez
35. J. P. Renier
36. D. Shieh
37. C. M. Smith
38-47. F. J. Sweeney
48. H. E. Trammell (Advisor)
49. D. B. Trauger
50. B. R. Upadhyaya
51. R. T. Wood
52-53. Laboratory Records
54. Laboratory Records, ORNL RC
55-56. Central Research Library
57. Y-12 Document Reference Sect.
58. ORNL Patent Section
59. I&C Publications Office

EXTERNAL DISTRIBUTION

62. R. W. Albrecht, The University of Washington, Nuclear Engineering Department, Seattle, WA 98195.
61. D. G. Cain, Nuclear Safety Analysis Center, Electric Power Research Institute, 3412 Hillview Ave., P. O. Box 10412, Palo Alto, CA 94304.
62. R. B. Duffey, Electric Power Research Institute, 3412 Hillview Avenue, P. O. Box 10412, Palo Alto, CA 94303.
63. G. B. Fader, Institute of Nuclear Power Operations, 1100 Circle 75 Parkway, Suite 1500, Atlanta, GA 30339.
64. W. S. Farmer, U.S. Nuclear Regulatory Commission, MS-1130SS, Washington, DC 20555.
65. G. P. Horne, Nuclear Engineering Services, Duke Power Company, P. O. Box 33189, Charlotte, NC 28242.
66. R. T. Jones, Philadelphia Electric Co., 2301 Market Street, Philadelphia, PA 19101.
67. N. N. Kondic, U.S. Nuclear Regulatory Commission, MS-NL5650, Washington, DC 20555.
68. G. Kosaly, Department of Nuclear Engineering, The University of Washington, Seattle, WA 98195.
69. G. S. Lewis, Office of Inspection and Enforcement, U.S. Nuclear Regulatory Commission, Washington, DC 20555.
70. L. Lois, U. S. Nuclear Regulatory Commission, MS P-924, Washington, DC 20555.
71. E. L. Machado, IPEN/CNEN RT, C. P. 11049, Pinheros, Sao Paulo SP 01000 Brazil.

72. J. Royce Maner, Tennessee Valley Authority, Chestnut Street Towers II, Room 740, Chattanooga, TN 37410.
73. C. W. Mayo, Science Applications, Inc., Jackson Plaza Tower, Suite 1000, 800 Oak Ridge Turnpike, Oak Ridge, TN 37830.
74. D. W. Miller, Ohio State University, 206 West 18th Avenue, Columbus, OH 43210.
75. A. Morris, Tennessee Valley Authority, 1300 Chestnut Street Towers II, Chattanooga, TN 37401.
76. C. Puyal, Electricite De France, 6, Quai Watier 78400, Chatou, France.
77. J. C. Robinson, Technology for Energy Corporation, One Energy Center, Pellissippi Parkway, Knoxville, TN 37922.
78. R. F. Saxe, Department of Nuclear Engineering, North Carolina State University, P. O. Box 5636, Raleigh, NC 27607.
79. J. Steelman, Baltimore Gas and Electric Co., Calvert Cliffs Nuclear Station, Lusby Post Office, Lusby, MD 20657.
80. R. Sunder, Gesellschaft für Reaakorsuherheit, Forschungsgelande, D-8046, Garching, Federal Republic of Germany.
81. E. Turkcan, Netherlands Energy Research Foundation ECN, 3 Westendurinweg, Petten, The Netherlands.
82. G. Weidenhamer, U.S. Nuclear Regulatory Commission, MS-1130SS, Washington, DC 20555.

83-84. Technical Information Center, Box 62, Oak Ridge, TN 37831.

85-359. Given distribution under NRC Category R-1, Water Reactor Safety Research (NTIS-10 copies).

NRC FORM 335 (11-81)

U.S. NUCLEAR REGULATORY COMMISSION

BIBLIOGRAPHIC DATA SHEET

1. REPORT NUMBER (Assigned by DDC)
NUREG/CR-3303
ORNL/TM-8774

4. TITLE AND SUBTITLE (Add Volume No., if appropriate)
Use of Neutron Noise for Diagnosis of In-Vessel Anomalies in Light-Water Reactors

2. (Leave blank)

3. RECIPIENT'S ACCESSION NO.

7. AUTHOR(S)
D. N. Fry, J. March-Leuba, F. J. Sweeney

5. DATE REPORT COMPLETED
MONTH June | YEAR 1983

9. PERFORMING ORGANIZATION NAME AND MAILING ADDRESS (Include Zip Code)
Oak Ridge National Laboratory
P. O. Box X
Oak Ridge, TN 37831

DATE REPORT ISSUED
MONTH | YEAR

6. (Leave blank)

8. (Leave blank)

12. SPONSORING ORGANIZATION NAME AND MAILING ADDRESS (Include Zip Code)
Office of Nuclear Regulatory Research
Division of Facility Operations
U.S. Nuclear Regulatory Commission
Washington, DC 20555

10. PROJECT/TASK/WORK UNIT NO.

11. FIN NO.
B0191

13. TYPE OF REPORT
NUREG/CR

PERIOD COVERED (Inclusive dates)

15. SUPPLEMENTARY NOTES

14. (Leave blank)

16. ABSTRACT (200 words or less)

The value of neutron noise analysis for diagnosis of in-vessel anomalies in light-water reactors (LWRs) was assessed by: (1) analyzing ex-core neutron noise from seven pressurized-water reactors (PWRs) to determine the degree of similarity in the noise signatures and the sources of ex-core neutron noise; (2) measuring changes in ex-core neutron noise over an entire fuel cycle at a commercial PWR; (3) applying PWR neutron noise analysis to diagnose a loose core barrel, to infer in-core coolant velocity, and to infer fuel assembly motion; and (4) applying BWR neutron noise analysis to diagnose in-core instrument tube vibrations and bypass coolant boiling, to infer in-core two-phase flow velocity and void fraction, and to infer stability associated with reactivity feedback.

This report summarizes these assessments and provides guidance for the acquisition and analysis of neutron noise in LWRs.

17. KEY WORDS AND DOCUMENT ANALYSIS

17a. DESCRIPTORS

17b. IDENTIFIERS/OPEN-ENDED TERMS

18. AVAILABILITY STATEMENT

19. SECURITY CLASS (This report)

20. SECURITY CLASS (This page)

21. NO. OF PAGES

22. PRICE
$

NRC FORM 335 (11-81)